

TA 7  
6  
2/73-33

LIBRARIES  
COLORADO STATE UNIVERSITY  
FORT COLLINS, COLORADO

STUDY OF PLANE COUETTE FLOW  
IN STRATIFIED FLUID

by

Sherman Chieh  
Everett C. Nickerson  
Virgil A. Sandborn



**FLUID MECHANICS PROGRAM  
ENGINEERING RESEARCH CENTER  
COLLEGE OF ENGINEERING  
COLORADO STATE UNIVERSITY  
FORT COLLINS, COLORADO**

STUDY OF PLANE COUETTE FLOW  
IN STRATIFIED FLUID

by

Sherman Chieh  
Everett C. Nickerson  
Virgil A. Sandborn

Prepared Under

National Science Foundation  
Grant Number GK-30556

Washington, D.C.

Fluid Dynamics and Diffusion Laboratory  
College of Engineering  
Colorado State University  
Fort Collins, Colorado

May 1973

CER72-73SC-ECN-VAS33

## ABSTRACT

### STUDY OF PLANE COUETTE FLOW IN STRATIFIED FLUID

The mechanism of turbulent plane Couette flow with a negative temperature gradient was examined theoretically. First, the instability of fluid under various conditions was examined by utilizing linear and nonlinear numerical models. From the results, it was confirmed that constant shear has a stabilizing effect on the perturbations. It is shown that the neutral Rayleigh numbers, found from linear and nonlinear models, are almost identical for non-longitudinal rolls, but quite different for longitudinal rolls.

The heat and momentum flux for the flow in a certain range of Reynolds numbers ( $Re \leq 500$ ) and Rayleigh numbers ( $Ra \leq 500,000$ ) were determined by integrating the Boussinesq equations numerically. In this range of Reynolds and Rayleigh numbers, the convection characteristic dominates the flow motion; hence the following occurs: a) Heat flux and momentum flux are linearly correlated; b) Both heat and momentum flux increase with the Rayleigh number, but decrease with an increasing wave angle; c) Heat flux increases as the Reynolds number decreases; d) Heat flux approximately follows the "one-thirds power law" to the Rayleigh number; and e) Heat flux attains its maximum at  $\alpha = 0$  (longitudinal roll). The nonlinear numerical model also shows that preferred mode of perturbation is a roll-type convection ( $\alpha = 0$ ); and the perturbation with a larger wave angle ( $\alpha \neq 0$ ) can exist only at smaller Rayleigh numbers for certain Reynolds number. The above conclusion confirms Chandra's (1938) laboratory results and Kuo's (1963) cloud-form assumption.

A theoretical approach based on Malkus' upper bound hypothesis was also investigated. Accordingly, two inequalities were derived to express the upper bound on heat and momentum flux for heated plane Couette flow.

## ACKNOWLEDGMENTS

Acknowledgment is made to the National Center for Atmospheric Research, which is sponsored by the National Science Foundation, for computer time used in this research.

The financial support for this study was provided by the National Science Foundation under grant number GK-30556.

## TABLE OF CONTENTS

<u>Chapter</u>	<u>Page</u>
ABSTRACT . . . . .	ii
ACKNOWLEDGMENTS . . . . .	iv
LIST OF TABLES . . . . .	vii
LIST OF FIGURES. . . . .	viii
LIST OF SYMBOLS . . . . .	x
 I	
INTRODUCTION . . . . .	1
1.1 General Remarks . . . . .	1
1.2 Theoretical Mathematics Model . . . . .	3
1.2.1 Boussinesq Approximation . . . . .	3
1.2.2 Boundary Conditions . . . . .	6
1.2.3 Heat Flux, Momentum Flux, and Energy Equations . . . . .	8
1.3 Brief Review on Previous Instability Studies . . . . .	11
1.3.1 Laboratory Experimentation . . . . .	11
1.3.2 Previous Linear Models . . . . .	13
1.3.3 Lipp's Nonlinear Model . . . . .	15
 II	
NUMERICAL EXPERIMENT . . . . .	16
2.1 Linear Method to Examine Flow Instability . . . . .	16
2.2 Nonlinear Method to Examine Flow Instability . . . . .	26
2.2.1 Governing Equations for Nonlinear Analysis . . . . .	27
2.2.2 Boundary Conditions for Stream Function and Vorticity. . . . .	30
2.2.3 Instability Criteria of Nonlinear Model . . . . .	33
2.2.4 Procedures of Integration . . . . .	34
2.2.5 Numerical Schemes . . . . .	35
2.2.5.1 Transport Equations . . . . .	35
2.2.5.2 Poisson's Equation . . . . .	40
2.2.6 Computer Programming . . . . .	43
2.2.7 Numerical Results of Nonlinear Stability Analysis . . . . .	45
2.3 Finite-amplitude Rolls at Steady-state. . . . .	47
2.3.1 Vertical Profiles of Mean Velocity and Temperature . . . . .	48
2.3.2 Heat and Momentum Flux . . . . .	49

TABLE OF CONTENTS (continued)

<u>Chapter</u>		<u>Page</u>
III	UPPER BOUNDS ON HEAT AND MOMENTUM FLUX . . . . .	52
	3.1 Power Integral Equations . . . . .	54
	3.2 Governing Inequalities . . . . .	58
	3.3 Bounding Procedure . . . . .	64
	3.3.1 Upper Bound on Momentum Flux . . . . .	64
	3.3.2 Upper Bound on Heat Flux . . . . .	70
	3.3.3 Absolute Upper Bounds . . . . .	76
	3.4 The Upper Bound on Heat Flux in Turbulent Convection . . . . .	79
IV	CONCLUSION . . . . .	81
	BIBLIOGRAPHY . . . . .	84
	APPENDIX I GALERKIN METHOD . . . . .	92
	APPENDIX II PROVE OF THE REAL PART OF WAVE SPEED IS ZERO . . . . .	99
	APPENDIX III DERIVATION OF EQUATIONS . . . . .	102
	APPENDIX IV TIME-SPLITTING METHOD . . . . .	112
	FIGURES . . . . .	115
	TABLES . . . . .	136

LIST OF TABLES

<u>Table</u>		<u>Page</u>
1	Experimental data for heated plane Couette flow . . . . .	137
2	Values of Rayleigh number for neutral stability obtained from linear stability theory . . . . .	138
3	Critical Rayleigh number with its corresponding Reynolds number for transverse roll . . . . .	139
4	Critical Reynolds number with its corresponding Rayleigh number for transverse roll . . . . .	140
5	Comparison of neutral Rayleigh number from linear and nonlinear methods . . . . .	141
6	Heat flux and momentum flux at various wave angles for $Re = 160$ and wave length is 4 . . . . .	142
7	Nusselt number for various Reynolds number and Rayleigh number at $\alpha = 0$ and $\alpha = \pi/2$ . . . . .	143
8	Experimental values of the constants in equation (273) as reported by various investigators . . . . .	144

## LIST OF FIGURES

<u>Figure</u>		<u>Page</u>
1	A vertical cross section of the model for thermal convection in the presence of vertical shear . . . . .	116
2	Neutral stability curves for various Reynolds numbers obtained from linear stability theory (Transverse roll). . . . .	117
3	Neutral stability curves for various Rayleigh numbers obtained from linear stability theory (Transverse roll) . . . . .	118
4A	Variation of kinetic energy of disturbance (unstable case) . . . . .	119
4B	Variation of kinetic energy of disturbance (neutral case) . . . . .	120
4C	Variation of kinetic energy of disturbance (stable case) . . . . .	121
5	Variation of Nusselt number as a function of time at three different vertical positions . . . . .	122
6	Nusselt number as a function of the dimensionless horizontal wave length for $Re = 160$ and $\alpha = 0$ . . . . .	123
7	Flow chart of nonlinear program . . . . .	124
8	Relation between $Nu$ and $-Mo$ for longitudinal rolls ( $\alpha = 0$ ) . . . . .	126
9	Mean temperature and velocity profiles for $Re = 160$ , $\alpha = 0$ , Wave length = 4 . . . . .	127
10	Nusselt number as a function of Rayleigh number in logarithmic scale . . . . .	128
11A	Upper bound on heat flux in terms of Rayleigh and Reynolds numbers ( $Pr = 0.7$ ) . . . . .	129
11B	Upper bound on momentum flux in terms of Rayleigh and Reynolds numbers ( $Pr = 0.7$ ) . . . . .	130
11C	Upper bound on heat flux in terms of Reynolds and Rayleigh numbers ( $Pr = 0.7$ ) . . . . .	131

LIST OF FIGURES (continued)

<u>Figure</u>		<u>Page</u>
11D	Upper bound on momentum flux in terms of Reynolds and Rayleigh numbers ( $Pr = 0.7$ ) . . . . .	132
12A	Upper bounds on heat and momentum flux in terms of Rayleigh and Reynolds numbers under additional single-wave-number assumption ( $Pr = 0.7$ ) . . . . .	133
12B	Upper bound on heat flux in terms of Reynolds and Rayleigh numbers under additional single-wave-number assumption ( $Pr = 0.7$ ) . . . . .	134
12C	Upper bound on momentum flux in terms of Reynolds and Rayleigh numbers under additional single-wave-number assumption ( $Pr = 0.7$ ) . . . . .	135

LIST OF SYMBOLS

<u>Symbol</u>	<u>Definition</u>
$A_n$	Coefficient of function $G_n$
$B_n$	Coefficient of function $H_n$
$C_{mn}$	Elements of matrix in Equation (79)
$D$	Depth between two parallel plates
$D_n$	Coefficient of function $L_n$
$e_n$	Coefficient of function $R_n$
$E$	$\frac{\text{Re}}{\sqrt{M_t}} \gamma$
$E_n$	Coefficient of function $M_n$
$f_n$	Coefficient of function $S_n$
$g$	Acceleration of gravity
$G$	$\left(\frac{1}{\lambda} \int_0^\lambda \beta^2 dz\right)^{\frac{1}{2}}$
$G_n$	Series expansion function for $W$
$H_n$	Series expansion function for $W$
$i$	$\sqrt{-1}$
$\vec{i}, \vec{j}, \vec{k}$	Unit vector in positive $x, y, z$ direction
$\vec{i}_*, \vec{j}_*$	Unit vector in positive $m, n$ direction
$I'$	Inertia energy of perturbation
$k$	$k_x^2 + k_y^2$
$k_x, k_y$	Wave number appropriate to the directions of $x$ and $y$
$k^*$	Corresponding wave number after Squire's transformation
$\bar{K}$	Kinetic energy of mean flow
$K'$	Kinetic energy of perturbation
$L_n$	Series expansion function for $\theta$
$L_x, L_y$	Wave length appropriate to the directions of $x$ and $y$

LIST OF SYMBOLS (continued)

<u>Symbol</u>	<u>Definition</u>
$m, n$	Cartesian coordinates, n-axis parallel to the center line of disturbance rolls
$\Delta m$	Grid size in m-direction
$M_n$	Series expansion function for $\theta$
$M_o$	Momentum flux
$M_t$	$-M_o$ , Momentum number
$Nu$	Nusselt number
$p$	Pressure derivation from hydrostatic equilibrium
$\hat{p}$	Pressure
$Pr$	$\frac{\nu}{\kappa}$ , Prandtl number
$q$	Wave number appropriate to y-direction for fixed side boundaries
$Ra$	$\frac{\epsilon g D^3 \Delta T}{\nu \kappa}$ , Rayleigh number
$Re$	$\frac{\Delta U D}{\nu}$ , Reynolds number
$Re^*$	Corresponding wave number after Squire's transformation
$R_n$	Series expansion function for $W$
$S_n$	Series expansion function for $\theta$
$t$	Time
$T$	Instantaneous temperature
$\bar{T}$	Horizontal mean temperature
$T_o$	Temperature on lower plate
$\Delta T$	Temperature difference between two parallel plates
$\bar{U}$	Horizontal mean velocity in x-direction
$\Delta U$	Relative velocity between two horizontal plates

LIST OF SYMBOLS (continued)

<u>Symbol</u>	<u>Definition</u>
$\tilde{v}$	Flucting velocity vector
$v_x, v_y, v_z$	Components of $\tilde{v}$
$\hat{v}$	Normalized flucting velocity vector
$\hat{v}_x, \hat{v}_y, \hat{v}_z$	Components of $\hat{v}$
$\vec{V}$	Velocity vector
$V_x, V_y, V_z$	Components of $\vec{V}$
$w$	Infinitesimal amplitude disturbances of $v_z$
$x, y, z$	Cartesian coordinates, $z$ ; vertically upward
$\hat{z}$	$z + \frac{1}{2}$
$z_v$	Boundary layer parameter of velocity
$z_\theta$	Thermal boundary layer parameter
$\Delta z$	Grid size in $z$ -direction
$\alpha$	Wave angle between the directions of mainflow and disturbance roll
$\beta$	$-\frac{d\bar{U}}{dz}$
$\Gamma$	$-\frac{d\bar{T}}{dz}$
$\epsilon$	Coefficient of density change produced by a unit change in temperature
$\eta$	Vorticity
$\theta$	Flucting temperature
$\hat{\theta}$	Normalized flucting temperature
$\theta_0$	Random flucting temperature
$\theta$	Infinitesimal amplitude disturbances of $\theta$
$\kappa$	Thermal diffusivity

LIST OF SYMBOLS (continued)

<u>Symbol</u>	<u>Definition</u>
$\kappa_n$	$2n\pi$ , n here is positive integer
$\lambda$	Critical boundary layer depth
$\lambda_n$	Roots of equation (73)
$\Lambda$	$\langle (1 - \overline{\hat{v}_x \hat{v}_z})^2 \rangle$
$\mu_n$	Roots of equation (74)
$\nu$	Kinematic viscosity
$\pi$	$\frac{P}{\rho_m \Delta U^2}$ , dimensionless pressure
$\rho$	Density
$\rho_m$	Reference density
$\rho_n$	$(2n-1)\pi$ , n here is positive integer
$\sigma$	Wave speed
$\sigma_r$	Real part of $\sigma$
$\sigma_i$	Imaginary part of $\sigma$
$\gamma$	$(1 + \frac{Ra}{Re^2 Pr^2} \frac{Nu-1}{M_t^{-1}})$
$\Phi$	$\langle  \nabla \times \hat{v} ^2 \rangle$
$\psi$	Stream function
$\Psi$	$\langle  \nabla \hat{\theta} ^2 \rangle$
$\Omega$	$\langle (1 - \overline{\hat{\theta} \hat{v}_z})^2 \rangle$

Operators

$$\nabla = \frac{\partial}{\partial x} \vec{i} + \frac{\partial}{\partial y} \vec{j} + \frac{\partial}{\partial z} \vec{k}$$

LIST OF SYMBOLS (continued)

<u>Operators</u>	<u>Definition</u>
$\nabla^2$	$\frac{\partial^2}{\partial x^2} + \frac{\partial^2}{\partial y^2} + \frac{\partial^2}{\partial z^2}$
—	Horizontal average
< >	Volume average
' , '' , 'V	(primes) derivatives with respect to the vertical coordinate

## Chapter I

### INTRODUCTION

#### 1.1 General Remarks

The objective of this study is to understand the mechanism of the turbulent plane Couette flow heated from below and to find its upper bounds on the momentum and heat flux. This problem has a wide range of geophysical application since thermal convection usually occurs in the presence of a mean velocity in the atmosphere and oceans and because the heat and momentum transfer through the atmospheric boundary layer and the upper levels of the ocean which are both independent of vertical coordinate.

The fluid is considered to be contained between plates of infinite horizontal extent. The lower plate, with temperature  $T_0$  moves with a velocity  $\Delta U/2$  while the upper plate with temperature  $T_0 - \Delta T$  moves with a velocity  $-\Delta U/2$  (See Fig. 1). The Boussinesq equation is used to model the flow field.

First, the instability of fluid is examined under various combination of shear (Reynolds number), stratification (Rayleigh number), and wave angle between the direction of mainflow and disturbance roll (we define  $\alpha=0$  for longitudinal rolls and  $\alpha=\pi/2$  for transverse rolls) by utilizing both linear and nonlinear numerical techniques. In this study all numerical experiments use air (Prandtl number is equal to 0.7).

The Galerkin method which transfers a system of differential equations (including boundary conditions) to a system of algebraic equations is used to solve the linearized Boussinesq equations.

As for the nonlinear model, a total of three numerical schemes (Arakawa's, Upstream difference, and Time-splitting) are used to solve the time dependent vorticity equation, energy equation, or momentum equation in the nonlinear Boussinesq model. The critical Rayleigh numbers, found from linear and nonlinear models, are almost identical for transverse rolls but are entirely different for longitudinal rolls.

Next, the heat and momentum transport for unstable flow are found. Since the linearized equations are only good for modeling the flow under neutral or stable conditions, the nonlinear model is used for this purpose.

The theoretical method which is being employed to determine the upper bounds of momentum and heat flux is Malkus' power-integral method which is a theoretical approach based on Malkus' upper bound hypothesis. This part is an extension of a technical report by Nickerson (1970) who found the upper bounds for heated plane Couette flow by power-integral method with additional "single horizontal wave number" assumption. A more general derivation will be shown for the same purpose, and the results will be compared to Nickerson's.

## 1.2 Theoretical Mathematics Model

### 1.2.1 Boussinesq approximation

In general, the Boussinesq approximation to the Navier-Stokes equations is a good mathematical model for parallel stratified incompressible fluid with small lapse rate; however, it must be based on the following assumptions:

- a. An incompressible fluid.
- b. A constant density except in the gravity body force terms.
- c. A linearized equation of state. (Barotropic fluid)
- d. The viscous dissipation term in the energy equation is neglected.

Basically, this approximation states that the density change caused by temperature nonhomogeneity effects only the body force, not the inertia terms. The major restriction on the use of this approximation is the avoidance of excessively high density difference. Detailed discussions on the Boussinesq approximation can be found in Spiegel & Veronis (1960), Mihaljan (1962), Malkus (1964), and Byatt-Smith (1971). The governing equations are:

$$\frac{d\vec{V}}{dt} + \frac{\nabla p}{\rho_m} + \frac{\rho}{\rho_m} g\vec{k} = \nu \nabla^2 \vec{V} \quad (1)$$

$$\nabla \cdot \vec{V} = 0 \quad (2)$$

$$\frac{dT}{dt} = \kappa \nabla^2 T \quad (3)$$

$$\rho = \rho_m (1 - \epsilon(T - \bar{T})) \quad (4)$$

or Eqs. 1-4 can be rewritten as:

$$\frac{d\vec{V}}{dt} + \frac{\nabla p}{\rho_m} - \epsilon g(T - \bar{T})\vec{k} = \nu \nabla^2 \vec{V} \quad (5)$$

$$\frac{dT}{dt} = \kappa \nabla^2 T \quad (3)$$

$$\nabla \cdot \vec{V} = 0 \quad (2)$$

Here  $T = \bar{T}(z,t) + \theta$  and  $P$  is the pressure derivation from hydrostatic equilibrium. It is convenient to have the nondimensional form of Eqs. 1-5 with the following parameters:

Reference Length	$D$
Reference Velocity	$\Delta U$
Reference Temperature	$\Delta T$
Reference Time	$D/\Delta U$

Here  $D$  is the depth between two parallel plates of infinite horizontal extent,  $\Delta T$  is temperature difference between two plates ( $T_0$  on lower plate, and  $T_0 - \Delta T$  on upper plate),  $\Delta U$  is relative velocity between two plates. Then the nondimensional equations will be:

$$\frac{\partial \vec{V}}{\partial t} + \vec{V} \cdot \nabla \vec{V} + \nabla \pi - \frac{Ra}{Re^2 Pr} \theta \vec{k} = \frac{1}{Re} \nabla^2 \vec{V} \quad (6)$$

$$\frac{\partial T}{\partial t} + \vec{V} \cdot \nabla T = \frac{1}{Re Pr} \nabla^2 T \quad (7)$$

$$\nabla \cdot \vec{V} = 0 \quad (8)$$

$$\text{here} \quad \text{Re} = \frac{\Delta U D}{\nu} \quad \text{Ra} = \frac{\epsilon g \Delta T D^3}{\nu \kappa}$$

$$\text{Pr} = \frac{\nu}{\kappa} \quad \pi = \frac{p}{\rho_m (\Delta U)^2}$$

Notice  $\vec{V}$  and  $T$  are now in dimensionless form in Eqs. 6-8.

The two systems of cartesian coordinate which can be chosen are  $(x,y,z)$  and  $(m,n,z)$ . Here  $z$ -axis is in vertical direction,  $x$  is the axis along the direction of main stream velocity, and  $n$  is the axis parallel to the center line of disturbance rolls. If we define  $\alpha$  as the angle between  $x$ -axis and  $n$ -axis, then  $\alpha = 0$  will be shown the longitudinal rolls, and  $\alpha = \pi/2$  will show transverse rolls. For the first system of cartesian coordinate, the vector operators can be defined as:

$$\nabla = \frac{\partial}{\partial x} \vec{i} + \frac{\partial}{\partial y} \vec{j} + \frac{\partial}{\partial z} \vec{k}$$

$$\nabla^2 = \frac{\partial^2}{\partial x^2} + \frac{\partial^2}{\partial y^2} + \frac{\partial^2}{\partial z^2} \quad (9)$$

For the second,

$$\nabla = \frac{\partial}{\partial m} \vec{i}_* + \frac{\partial}{\partial z} \vec{k}$$

$$\nabla^2 = \frac{\partial^2}{\partial m^2} + \frac{\partial^2}{\partial z^2} \quad (10)$$

Here we set  $\partial(\ )/\partial n = 0$  since we assume that there are no variations along the axes of disturbance rolls. This assumption transfers the three dimensional problem to a two dimensional one.

### 1.2.2 Boundary Conditions

In this section, the proper boundary conditions for both main-stream flow and its fluctuation on the upper or lower plates are developed. It is convenient to separate the velocity and temperature in the following manner:

$$\begin{aligned}\vec{V} &= \bar{U}(z,t)\vec{i} + \tilde{v}(x,y,z,t) = (\bar{U} + v_x)\vec{i} + v_y\vec{j} + v_z\vec{k} \\ &= (\bar{U}\sin\alpha + v_m)\vec{i}_* + (\bar{U}\cos\alpha + v_n)\vec{j}_* + v_z\vec{k}\end{aligned}\quad (11)$$

$$T = \bar{T}(z,t) + \theta(x,y,z,t) = \bar{T}(z,t) + \theta(m,z,t) \quad (12)$$

and

$$v_m = v_x \sin(\alpha) - v_y \cos(\alpha) \quad (11a)$$

$$v_n = v_x \cos(\alpha) + v_y \sin(\alpha) \quad (11b)$$

$$v_x = v_n \cos(\alpha) + v_m \sin(\alpha) \quad (11c)$$

$$v_y = v_n \sin(\alpha) - v_m \cos(\alpha) \quad (11d)$$

here  $\tilde{v}$  and  $\theta$  are the fluctuating velocity and temperature.

For this specific problem,

$$\bar{U} = \Delta U/2, \quad \bar{T} = T_0 \quad \text{at} \quad z = -\frac{D}{2} \quad (13)$$

$$\bar{U} = -\Delta U/2, \quad \bar{T} = T_0 - \Delta T \quad \text{at} \quad z = \frac{D}{2} \quad (14)$$

And after dimensionalization

$$\bar{U} = \frac{1}{2}, \quad \bar{T} = T_0/\Delta T \quad \text{at} \quad z = -\frac{1}{2} \quad (15)$$

$$\bar{U} = -\frac{1}{2}, \quad \bar{T} = T_0/\Delta T - 1 \quad \text{at} \quad z = \frac{1}{2} \quad (16)$$

In general, two sets of boundary conditions can be chosen for fluctuating velocity and temperature. Free surface means there is no tangential stresses and heat flux is constant on the surface. However, rigid surface indicates that there is no slip, and the temperature is

constant on the surface. In mathematical terms, these boundary conditions at the surfaces may be expressed as follows:

A) Rigid surface

$$\begin{aligned} v_x = v_y = v_m = v_n = v_z = 0 \\ \theta = 0 \end{aligned} \quad (17)$$

B) Free surface

$$\begin{aligned} \frac{\partial v_x}{\partial z} = \frac{\partial v_y}{\partial z} = \frac{\partial v_m}{\partial z} = \frac{\partial v_n}{\partial z} = v_z = 0 \\ \frac{\partial \theta}{\partial z} = \text{constant} \end{aligned} \quad (18)$$

Also, from the equation of continuity, these additional conditions can be found:

$$\frac{\partial v_z}{\partial z} = 0 \quad \text{for rigid surface} \quad (17a)$$

and

$$\frac{\partial^2 v_z}{\partial z^2} = 0 \quad \text{for free surface} \quad (18a)$$

In this case, it can be assumed that both lower and upper boundaries are rigid.

As for initial condition, it can be assumed that both  $\bar{U}(z)$  and  $\bar{T}(z)$  are a linear function with respect to vertical coordinate  $z$ .

i.e;

$$\bar{U}(z) = -z \quad \text{at } t = 0 \quad (19)$$

$$\bar{T}(z) = T_0/\Delta T - z - \frac{1}{2} \quad \text{at } t = 0 \quad (20)$$

The two equations above are dimensionless in form.

### 1.2.3 Heat flux, momentum flux, and energy equations.

In this section the energy flux and transformation which occur in thermal convection with vertical shear is considered.

Nusselt number, a dimensionless form of vertical heat flux, is defined as the ratio of actual vertical heat flux to pure conductive vertical heat flux per unit horizontal area, which can be found by taking the horizontal average of the steady-state thermodynamic equation (Eq. 7):

$$\text{Nu} = - \frac{d\bar{T}}{dz} + \text{RePr}(\overline{v_z \theta}) \quad (21)$$

Similarly, the momentum flux can be determined by taking the horizontal average of the steady-state momentum equation (Eq. 6):

$$\text{Mo} = \frac{d\bar{U}}{dz} - \text{Re}(\overline{v_x v_z}) \quad (\text{along x-axis}) \quad (22)$$

or

$$\text{Mom} = \frac{d\bar{U}}{dz} \sin(\alpha) - \text{Re}(\overline{v_m v_z}) \quad (\text{along m-axis}) \quad (23)$$

$$\text{Mon} = \frac{d\bar{U}}{dz} \cos(\alpha) - \text{Re}(\overline{v_n v_z}) \quad (\text{along n-axis}) \quad (24)$$

The derivations of equations 21 to 24 are in Appendix III. These equations show that for turbulent flow as well as for laminar flow, the heat and momentum flux are independent of vertical coordinate:

$$\overline{(\quad)} = \frac{1}{A} \int_A (\quad) dA \quad (25)$$

A is a horizontal area bounded by the two wave lengths in the horizontal direction.

Herein is described the energy conversion mechanism of the problem. The equations for kinetic energy of perturbations and mean flow can be derived from Eq. 6 by taking a dot product of it with  $\tilde{v}$

or  $\vec{V}$ , and by taking the average over the volume. After several mathematical derivations (see Appendix III) the following equations is obtained:

$$\begin{aligned} \frac{d}{dt} K' = & - \left\langle \overline{v_x v_z} \frac{d\bar{U}}{dz} \right\rangle + \frac{Ra}{PrRe^2} \left\langle \overline{v_z \bar{\theta}} \right\rangle \\ & - \frac{1}{Re} \left\langle |\nabla_x \tilde{v}|^2 \right\rangle \end{aligned} \quad (26)$$

and

$$\begin{aligned} \frac{d}{dt} \bar{K} = & \left\langle \overline{v_x v_z} \frac{d\bar{U}}{dz} \right\rangle - \frac{1}{Re} \int_{-1/2}^{1/2} \left( \frac{d\bar{U}}{dz} \right)^2 dz \\ & + \frac{1}{2Re} \left. \frac{d(\bar{U}^2)}{dz} \right|_{-1/2}^{1/2} \end{aligned} \quad (27)$$

where  $K'$  is the kinetic energy of perturbation and is defined as

$$\begin{aligned} K' = \frac{1}{2} \langle \tilde{v} \cdot \tilde{v} \rangle & = \frac{1}{2} \int_{-1/2}^{1/2} (\overline{v_x^2} + \overline{v_y^2} + \overline{v_z^2}) dz \\ & = \frac{1}{2} \int_{-1/2}^{1/2} (\overline{v_m^2} + \overline{v_n^2} + \overline{v_z^2}) dz . \end{aligned} \quad (28)$$

And  $\bar{K}$  is the kinetic energy of the mean flow which is

$$\bar{K} = \frac{1}{2} \int_{-1/2}^{1/2} \bar{U}^2 dz . \quad (29)$$

The angular brackets  $\langle \rangle$  denote an average over a volume which is defined as:

$$\langle ( \quad ) \rangle = \frac{1}{A \cdot 1} \iiint_V ( \quad ) dAdz = \int_{-1/2}^{1/2} ( \quad ) dz \quad (30)$$

The first term of the right-hand side of Eq. 26 indicates the conversion between the kinetic energy of the mean flow and that of the perturbation and is denoted as:

$$\{K', \bar{K}\} \equiv \left\langle \overline{v_x v_y} \frac{d\bar{U}}{dz} \right\rangle \quad (31)$$

The second term indicates the conversion between the potential energy and the kinetic energy of the perturbation. The last term expresses dissipation due to viscous friction. The second term of the right-hand side of Eq. 27 is the dissipation due to shear friction between layers. Eqs. 26 and 27 clearly show that the energy is transferred from mean flow to the perturbation if  $\{K', \bar{K}\}$  is negative and vice versa.

Similarly, the equation for inertia energy of perturbations can be derived from equation (7) by multiplying  $\theta$  on it and by taking the average over the volume. It gives

$$\left\langle \theta \frac{\partial T}{\partial t} \right\rangle + \left\langle \theta \vec{V} \cdot \nabla T \right\rangle = \left\langle \frac{\theta}{\text{RePr}} \nabla^2 T \right\rangle \quad (32)$$

Then it can be found (see Appendix III),

$$\frac{\partial I'}{\partial t} + \left\langle \theta v_z \frac{d\bar{T}}{dz} \right\rangle = \frac{-1}{\text{RePr}} \left\langle |\nabla \theta|^2 \right\rangle \quad (33)$$

where

$$I' = \frac{1}{2} \left\langle \theta^2 \right\rangle \quad (34)$$

### 1.3 Brief Review on Previous Instability Studies

#### 1.3.1 Laboratory experimentation

Laboratory experiments involving convection and vertical shear flow in fluids were carried out by Terada (1928), Phillips & Walker (1932), Graham (1934), Dassanayake (1937), Chandra (1938), Brunt (1951), and Ingersoll (1965). Although the experimental apparatus and the fluid used in the above experiments were quite different, they gave almost the same physical sketch of the flow.

In Ingersoll's experiments the liquid, with moderately larger Prandtl number, was confined between two concentric vertical cylinders and two horizontal plates. Hence, the fluids were effected only slightly by curvature and centrifugal acceleration. For this reason, the results were not exactly what we had wanted for describing the flow phenomenon.

In Chandra's experiments, the base of the chamber consisted of a flat stainless steel plate which could be heated from below by passing a current through a number of coils of thin wire arranged at the bottom of the box. The top of the chamber consisted of a plane sheet of glass which could be drawn over the channel to produce a shear. The sides of the chamber were filled in by layers of felt, sufficient to prevent a rapid leakage of air into or out of the chamber. The motion within the chamber was made visible with cigarette smoke, injected by means of a two way pump. The results of Chandra's experiments are reviewed below:

a) When there is no shearing motion, the chamber (12"X12") is filled with polygonal convection cells, also referred to as Benard cells.

b) For a very small Reynolds number (small shearing motion), the original convection cells are distorted into a horseshoe pattern.

c) If the Reynolds number is increased but does NOT exceed another limiting value, the chamber is filled with transverse rolls.

d) If the Reynolds number exceeds a certain value (say  $Re = 3.19$  for  $Ra = 4132.45$  , or  $Re = 8.67$  for  $Ra = 4760.58$  ), the chamber becomes filled with longitudinal rolls. The greater the  $Ra$  , the greater the shear necessary to arrange the patterns longitudinally.

e) The edge of longitudinal rolls were wavy at  $Re = 61.22$  and  $Ra = 42316.29$  , but the waviness disappeared when the rate of shear was further increased.

f) For a relatively larger Rayleigh number, the perturbation will skip transverse rolls and change directly from polygonal cells to longitudinal rolls as we increase Reynolds number.

g) Longitudinal waves are the most probable form of unstable disturbance.

However, Chandra's model is not exactly the same as the mathematical model which was shown in 1.2, because the transverse direction is confined instead of being theoretically unbounded horizontally. The mathematical model for this bounded flow will be shown in 2.1.

Experimental data from previous reports are shown in Table 1.

### 1.3.2 Previous linear models

To solve the problem of hydrodynamic stability, one must follow the solution of a system of non-linear (quasi-linear) partial differential equations. In the classic approaches to the problem, it is assumed that for small disturbances (infinitesimal disturbances) the equations may be linearized; that is, quadratic or higher terms in the disturbances and derivatives will be neglected. It is obvious that the linearization method can not be applied to a system in which the disturbances are no longer small (finite disturbances).

Recently, Deardorff (1965), Gallagher & Mercer (1965), Ingersoll (1966a), Asai & Nakasuji (1968), and Asai (1969), analyzed the heated plane Couette flow problem utilizing the linearized equations. The equations can be solved numerically by using either finite-difference method (Asai & Nakasuji, and Asai), or series-expansion method (others). The results were obtained independently, using different procedures but are in general agreement. Curves of neutral stability were calculated by relating the five physical parameters of the problem: Reynolds number, Rayleigh number, Prandtl number, horizontal wave-numbers, and phase speed. In order to compare the results to a nonlinear model, the same problem was done independently. The details will be shown in Chapter 2.

The results of linear models discussed in previous papers can be summarized as follows:

1. Shear has a stabilizing influence on the thermal convection if we assume the disturbance are not purely longitudinal.
2. For pure longitudinal rolls, the equations reduce to those of the Rayleigh convection problem. Thus all fluids will become

unstable at the same value of Rayleigh number whether shear is present or not.

3. The wavelength of the disturbance increases with the Reynolds number.

4. The stabilizing effect of shear becomes increasingly strong with increasing Prandtl number for non-pure longitudinal rolls. However, there is no effect for pure longitudinal rolls.

5. A stabilization of the vertical shear is more effective in a perturbation of shorter wave length. Hence an appearance of the most unstable perturbation shifts toward a longer wave length with an increasing shear.

6. The suppressing effect of the vertical shear is much more striking on a transverse perturbation when compared with a longitudinal one. This gives a preference for the longitudinal convection rolls in an atmosphere with a vertical shear.

The stability of both stably- and unstably-stratified plane Couette flow were studied theoretically by Kuo (1963). However, his results are not included because the effects of molecular diffusion were not taken into account in his paper.

### 1.3.3 Lipps' nonlinear model

During the last few years, particular emphasis has been placed on studying nonlinear stability problems. These were successfully solved by Ogura & Yagihashi (1969) on force convection, and Crowder & Dalton (1971) on pipe flow.

As for our problem, Lipps was the first to analyze with the nonlinear method. He discussed the instability for transverse rolls and determined the heat flux for longitudinal rolls. Since Lipps' interest is restricted to two dimensional flow, a more general but different analysis will be shown in 2.3. The instability for various wave-angles (including transverse roll and longitudinal roll) will be discussed, and the results will be compared to those from the linear method.

## Chapter II

## NUMERICAL EXPERIMENT

## 2.1 Linear Method to Examine Flow Instability

As previously mentioned, two systems of coordinates can be used for the mathematical model. Here, the governing equations for these two choices are derived. In addition, the governing equations for the one with confined boundaries in the y-direction will also be shown.

After substituting Eqs. 11 & 12 into Eqs. 6-8, two sets of equations can be found for different coordinates:

$$\frac{\partial v_x}{\partial t} + \bar{U} \frac{\partial v_x}{\partial x} + v_z \frac{\partial \bar{U}}{\partial z} + \frac{\partial \pi}{\partial x} = \frac{1}{Re} \nabla^2 v_x \quad (35)$$

$$\frac{\partial v_y}{\partial t} + \bar{U} \frac{\partial v_y}{\partial y} + \frac{\partial \pi}{\partial y} = \frac{1}{Re} \nabla^2 v_y \quad (36)$$

$$\frac{\partial v_z}{\partial t} + \bar{U} \frac{\partial v_z}{\partial z} - \frac{Ra}{Re^2 Pr} \theta + \frac{\partial \pi}{\partial z} = \frac{1}{Re} \nabla^2 v_z \quad (37)$$

$$\frac{\partial \theta}{\partial t} + \bar{U} \frac{\partial \theta}{\partial x} + v_z \frac{\partial \bar{T}}{\partial z} = \frac{1}{Re Pr} \nabla^2 \theta \quad (38)$$

$$\frac{\partial v_x}{\partial x} + \frac{\partial v_y}{\partial y} + \frac{\partial v_z}{\partial z} = 0 \quad (39)$$

and

$$\frac{\partial v_m}{\partial t} + \bar{U} \sin \alpha \frac{\partial v_m}{\partial m} + v_z \frac{\partial \bar{U}}{\partial z} \sin \alpha + \frac{\partial \pi}{\partial m} = \frac{1}{Re} \nabla^2 v_m \quad (40)$$

$$\frac{\partial v_n}{\partial t} + \bar{U} \sin \alpha \frac{\partial v_n}{\partial m} + v_z \frac{\partial \bar{U}}{\partial z} \cos \alpha = \frac{1}{Re} \nabla^2 v_n \quad (41)$$

$$\frac{\partial v_z}{\partial t} + \bar{U} \sin \alpha \frac{\partial v_z}{\partial m} - \frac{Ra}{Re^2 Pr} \theta + \frac{\partial \pi}{\partial z} = \frac{1}{Re} \nabla^2 v_z \quad (42)$$

$$\frac{\partial \theta}{\partial t} + \bar{U} \sin \alpha \frac{\partial \theta}{\partial m} + v_z \frac{\partial \bar{T}}{\partial z} = \frac{1}{Re Pr} \nabla^2 \theta \quad (43)$$

$$\frac{\partial v_m}{\partial m} + \frac{\partial v_z}{\partial z} = 0 \quad (44)$$

In these, the nonlinear terms  $\tilde{v} \cdot \nabla \tilde{v}$  and  $\tilde{v} \cdot \nabla \theta$  were neglected to linearize the equations and also use a relationship among  $\bar{U}$ , and  $\bar{T}$ , since the mean flow satisfies the Boussinesq equation. There are now five equations and five unknowns in equations 35-39. After eliminating the nondimensional unknowns  $v_x$ ,  $v_y$ , and  $\pi$ , the linearized equations are

$$\left( \frac{\partial}{\partial t} + \bar{U} \frac{\partial}{\partial x} - \frac{1}{Re} \nabla^2 \right) \nabla^2 v_z - \frac{Ra}{Pr Re^2} \nabla_H^2 \theta = \frac{\partial^2 \bar{U}}{\partial z^2} \frac{\partial v_z}{\partial x} \quad (45)$$

$$\left( \frac{\partial}{\partial t} + \bar{U} \frac{\partial}{\partial x} - \frac{1}{Re Pr} \nabla^2 \right) \theta + v_z \frac{\partial \bar{T}}{\partial z} = 0 \quad (46)$$

here

$$\nabla^2 = \frac{\partial^2}{\partial z^2} + \nabla_H^2$$

$$\nabla_H^2 = \frac{\partial^2}{\partial x^2} + \frac{\partial^2}{\partial y^2}$$

As for boundary conditions for the fluctuating velocity  $v_z$  and  $\theta$ , it is assumed that both upper and lower boundaries are rigid surfaces:

$$v_z = \theta = \frac{\partial v_z}{\partial z} = v_z = 0 \quad \text{at } z = \pm \frac{1}{2} \quad (47)$$

Classically, it is assumed that the disturbance functions  $v_x$ ,  $v_y$ ,  $v_z$  and  $\theta$ , are all proportional to  $\exp(i(k_x x + k_y y - \sigma t))$ , so that we consider a single component of a Fourier series in  $x$  and  $y$  directions to represent the flow. The assumption also ensures that the velocities are bounded at infinite. The quantities  $k_x$  and  $k_y$  are real and are the wave numbers appropriate to the directions  $x$  and  $y$ , which are related to the wave length of the disturbances by  $L_x = 2\pi/k_x$ ,  $L_y = 2\pi/k_y$ . Also,  $\sigma = \sigma_r + i\sigma_i$  is the wave (or phase) speed;  $\sigma_i$  represents the amplification or damping of the oscillation with the passage of time. If  $\sigma_i$  is positive, the disturbance amplifies and is unstable; however, if it is negative, the disturbance decays and is stable. The situation in neutral stability is governed by  $\sigma_i = 0$ .

In mathematical terms, it can be written as:

$$v_z(x, y, z, t) = W(z) \exp(i(k_x x + k_y y - \sigma t)) \quad (48)$$

$$\theta(x, y, z, t) = \Theta(z) \exp(i(k_x x + k_y y - \sigma t)) \text{RePr} \quad (49)$$

Then Eqs. 45-49 give:

$$\begin{aligned} \bar{L}_1 &= W''v - 2k^2 W'' + k^4 W - \text{Ra} k^2 \theta \\ &- i k_x \text{Re} \left[ \left( \bar{U} - \frac{\sigma}{k_x} \right) (W'' - k^2 W) - \bar{U}'' W \right] = 0 \end{aligned} \quad (50)$$

$$\bar{L}_2 = \theta'' - k^2 \theta - \bar{W}'' - i k_x \text{RePr} \left( \bar{U} - \frac{\sigma}{k_x} \right) \theta = 0 \quad (51)$$

$$\theta(\pm \frac{1}{2}) = W(\pm \frac{1}{2}) = W'(\pm \frac{1}{2}) = 0 \quad (52)$$

here  $k^2 = k_x^2 + k_y^2$ . Eqs. 51-52 are the governing equations for the linear method.

Similarly, the equations for  $v_z$  and  $\theta$  also can be found after eliminating unknowns  $v_m$ ,  $v_n$ , and  $\pi$  in Eqs. 40-44.

$$\left(\frac{\partial}{\partial t} + \bar{U}\sin\alpha \frac{\partial}{\partial m} - \frac{1}{\text{Re}} \nabla^2\right) \nabla^2 v_z - \frac{\partial^2 \bar{U}}{\partial z^2} \sin\alpha \frac{\partial v_z}{\partial z} = \frac{\text{Ra}}{\text{Re}^2 \text{Pr}} \frac{\partial^2 \theta}{\partial m^2} \quad (53)$$

$$\left(\frac{\partial}{\partial t} + \bar{U}\sin\alpha - \frac{1}{\text{RePr}} \nabla^2\right) \theta + v_z \frac{\partial \bar{T}}{\partial z} = 0 \quad (54)$$

here

$$\nabla^2 = \frac{\partial^2}{\partial m^2} + \frac{\partial^2}{\partial z^2}$$

The boundary conditions are the same as for Eq. 47. With the same procedure, the Fourier component for  $v_z$  and  $\theta$  can be defined as follows:

$$v_z(m, z, t) = W(z) \exp(i(km - \sigma t)) \quad (55)$$

$$\theta(m, z, t) = \Theta(z) \exp(i(km - \sigma t)) \text{RePr} \quad (56)$$

then Eqs. 52-56 give:

$$\begin{aligned} \bar{L}_1 &= W'V - zk^2 W'' + k^4 W - \text{Ra}k^2 \Theta \\ &- i\text{Re}k \sin\alpha \left[ \left( \bar{U} - \frac{\sigma}{k \sin\alpha} \right) (W'' - k^2 W) - \bar{U}'' W \right] = 0 \end{aligned} \quad (57)$$

$$\bar{L}_2 = \Theta'' - k^2 \Theta - W\bar{T}' - i k \sin\alpha \text{RePr} \left( \bar{U} - \frac{\sigma}{k \sin\alpha} \right) \Theta = 0 \quad (58)$$

here the boundary conditions will be the same as Eq. 52.

From our definition of coordinate, the geometric relation shows

$$k_x = k \sin(\alpha) \quad (59)$$

$$k_y = k \cos(\alpha) \quad (60)$$

and  $k^2 = k_x^2 + k_y^2 \quad (61)$

If Eqs. 50-61 are substituted into Eqs. 57 and 58 and compared to Eqs. 50 and 51, it is found that the two sets of equations are the same. This means that the assumption made (that is  $\partial(\ )/\partial n = 0$ ) in 1.2.1 is consistent.

Next the governing equations for the case with confined boundaries in y-direction will be determined. For fixed side boundaries, an additional boundary condition can be used:

$$v_x = v_y = v_z = \theta = 0 \quad \text{at } y = 0 \text{ and } B \quad (62)$$

here  $B$  is the dimensionless width of the chamber. The side boundary condition allows the separation of variables by assuming that

$$v_z(x,y,z,t) = W(z)\exp(i(k_x x - \sigma t))\sin(qy) \quad (63)$$

$$\theta(x,y,z,t) = \Theta(z)\exp(i(k_x x - \sigma t))\sin(qy) \quad (64)$$

$$\text{here } q = \lambda\pi/B \quad \lambda = 1,2,3,\dots \quad (65)$$

$\lambda = 1$  or  $2$  is used since this gives the most unstable mode.

Substituting Eqs. 63 and 64 into Eqs. 45 and 46, results in the same set of equations as Eqs. 50-52, except the definition of  $k$  which is

$$k^2 = k_x^2 + q^2 \quad (66)$$

Therefore, Eqs. 50-52 are the only equations which need to be solved numerically regardless of boundary conditions (infinite extent or confined) and no matter what kind of cartesian coordinate system that is chosen.

Next, Eqs. 50-52 must be solved numerically. These non-Hermitian equations will be solved by the "Galerkin method" (see appendix 1 for detail) which transfers a system of differential equations (including boundary conditions) to a system of algebraic equations. Then these equations were solved numerically with the aid of CDC 6400 high speed computer at Colorado State University. Accordingly, the variables  $W(z)$  and  $\Theta(z)$  can be expanded as:

$$W(z) = \sum_{n=1}^N (e_n R_n) = \sum_{n=1}^N (A_n G_n(z) + iB_n H_n(z)) \quad (67)$$

$$\Theta(z) = \sum_{n=1}^N (f_n S_n) = \sum_{n=1}^N (D_n L_n(z) + iE_n M_n(z)) \quad (68)$$

here  $R_n$  and  $S_n$  individually should satisfy the boundary conditions (Eq. 52) and also orthogonalized with respect to  $R_n$ 's and  $T_n$ 's, and the functions  $G_n$ ,  $H_n$ ,  $L_n$ , and  $M_n$  are real. For this problem, the following are defined:

$$G_n(z) = \cosh(\lambda_n z) / \cosh(\lambda_n / 2) - \cos(\lambda_n z) / \cos(\lambda_n / 2) \quad (69)$$

$$H_n(z) = \sinh(\mu_n z) / \sinh(\mu_n / 2) - \sin(\mu_n z) / \sin(\mu_n / 2) \quad (70)$$

$$M_n(z) = \sin(\kappa_n z) \quad (71)$$

$$L_n(z) = \cos(\rho_n z) \quad (72)$$

in order to satisfy the boundary conditions. Here  $\lambda_n$  and  $\mu_n$  are the roots of

$$\tanh(\lambda/2) + \tan(\lambda/2) = 0 \quad (73)$$

$$\operatorname{ctnh}(\mu/2) + \operatorname{ctn}(\mu/2) = 0 \quad (74)$$

$$\text{and } \rho_n = (2n-1)\pi \quad n = 1, N \quad (75)$$

$$\kappa_n = 2n\pi \quad n = 1, N \quad (76)$$

From the principle of Galerkin method, the following conditions should be satisfied:

$$\int_{-1/2}^{1/2} \bar{L}_1 R_m dz = 0 \quad m = 1, N \quad (77)$$

$$\int_{-1/2}^{1/2} \bar{L}_2 S_m dz = 0 \quad m = 1, N \quad (78)$$

After substituting Eqs. 67 and 68 into Eqs. 77 and 78, a system of simultaneous linear equations are obtained (see appendix 1 for detail).



Physically, Eq. 80 specifies the states of neutral stability when  $\sigma_i = 0$ . As for  $\sigma_r$ , Vest & Arpaci (1969) have proved that  $\sigma_r = 0$  if the functions are defined as in Eqs. 69-72. This is because of the orthogonalized property of  $G_n$ ,  $H_n$ ,  $L_n$ , and  $M_n$  (see Appendix 2). Hence  $\sigma = 0$  can be set in Eqs. 50 and 51 before determining Eq. 80. Now Eq. 80 becomes:

$$F(\alpha, k, Ra, Re, Pr) = 0 \quad (81)$$

It is found that the secular equation 80 approximately converges at  $N = 4$ .

The computer programs have been tested, that is; the following were set  $k_y = 0$  (or  $\alpha = \pi/2$ ) and  $Re = 0$ , meaning there is no shear present and the disturbance is only a function of  $x$ . Then Eqs. 50-52 will become the governing equations for the Benard problem (pure thermal convection instability problem). The calculated critical Rayleigh number  $Ra = 1707.784$  differs only slightly from the well-known result  $Ra = 1707.762$ . Here  $N = 5$  and the wave number  $k = 3.116$  instead of the classic result  $k = 3.117$ .

Next  $Ra$  and  $k_y$  are set equal to zero; then Eqs. 50-52 approach the well known Orr-Sommerfeld equation for plane Couette flow. When  $k_x = 0.41$  the Reynolds number is 189894.624. This result is close to Kuwabara's (1967),  $Re_{crit} = 1.9 \times 10^5$ . A contradiction was found in Gallagher and Mercer's (1961) paper in which they concluded that plane Couette flow is stable at all Reynolds numbers. A possible explanation for their discrepancy is that they only considered the real part, as

they expanded the variables in series form and also only considered the real growth rate as they checked the flow instability. However, further proof is needed to substantiate the above explanation.

Numerical results for neutral stability are shown in Table 2-4 and Figs. 2 and 3 for various cases. The values of Rayleigh number at neutral stability under different Reynolds numbers for the transverse roll are shown in Table 2; also for comparison the data of Gallagher & Mercer (1965) are listed. This clearly shows that the results of the two different sources are close. Table 3 shows the critical Rayleigh number with its corresponding Reynolds number; Table 4 shows the critical Reynolds number with its corresponding Rayleigh number. Neutral stability curves for various Reynolds numbers in the  $Re$ - $k$  plane are shown in Fig. 2, and neutral stability curves for various Rayleigh number in the  $Re$ - $k$  plane are shown in Fig. 3.

Only the transverse rolls are considered in Tables 2-4 and Figs. 2-3 because the non-transverse cases ( $\alpha$  is not equal to  $\pi/2$ ) can be transferred to the case  $\alpha = \pi/2$  by Squire's transformation. From Eqs. 50 and 51 the following can be set:

$$Re \sin(\alpha) = k^* Re^* \sin(\pi/2) \quad (82)$$

$$k = k^* \quad (83)$$

or

$$Re^* = Re \sin(\alpha) \quad (84)$$

to transfer the three dimensional disturbance to a two dimension one. Eq. 84 is called the Squire's transformation, where  $Re^*$  and  $k^*$  are the corresponding Reynolds number and wave number after transformation. Thus; the problem of a three dimensional disturbance is equivalent

to a problem of a two dimensional one with the same Rayleigh number but lower Reynolds numbers. Also, from Eq. 84 it is evident that the pure longitudinal wave ( $\alpha = 0$ ) should become critically stable at the same value of the Rayleigh number as for the Benard problem.

## 2.2 Nonlinear Method to Examine Flow Instability

In the basic ideas of linearized theory, the second and higher powers of the disturbance amplitude and their derivatives are ignored. For plane Poiseuille flow, Meksyn & Stuart (1951) suggested that, even if the Reynolds number is less than the critical Reynolds number determined from the linear method (Thomas (1950) found  $Re_{crit} = 5780$ ), the nonlinear effects might provide a threshold amplitude above which velocity perturbations could grow and stimulate turbulence. Their approximate theory yielded an amplitude-dependent critical Reynolds number as low as 3000.

Ellingsin & Palm (1970) discussed the nonlinear effect on pure plane Couette flow and found the nonlinear terms are destabilizing for small amplitudes. The nonlinear effect might also be important for heated plane Couette flow. Hence it is necessary to determine the contribution of the nonlinear term when considering flow instability. Also, if the amplitude of disturbance becomes too large, the linear theory is no longer applicable, and a nonlinear theory is required in order to follow the evolution of such perturbations for the purpose of finding the heat and momentum flux.

A single-wave-number assumption is made in the nonlinear numerical model.

### 2.2.1 Governing equations for nonlinear analysis

For the convenience of analysis, a cartesian coordinate system  $(m,n,z)$  is chosen with its  $n$ -axis parallel to central lines of disturbance rolls. This coordinate system can simplify the problem and can transfer the three dimensional problem to a two dimensional one under the assumption that there is no variation along the axis of disturbance rolls. It has been shown in 2.1 that the results of a linear model are independent of the chosen coordinates. For equations 6-10, the governing equations for the nonlinear model will be:

$$\frac{\partial V_n}{\partial t} + V_m \frac{\partial V_n}{\partial m} + V_z \frac{\partial V_n}{\partial z} = \frac{1}{Re} \nabla^2 V_n \quad (85)$$

$$\frac{\partial V_m}{\partial t} + V_m \frac{\partial V_m}{\partial m} + V_z \frac{\partial V_m}{\partial z} = \nabla^2 V_m - \frac{\partial \pi}{\partial m} \quad (86)$$

$$\frac{\partial V_z}{\partial t} + V_m \frac{\partial V_z}{\partial m} + V_z \frac{\partial V_z}{\partial z} = \frac{1}{Re} \nabla^2 V_z - \frac{\partial \pi}{\partial z} + \frac{Ra}{Re^2 Pr} (T - \bar{T}) \quad (87)$$

$$\frac{\partial T}{\partial t} + V_m \frac{\partial T}{\partial m} + V_z \frac{\partial T}{\partial z} = \frac{1}{Re Pr} \nabla^2 T \quad (88)$$

$$\frac{\partial V_m}{\partial m} + \frac{\partial V_z}{\partial z} = 0 \quad (89)$$

where

$$\nabla^2 = \frac{\partial^2}{\partial m^2} + \frac{\partial^2}{\partial z^2} \quad (90)$$

From Eq. 89, a stream function  $\psi$  can be introduced such that

$$V_m = -\frac{\partial \psi}{\partial z} \quad (91)$$

$$V_z = \frac{\partial \psi}{\partial m} \quad (92)$$

Also, the vorticity  $\eta$  can be defined as

$$\eta = \frac{\partial V_z}{\partial m} - \frac{\partial V_m}{\partial z} = \frac{\partial^2 \psi}{\partial m^2} + \frac{\partial^2 \psi}{\partial z^2} = \nabla^2 \psi \quad (93)$$

The vorticity equations are established after eliminating the nondimensional pressure  $\pi$  from Eqs. 86 and 87:

$$\frac{\partial \eta}{\partial t} + V_m \frac{\partial \eta}{\partial m} + V_z \frac{\partial \eta}{\partial z} = \frac{1}{Re} \nabla^2 \eta + \frac{Ra}{PrRe^2} \frac{\partial T}{\partial m} \quad (94)$$

As for initial conditions, the basic state consisted of a linear temperature gradient and linear shear flow. A random temperature distribution was superimposed on the linear temperature gradient in order to have a disturbance source for the purpose of checking flow stability. The random field was obtained from a pseudo-random number generator and contained a random number in the range  $\pm 0.5 \times 10^{-m}$ .  $m$  is a chosen integer between 2-6. Experience shows that  $m$  has no affect on the problem. The velocity components and temperature field of upper and lower are kept constant during integration. Eqs. 11, 12, 19, and 20 give:

$$V_m = \bar{U}(z) \sin(\alpha) + v_m = -z \sin(\alpha) + 0 \quad \text{at } t=0 \text{ \& } z = \pm 1/2 \quad (95)$$

$$V_n = \bar{U}(z) \cos(\alpha) + v_n = -x \cos(\alpha) + 0 \quad \text{at } t=0 \text{ \& } z = \pm 1/2 \quad (96)$$

$$V_z = v_z = 0 \quad \text{at } t=0 \text{ \& } z = \pm 1/2 \quad (97)$$

$$T = \bar{T} + \theta_0 = T_0/\Delta T - z - \frac{1}{2} + \theta_0 \quad \text{at } t=0 \text{ \& } z = \pm 1/2 \quad (98)$$

$$\theta_0 = 0 \quad \text{at } z = \pm 1/2 \quad (99)$$

Hence, all disturbances vanish at  $t = 0$  and  $z = \pm \frac{1}{2}$ .

Physically speaking, no experiment is performed with an apparatus of infinite dimensions. But mathematically, it is possible to circumvent the difficulty by limiting the discussion to disturbances which are spatially periodic in the directions in which the fluid extends to infinite. The flow must be periodic at the lateral boundaries,  $m = 0$  and  $m = L = 2\pi/k$ . In mathematical expression:

$$\vec{V}(0, z, t) = \vec{V}(L, z, t) \quad (100)$$

$$T(0, z, t) = T(L, z, t) \quad (101)$$

$$\psi(0, z, t) = \psi(L, z, t) \quad (102)$$

$$\eta(0, z, t) = \eta(L, z, t) \quad (103)$$

Therefore all variables at the downstream boundary become the new boundary values at the upstream boundary during the numerically integraticn.

### 2.2.2 Boundary conditions for stream function and vorticity

Boundary conditions for the vorticity transport equation cannot be given directly. However, they are closely related to interior values of vorticity and stream functions by means of a Taylor's series expansion. For rigid boundaries this relation is simple and may be derived analytically from the known boundary conditions of velocities and stream functions. The initial condition for vorticity  $\eta$  can be determined numerically from the definition of vorticity

$$\eta = \frac{\partial V_z}{\partial m} - \frac{\partial V_m}{\partial z} = - \frac{\partial V_m}{\partial z} \quad \text{at } t = 0 \quad (104)$$

$$\eta(z) = - \frac{V_m(z+\Delta z) - V_m(z)}{\Delta z} \quad \text{at } t = 0 \quad (105)$$

The Taylor's series expansion of the stream function is the basic equation to determine the boundary conditions of vorticity  $\eta$  at upper and lower planes. Since

$$\begin{aligned} \psi(B \pm \Delta z) &= \psi(B) \pm \frac{\partial \psi(B)}{\partial z} \Delta z + \frac{(\Delta z)^2}{2!} \frac{\partial^2 \psi(B)}{\partial z^2} \\ &\pm \frac{(\Delta z)^3}{3!} \frac{\partial^3 \psi(B)}{\partial z^3} + \dots \\ &= \psi(B) \mp V_m(B) \Delta z + \frac{(\Delta z)^2}{2!} (\eta(B) - \frac{\partial^2 \psi(B)}{\partial m^2}) \\ &\pm \frac{(\Delta z)^3}{6} \frac{\partial}{\partial z} (\eta(B) - \frac{\partial^2 \psi(B)}{\partial m^2}) + \\ &= \psi(B) \mp V_m(B) \Delta z + \frac{(\Delta z)^2}{2} \eta(B) \pm \frac{(\Delta z)^3}{6} \frac{\partial \eta(B)}{\partial z} + \\ &= \psi(B) \mp V_m(B) \Delta z + \frac{(\Delta z)^2}{2} \eta(B) + \frac{(\Delta z)^3}{6} (\frac{\eta(B \pm \Delta z) - \eta(B)}{\Delta z}) + \\ &= \psi(B) \mp V_m(B) \Delta z + \frac{(\Delta z)^2}{3} \eta(B) + \frac{(\Delta z)^2}{6} \eta(B \pm \Delta z) + \dots \end{aligned}$$

or

$$\eta(B) = \frac{3}{(\Delta y)^2} (\psi(B \pm \Delta z) - \psi(B)) \pm V_m(B) \cdot \Delta z$$

$$- \frac{1}{2} \eta(B \pm \Delta z) \quad \text{at } B = z = \pm 1/2 \quad (106)$$

At lower surface,

$$\eta(-1/2) = \frac{3}{(\Delta z)^2} [\psi(-1/2 + \Delta z) - \psi(-1/2)]$$

$$+ V_m(-1/2) \Delta z - 1/2 \eta(-1/2 + \Delta z) \quad (107)$$

At upper surface,

$$\eta(1/2) = \frac{3}{(\Delta z)^2} [\psi(1/2 - \Delta z) - \psi(1/2)]$$

$$- V_m(1/2) - 0.5 \eta(1/2 - \Delta z) \quad (108)$$

Notice that the vorticity is independent of the m-axis at the boundaries.

The boundary conditions and initial conditions for the stream function follow from Eq. 92 and Eq. 97

$$V_z = \frac{\partial \psi}{\partial m} = 0 \quad \text{at } t = 0 \text{ \& } z = \pm 1/2 \quad (109)$$

This shows the stream function has no variation along the m-axis direction on the upper and lower plates or at the initial time. This allows equation 91 to change to:

$$V_m = - \frac{d\psi}{dz} \quad \text{at } t = 0 \text{ \& } z = \pm 1/2 \quad (110)$$

or

$$\int_{z-\Delta z}^z d\psi = - \int_{z-\Delta z}^z V_m dz \quad \text{at } t = 0 \text{ \& } z = \pm 1/2 \quad (111)$$

then

$$\psi(z) - \psi(z - \Delta z) = - \int_{z-\Delta z}^z V_m dz$$

$$\approx - \frac{V_m(z) + V_m(z - \Delta z)}{2} \Delta z \quad \text{at } t = 0 \text{ \& } z = \pm 1/2$$

or

$$\psi(z) = - \frac{V_m(z) + V_m(z - \Delta z)}{2} \Delta z + \psi(z - \Delta z) \quad \text{at } t = 0 \text{ \& } z = \pm 1/2 \quad (112)$$

Equation 112 is based on the mean-value theorem for very small  $\Delta z$ . The stream function for various depths at initial time can be found from Eq. 112 by assigning a zero value to the horizontal plane of the bottom boundary. The stream function for both upper and lower planes will remain unchanged as time increases.

### 2.2.3 Instability criteria of nonlinear model

There are two basic methods to treat instability problems. The first is the classic linear theory method which assumes that the perturbation is of the form of  $\exp(-i(k_x x + k_y y - \sigma t))$  to check the flow instability by the sign of  $\sigma$ , as was done in section 2.1. The second is called the energy method since the rate change of kinetic energy is checked to distinguish the state of flow. A disturbance source is given at initial time and checked later. The flow is considered stable if the rate change of kinetic energy of the perturbation is negative, and called unstable if it is positive. The criteria is

$$\frac{dK'}{dt} < 0 \quad \text{stable} \quad (113)$$

$$\frac{dK'}{dt} = 0 \quad \text{neutral} \quad (114)$$

$$\frac{dK'}{dt} > 0 \quad \text{unstable} \quad (115)$$

where  $K'$  is defined in Eq. 28. The kinetic energy will be checked after 2000 time-steps in a computer program, while the flow is approaching a numerically steady-state.

Figs. 4a-4c are directly drawn from a digital computer and show the variation of perturbation kinetic energy as the time integration proceeded. Fig. 4a shows the variation of  $K'$  which is a typical type for unstable flow, Fig. 4b shows a neutral case, and Fig. 4c shows a stable case. It can be seen in those figures that the dimensionless time of approximately 20 is required for the calculation settling.

#### 2.2.4 Procedures of integration

Equations 85 and 88-94 are the governing equations for a nonlinear model which can be integrated numerically with the following procedures:

Step 1. From initial conditions (Eqs. 95-98, 105-112), the vorticity  $\eta$  can be determined numerically by Eq. 94.

Step 2. Find the stream function  $\psi$  by solving Poisson's equation (Eq. 93) with the latest vorticity from step 1. The boundary conditions for  $\psi$  are shown in Eq. 112.

Step 3.  $V_m$  and  $V_z$  are determined from Eqs. 91 and 92.

Step 4. Equations 85 and 88 are integrated numerically with the same numerical scheme used in step 1 to determine the temperature field  $T$  and the velocity component in the  $n$ -direction. The boundary conditions for  $T$  and  $V_n$  are shown in Eqs. 96.

Step 5. The vorticity function for the new time-step are found by solving the vorticity equation given in step 1. The variables  $V_m$ ,  $V_z$ , and  $T$  in the equation are all new values calculated from step 3 and step 4. Boundary conditions for vorticity during integration are shown in Eqs. 107 and 108.

A set of calculations, step 2-step 5, is repeated until a pre-specified time period has past.

By definition (Eq. 23), the Nusselt number must be independent of the vertical coordinate,  $z$ , under the steady-state condition. Hence, all time-integrations are continued until the vertical distribution of the Nusselt number becomes independent of  $z$  within an error of less than 5% for the purpose of finding heat and momentum flux in steady-state.

## 2.2.5 Numerical schemes

### 2.2.5.1 Transport equations

Three different transport equations in the nonlinear model need to be integrated numerically: vorticity equation (Eq. 94), energy transport equation (Eq. 88), and momentum equation (Eq. 85). These three equations may be summarized and integrated with the same numerical scheme. This is defined as:

$$\frac{\partial P}{\partial t} + V_m \frac{\partial P}{\partial m} + V_z \frac{\partial P}{\partial z} = C_1 \nabla^2 P + C_2 \frac{\partial Q}{\partial m} \quad (116)$$

where

$$P = \eta$$

$$Q = T$$

$$C_1 = 1/Re$$

$$C_2 = Ra/PrRe^2 \quad (117)$$

for vorticity transport equation; and

$$P = T$$

$$C_1 = 1/RePr$$

$$C_2 = 0 \quad (118)$$

for energy transport equation; and

$$P = V_n$$

$$C_1 = 1/Re$$

$$C_2 = 0 \quad (119)$$

for momentum transport equation.

Three different numerical schemes can be utilized to integrate the time-dependent transport equation (Eq. 116): Arakawa's finite difference scheme, Upstream finite difference scheme, and Time-splitting

finite difference scheme. The third is adopted more often in numerical calculation because of its accuracy.

Arakawas (1966) developed his finite difference scheme for the vorticity transport equation in such a manner that it conserves the mean vorticity, the mean kinetic energy, and the mean square vorticity in a closed domain. The same scheme can be applied to the other two transport equations. Accordingly, Eq. 116 can be put in the finite difference form as follows:

$$\begin{aligned}
 P_{j,k}^{\ell+1} = & P_{j,k}^{\ell-1} - \frac{\Delta t}{6h^2} [(\psi_{j,k-1}^{\ell} + \psi_{j+1,k-1}^{\ell} - \psi_{j,k-1}^{\ell} - \psi_{j+1,k+1}^{\ell}) \\
 & (P_{j+1,k}^{\ell} - P_{j,k}^{\ell}) + (\psi_{j-1,k-1}^{\ell} + \psi_{j,k-1}^{\ell} - \psi_{j-1,k+1}^{\ell} - \psi_{j,k+1}^{\ell}) \\
 & (P_{j,k}^{\ell} - P_{j-1,k}^{\ell}) + (\psi_{j+1,k}^{\ell} + \psi_{j+1,k+1}^{\ell} - \psi_{j-1,k}^{\ell} - \psi_{j-1,k+1}^{\ell}) \\
 & (P_{j,k+1}^{\ell} - P_{j,k}^{\ell}) + (\psi_{j+1,k-1}^{\ell} + \psi_{j+1,k}^{\ell} - \psi_{j-1,k-1}^{\ell} - \psi_{j-1,k}^{\ell}) \\
 & (P_{j,k}^{\ell} - P_{j,k-1}^{\ell}) + (\psi_{j+1,k}^{\ell} - \psi_{j,k+1}^{\ell}) (P_{j+1,k+1}^{\ell} - P_{j,k}^{\ell}) \\
 & + (\psi_{j,k-1}^{\ell} - \psi_{j-1,k}^{\ell}) (P_{j,k}^{\ell} - P_{j-1,k-1}^{\ell}) + (\psi_{j,k+1}^{\ell} \\
 & - \psi_{j-1,k}^{\ell}) (P_{j-1,k+1}^{\ell} - P_{j,k}^{\ell}) + (\psi_{j+1,k}^{\ell} - \psi_{j,k-1}^{\ell}) (P_{j,k}^{\ell} \\
 & - P_{j+1,k-1}^{\ell})] + \frac{2\Delta t}{h^2} C_1 (P_{j+1,k}^{\ell} + P_{j-1,k}^{\ell} + P_{j,k+1}^{\ell} + P_{j,k-1}^{\ell} \\
 & - 4P_{j,k}^{\ell}) + \frac{\Delta t}{h} C_2 (Q_{j+1,k}^{\ell} - Q_{j-1,k}^{\ell})
 \end{aligned}
 \tag{118}$$

where  $h = \Delta m = \Delta z$ ; and  $\psi_{j,k}^\ell$  is the stream function defined in Eqs. 91 and 92. A test program shows that Arakawa's scheme will blowup easily, and smaller time-step are necessary in order to overcome the numerical instability. Finally, this scheme was not employed due to the excess required computer time.

The upstream finite difference scheme gives the difference form of equation 116 as follows:

$$\begin{aligned}
 P_{j,k}^{\ell+1} = & P_{j,k}^\ell + \frac{\Delta t}{(\Delta m)^2} (P_{j+1,k}^\ell - 2P_{j,k}^\ell + P_{j-1,k}^\ell) C_1 \\
 & + \frac{\Delta t}{(\Delta z)^2} (P_{j,k+1}^\ell - 2P_{j,k}^\ell + P_{j,k-1}^\ell) C_1 + \frac{\Delta t}{2\Delta m} (Q_{j+1,k}^\ell \\
 & - Q_{j-1,k}^\ell) C_2 - \frac{\Delta t}{\Delta m} (V_m)_{j,k}^\ell [A_1 (P_{j,k}^\ell - P_{j-1,k}^\ell) \\
 & + A_2 (P_{j+1,k}^\ell - P_{j,k}^\ell)] - \frac{\Delta t}{\Delta z} (V_z)_{j,k}^\ell [A_3 (P_{j,k}^\ell \\
 & - P_{j,k-1}^\ell) + A_4 (P_{j,k+1}^\ell - P_{j,k}^\ell)] \quad (121)
 \end{aligned}$$

where

	$A_1 = 1, A_2 = 0$	$\text{for } V_m \geq 0$
	$A_1 = 0, A_2 = 1$	$\text{for } V_m < 0$
	$A_3 = 1, A_4 = 0$	$\text{for } V_z \geq 0$
	$A_3 = 0, A_4 = 1$	$\text{for } V_z < 0$

(122)

The difference form for the convection terms,  $V_m \frac{\partial P}{\partial m} + V_z \frac{\partial P}{\partial z}$ , depend on the signs of  $V_m$  and  $V_z$ . Backward differences are used if both  $V_m$  and  $V_z$  are positive; and forward differences are used if both are negative. If  $V_m$  and  $V_z$  have different signs, then convection terms are approximated according to the upstream difference; i.e. one is backward and another is forward depending on the signs of  $V_m$  and  $V_z$ .

A larger time step, one which is within the computational stability criterion, is desired in order to save computation time. Hence an accurate stability analysis for the upstream finite scheme is an important requirement. It is difficult to derive the exact solution of stability criterion by Von Neuman stability analysis if the difference equation is nonlinear. Additional assumptions have been made by numerous authors to analyze the numerical stability. Yamada (1971) suggested that

$$\Delta t \leq \frac{0.8}{\frac{|V_m|_{\max}}{\Delta m} + \frac{|V_z|_{\max}}{\Delta z} + \frac{2\delta}{\Delta m} + \frac{2\delta}{\Delta z}} \quad (123)$$

$\delta$  is the number of integration. Also the well-known Courant-Friedrichs-Levy requirements are:

$$\Delta t \leq \frac{\text{RePr}}{4\left(\frac{1}{(\Delta m)^2} + \frac{1}{(\Delta z)^2}\right)} \quad (124)$$

$$\Delta t \leq \frac{1}{\frac{|V_m|_{\max}}{\Delta m} + \frac{|V_z|_{\max}}{\Delta z}} \quad (125)$$

However, from practical experiences, it is suggested that

$$t \leq \frac{\text{Re}}{300\left(\frac{|V_m|_{\max}}{\Delta m} + \frac{|V_z|_{\max}}{\Delta z}\right)} \quad (126)$$

In the computer program,  $\Delta t$  was checked at each time step; and a new  $\Delta t$  was assigned, based on Eq. 126, if the new one is smaller than the old one. This procedure insures the computational stability of the scheme for the transport equations.

The time-splitting finite difference scheme was first derived by Crowley (1968, 1970) who followed Marchnk's (1964) original ideal. Crowley (1970), Chan (1970), and Derickson (1972) applied this scheme successfully to solve transport equations. They found that the truncation error caused by this scheme is smaller than by others. Accordingly, the finite difference form of equation 111 is:

$$\begin{aligned}
 P_{j,k}^{\ell+1/2} &= P_{j,k}^{\ell} - \frac{\Delta t}{2\Delta m} (V_m)_{j,k} (P_{j+1,k}^{\ell} - P_{j-1,k}^{\ell}) + \left[ \frac{1}{2} \left( \frac{\Delta t}{\Delta m} (V_m)_{j,k}^{\ell} \right)^2 \right. \\
 &+ \left. \frac{\Delta t}{(\Delta m)^2} C_1 \right] (P_{j+1,k}^{\ell} - 2P_{j,k}^{\ell} + P_{j-1,k}^{\ell}) + \frac{\Delta t}{2\Delta m} C_2 (Q_{j+1,k}^{\ell} \\
 &- Q_{j-1,k}^{\ell}) \quad (127)
 \end{aligned}$$

and

$$\begin{aligned}
 P_{j,k}^{\ell+1} &= P_{j,k}^{\ell+1/2} - \frac{\Delta t}{2\Delta z} (V_z)_{j,k}^{\ell+1/2} (P_{j,k+1}^{\ell+1/2} - P_{j,k-1}^{\ell+1/2}) \\
 &+ \left[ \frac{1}{2} \left( \frac{\Delta t}{\Delta z} (V_m)_{j,k}^{\ell+1/2} \right)^2 + \frac{\Delta t}{(\Delta z)^2} C_1 \right] (P_{j,k+1}^{\ell+1/2} \\
 &- 2P_{j,k}^{\ell+1/2} + P_{j,k-1}^{\ell+1/2}) \quad (128)
 \end{aligned}$$

The derivation of equations 127 and 128 are shown in Appendix 4. Crowley (1970) did the stability analysis for this scheme and gave a stability criteria; for complete details the reader should refer to his paper. Fortunately, the result of Eq. 126 is within the limitation of Crowley's criteria. For convenience, Eq. 126 is also used for a time-splitting scheme.

### 2.2.5.2 Poisson's equation

The stream function is obtained by solving the Poisson's equation with known vorticity values. There are many computer subprograms available to solve such an elliptic equation numerically with different theoretical background. Basically the S.O.R. (successive over relaxation) method, A.D.I. (alternation direction implicit) method, and F.F.T. (fast Fourier transformation) method are the most popular schemes. After comparing and testing several available computer subprograms, a most effective and economic one called "POISDP" was chosen. This subroutine was written by Mr. Roland Sweet on September 1971 for the NCAR (National Center for Atmospheric Research) computer center library. "POISDP" is based on a modified A.D.I. Method to solve Poisson's equation with Dirichlet boundary conditions in one direction and periodic boundary conditions in the other direction. The theoretical background of this subroutine is from a publication "On direct methods for solving Poisson's equation" by Busbee, Bolub, and Nielson (1970). A new algorithm is introduced in this paper called CORF (cyclic odd-even reduction and factorization) algorithm to solve the finite difference form of Poisson's equation. From Eq. 93, the finite difference approximation to Poisson's equation can be written as

$$\frac{2\psi_{j,k} - \psi_{j-1,k} - \psi_{j+1,k}}{(\Delta m)^2} + \frac{2\psi_{j,k} - \psi_{j,k-1} - \psi_{j,k+1}}{(\Delta z)^2} = -\eta_{j,k} \quad 1 \leq j \leq J, \quad 2 \leq k \leq K \quad (129)$$

with boundary conditions

$$\psi_{j,1} = g_0(m_j)$$

$$1 \leq j \leq J \quad (130)$$

$$\psi_{j,k+1} = g_1(m_j)$$

$$\psi_{0,k} = \psi_{J,k}$$

$$2 \leq k \leq K \quad (131)$$

$$\psi_{1,k} = \psi_{J+1,k}$$

The equations 129 to 130 form a linear system of equations of dimension  $J \times (N-1)$  for the unknown  $\psi_{j,k}$ . This system is solved by a modification of the Buneman variant of the CORF algorithm. The primary advantage of this algorithm is to avoid iteration procedure process. The difficulty of convergence has always existed in iteration methods. Hence, the implicit scheme used in "POISDP" can save a significant amount of computer time.

### 2.2.6 Computer programming

The program consists of one main program, "CHIEH", and six subprograms: "UPSTRE", "TIMESP", "POISDP", "QSF", "DET3", and "NONLIN". All data and constants necessary for the calculations are read in by "CHIEH." The purpose of subroutine "UPSTRE" is to integrate the transport equation (Eq. 116) numerically by the upstream finite difference scheme (Eq. 121 and 130) in order to determine the new values for the next time step. "TIMESP" has the same purpose as "UPSTRE" except that the time-splitting scheme (Eqs. 127 and 128) is adopted. "POISDP" was supported by the NCAR computer center library; the stream function is obtained by solving the Poisson's equation (Eq. 93 or Eq. 129) with known vorticity values. Subroutines "QSF" and "DET3" were copied from IBM Scientific subroutine Package (1970). "QSF" determines the integration of the equidistantly tabulated function by Simpson's rule, and "DET3" determines the differentiation of an equidistantly tabulated function. All subroutines mentioned above are called from subroutine "NONLIN". The Multi-purpose assigned to "NONLIN" included:

- A). Generate the functions or constants necessary for this program or other subroutines.
- B). Calculating the initial values of variables defined in Eqs. 95-98, 108 and 109. If the computation is a continuation of a previous run, then the values of variables are read from a magnetic tape.
- C). Calling subroutines "UPSTRE" or "TIMESP" to calculate new vorticities.
- D). Call "POISDP" to determine the stream function using the vorticities obtained from the last step. The value at upper or lower boundaries remain unchanged during integration.

- E). Obtain velocity components ( $V_m$  and  $V_z$ ) from the finite difference definition of stream function (Eqs. 91 and 92). Central differences are used to evaluate interior values, and forward or backward differences are used to evaluate boundary values.
- F). Obtain the maximum values of  $V_m$  and  $V_z$  in order to find the new size of time-step; this insures the computational stability for the next calculation. No size will be changed if the new one is larger than the old one.
- G). Employ equations 111 and 112 to compute new boundary values of vorticity along two rigid boundaries.
- H). Call "UPSTRE" of "TIMESP" to find the new temperature field.
- I). Call "UPSTRE" of "TIMESP" to determine the velocity component in the n-direction which was paralleled to the central line of the disturbances.
- J). Calculate the kinetic energy of perturbation, based on equation 28, at each 20th time steps.
- K). Terminate the program at the 2000th time-step if the purpose of running is to check the instability of flow. If this is not done, the program will keep going until the vertical distribution of the Nusselt number becomes independent of  $z$  for the purpose of finding heat and momentum flux.
- L). Record all final values of variables on a magnetic tape to be the initial values of the next run if it is necessary.

The flow chart for subroutine "NONLIN" is shown in Fig. 7. In general, the number of grid points taken are 17 in the vertical direction and 17, 33, or 65 in the horizontal, dependent on the magnitude of the Reynolds number.

All numerical experiments were run on the CDC 7600 digit computer installed in the National Center for Atmospheric Research.

### 2.2.7 Numerical results of nonlinear stability analysis

After investigating approximately one hundred cases, in order to survey the instability of flow, it was found that all results are independent of the grid size and the temperature difference set on the upper and lower boundaries. Usually, the number of grid point is 17 in the vertical direction ( $\Delta z = 0.0625$ ) and 65 in the m-direction for the instability analysis. The grid size in the m-direction,  $\Delta m$ , can be determined by the following equation:

$$\Delta m = (\text{Wave length}) / (MT - 1) \quad (132)$$

where  $MT$  is the chosen number of grid point in the m-direction. The nondimensional temperature is set at 3.53 on the upper boundary and 2.53 on the lower boundary.

The values of the Rayleigh number for neutral stability were determined to distinguish the flow state under varying conditions. It is difficult to determine the neutral Rayleigh number directly with a computer program. Hence the trial-and-error method is used to find two neighboring points with a different sign of rate change for  $K'$  (defined in Eq. 28). Then the exact neutral value with zero rate change of  $K'$  is calculated by linear extrapolation from two reference Rayleigh numbers. For example, the rate change of  $K'$  is  $-0.9157 \times 10^{-14}$  for  $Ra = 10600$ , and is  $0.5969 \times 10^{-14}$  for  $Ra = 10700$ ; then the zero rate change of  $K'$  is  $Ra = 10660$  for the case of  $Re = 160$  and  $\alpha = \pi/2$ . Table 5 shows the numerical results from a nonlinear model, a linear model, and Lipp's (1971) nonlinear model in different wave angles for  $Re = 160$  and  $Re = 320$ . The comparison of neutral Rayleigh numbers calculated from nonlinear and linear numerical models are also

shown in Table 5 for  $Re = 160$  and  $\alpha = \pi/2$ . The results of the two nonlinear models are extremely close, although the numerical schemes adopted are quite different. Also as Table 5 shows, the linear and nonlinear models gave very close results both for various wave lengths and wave lengths (except the longitudinal roll). This proves the assumption of linearization is valid for non-longitudinal roll. It takes almost 500 seconds of CDC 7600 computing time to get one point of a neutral curve for the nonlinear model as opposed to 0.3 seconds for the linear model. Hence the linear model is the most economical method to survey flow instability if the non-longitudinal roll is examined.

Finally, it was concluded that both linear and nonlinear models give almost identical results, except for pure longitudinal rolls ( $\alpha = 0$ ); and hence the previous summary shown in 1.3.2 is accepted.

### 2.3 Finite-amplitude Rolls at Steady-state

Laboratory studies by Chandra and others have shown that the amplified disturbances of unstable flow can approach the finite-amplitude rolls at steady-state. Thus, in this section, some characters of disturbance rolls are investigated. The numerical model is the same one discussed in 2.2; however, the time integration is extended until the vertical distribution of Nusselt number becomes independent of  $z$  to insure that the flow is in steady-state. Fig. 5 shows the variation of Nusselt numbers at  $z = 0.125$ ,  $0.5$ , and  $0.9375$  as time increases and they approach the same value after the flow is in steady-state.

### 2.3.1 Vertical profiles of mean velocity and temperature

Both mean velocity and temperature of heated plane Couette flow are linear distributed along the vertical direction, while the flow is in laminar. However, numerical experimentation has shown that the profiles of mean temperature and velocity have the shape of inclined sine curve as the flow becomes turbulent. The difference between the turbulent profile and the laminar profile is dependent on the magnitude of the Rayleigh number, i.e., the larger the Rayleigh number, the larger the difference. This difference is not sensitive to the change of wave length, but it is increased by enlarging the wave angle (maximum is  $\pi/2$ ) and decreasing the Reynolds number. Also it can easily be determined that all points, except those near or on the two boundaries, have a tendency to approach the same quantities of mean velocity and temperature as the central point. The percentage of achievement is sensitive and proportional to the increase of the Rayleigh number. Fig. 9 shows the typical variation of turbulent profiles of mean velocity and temperature where the Rayleigh number increases for  $Re = 160$ ,  $\alpha = 0$ , and the wave length is 4.

### 2.3.2 Heat and momentum flux

To compute the heat and momentum flux under varying conditions about 80 cases were run. In general, both  $Nu$  and  $Mo$  take a maximum value at a certain wave length and  $\alpha = 0$  (longitudinal rolls) for each value of Rayleigh number; and the flux increases with the Rayleigh number under certain conditions. Fig. 6 shows the Nusselt number as a function of the nondimensional horizontal wave length at  $Re = 160$  and  $\alpha = 0$ . It is easy to determine that both momentum and heat flux change with various horizontal wave lengths but within a limit. For convenience, however, only the wave length near the critical wave length (where the critical Rayleigh number occurred in the stability problem) for each Reynolds number was investigated. For example, 4.0 is taken for  $Re = 160$ , 6.0 for  $Re = 320$ , and 9.0 for  $Re = 500$  during the computation of flux.

Table 6 shows the heat and momentum flux at various wave angles when  $Re = 160$  and the wave length is 4. While there are some exceptions in Table 6, an obvious conclusion can be made: both heat and momentum flux increase with the Rayleigh number but decrease with an increasing wave angle. In other words, longitudinal rolls hold maximum heat and momentum flux.

According to Eq. 22, momentum flux should be independent of a vertical coordinate in steady-state. But from the numerical experimentation, the momentum flux does vary with respect to the vertical coordinate, although the Nusselt number shows the flow has already been in steady-state for some cases where the wave angle is not zero (non-longitudinal roll). Physically speaking, the disturbance is still unsettled with unbalanced momentum flux. In this situation the wave angle of the

disturbance roll becomes smaller in order to have the momentum flux balanced. This confirms Kuo's (1963) conclusion that the preferred mode of perturbation is a roll-type convection parallel to the main flow for plane Couette flow heated from below. Kuo also found that it has the same type of roll for the flow in dry convection with the wind shear in atmosphere. Thus, another conclusion can be drawn from our numerical results; that is, the transverse roll with balanced momentum flux can exist only at the smaller Reynolds number and Rayleigh number. This conclusion coincides exactly with the results of the laboratory experimentation reviewed in 1.3.1 (summary D).

Next the relationship between heat and momentum flux must be determined. Ingersoll (1966b) used a mixing length theory of Kraichnan (1962) to show that  $Mo$  and  $Nu$  should be related. Fortunately, present data fit the linear relation quite well as shown in Fig. 8, and the regression curve is

$$Mo = -q \times Nu = -1.165 Nu \quad \text{for } \alpha = 0 \quad (133)$$

which is a universal relation and is independent of the Reynolds number, the Rayleigh number, and the wave number. Where  $q$  is a constant decreasing as  $\alpha$  is increased,  $q = 0.93$  for  $\alpha = \pi/8$  and  $q = 0.6$  for  $\alpha = \pi/4$ .

Stability theory shows that shear has a stabilization effect. Similarly, it is obvious from Table 7,  $Nu$  decreases as the Reynolds number increases. Also the decreasing rate is small for the longitudinal roll, but is large for the transverse roll. In other words, the affection increases with wave angle. Thus it can be concluded that the upper bonds of heat transfer for heated plane Couette flow will be the heat transfer with the shear absent (Benard problem).

The relation between Rayleigh number and Nusselt number for  $Re = 160$  and  $\alpha = 0$  is shown in Fig. 10 on a logarithm scale. This relation may be expressed with accuracy by

$$Nu = 0.129 Ra^{0.323} \quad (134)$$

It is interesting to point out that the relation

$$Nu \sim Ra^{1/3} \quad (135)$$

has been predicted on the basis of dimensional reasoning for Benard convection at high Rayleigh numbers and has been verified both experimentally and numerically (see Herring (1963)). Ogura and Yagihashi (1969) also found the relation

$$Nu \sim Ra^{0.328} \quad (136)$$

while studying the parabolic flow between horizontal parallel plates heated from below. Figure 12 appears to show that a similar relation also exists in our problem and also in the range of a rather low Rayleigh number ( $Ra \geq 11000$ ).

## Chapter III

## UPPER BOUNDS ON HEAT AND MOMENTUM FLUX

A simple variational approach to the turbulent transfer problem will be applied to the analytical prediction of upper bounds on the vertical transport of heat and momentum flux in the heated plane Couette flow. Since the exact solutions to the Navier-Stokes equations are still beyond the current mathematical knowledge, it is reasonable to determine the upper bounds of some important physical quantities to describe the fluid field. This variational analysis is based on Malkus' (1954) power integral hypothesis. He states that for the turbulent convection problem the heat transport which actually occurs for the larger Rayleigh number is not only the solution of Boussinesq equations, but also that it exists in larger upper bound solutions which no longer satisfy the governing equations. The larger upper bound solution is restricted up a) continuity equation, b) boundary conditions, c) the requirements of homogeneity, and d) the power integral equations. Howard (1963) is the first one who applied the power integral method to predict the upper bound on heat flux in parallel plate convection under the additional hypothesis that the solution has a single horizontal wave number. He found

$$\text{Nu} \leq \left(\frac{\text{Ra}}{248}\right)^{3/8} \quad (137)$$

The same problem had also been solved by Halpern (1964) and Basse (1969). Halpern restricted his work to the infinite Prandtl number and the larger Rayleigh number but adopted the same single-wave-number assumption. His results indicate that

$$\text{Nu} < c \text{ Ra}^{1/3} \quad (138)$$

where  $c$  is a constant. Busse, however, claimed that Howard's single-wave-number assumption is true only for a limited range of the Rayleigh number. Instead he proposed a multi-wave-number assumption which

$$\text{Nu} \leq \left(\frac{\text{Ra}}{1035}\right)^{\frac{1}{2}} \quad (139)$$

In recent years the same variational technique with an additional single- or multi-wave-number assumption was widely applied to similar fluid dynamic problems. See Malkus (1968), Nickerson (1969, 1970), Busse (1969a, 1969b, 1970), Lindberg (1971). Recently, Nickerson (1973) developed a new variational technique to determine the upper bound on momentum flux in plane Couette flow without any simplifying assumptions concerning the dependence in horizontal wave number space. This method avoids the extreme mathematical difficulty which Busse (1968, 1969a, 1969b, 1970) used in his papers, and gives satisfactory results.

Nickerson found

$$- \text{Mo} - 1 \leq 0.63 \text{Re}^{2/3} \quad (140)$$

In this chapter, the upper bounds of heat and momentum flux in heated plane Couette flow will be determined by adopting Nickerson's new variational technique; then the results will be compared to previous works.

### 3.1 Power Integral Equations

The power integrals derived from the dimensionless statistically steady Boussinesq equations will be the initial step of the analysis.

The first power integral equation is the steady-state form of equation 26.

$$\frac{Ra}{PrRe} \langle v_z \theta \rangle + Re \langle \overline{v_x v_z} \beta \rangle = \langle |\nabla \times \tilde{v}|^2 \rangle \quad (141)$$

where

$$\beta = - \frac{d\bar{U}}{dz} \quad (142)$$

The second power integral equation is the steady-state form of equation 33.

$$\langle \overline{\theta v_z} \Gamma \rangle = \frac{1}{RePr} \langle |\nabla \theta|^2 \rangle \quad (143)$$

where

$$\Gamma = - \frac{dT}{dz} \quad (144)$$

The momentum and heat transfer can be determined from Eqs. 21 and 22:

$$M_t = - Mo = \beta + Re \langle \overline{v_x v_z} \rangle \quad (145)$$

and

$$Nu = \Gamma + RePr \langle \overline{\theta v_z} \rangle \quad (146)$$

By integrating equations (145) and (146) throughout the depth of the fluid, the following can be determined:

$$M_t = 1 + Re \langle \overline{v_x v_z} \rangle \quad (147)$$

and

$$Nu = 1 + RePr \langle \overline{\theta v_z} \rangle \quad (148)$$

Then equations (145) and (147) give

$$\beta = 1 + \text{Re} \left[ \langle v_x v_z \rangle - \overline{(v_x v_z)} \right] \quad (149)$$

and equations (146) and (148) gives

$$\Gamma = 1 + \text{RePr} \left[ \langle \theta v_z \rangle - \overline{(\theta v_z)} \right] \quad (150)$$

The dissipation term now can be expressed in terms of  $\langle v_x v_z \rangle$ .

Equations (141) and (149) give:

$$\begin{aligned} \langle |\nabla \times \tilde{v}|^2 \rangle &= \frac{\text{Ra}}{\text{PrRe}} \langle \theta v_z \rangle + \text{Re} \langle v_x v_z \rangle \\ &- \text{Re}^2 \langle (\langle v_x v_z \rangle - \overline{v_x v_z})^2 \rangle \end{aligned} \quad (151)$$

Similarly, equations (143) and (150) give:

$$\begin{aligned} \langle |\nabla \hat{\theta}|^2 \rangle &= \text{RePr} \langle \theta v_z \rangle \\ &- \text{Re}^2 \text{Pr}^2 \langle (\langle \theta v_z \rangle - \overline{\theta v_z})^2 \rangle \end{aligned} \quad (152)$$

Equations (151) and (152) show that both  $\langle v_x v_z \rangle$  and  $\langle \theta v_z \rangle$  are positive. Also, from (147) and (148),  $M_t$  and  $Nu$  are always positive.  $M_t$  represents the ratio of total stress to viscous stress; thus, it is the equivalent of a Nusselt number in parallel plate convection. Hence, it is then seen that the total stress in this problem is always greater than or equal to the viscous stress. Similarly, by definition of the Nusselt number, the actual heat flux is always greater than or equal to the pure heat conduction in this problem.

It is convenient to normalize the fluctuation temperature and velocity fields in the following manner:

$$\hat{\theta} = \langle v_x v_z \rangle^{1/2} \langle \theta v_z \rangle^{-1} \theta \quad (153)$$

$$\hat{v} = \langle v_x v_z \rangle^{-1/2} \tilde{v} \quad (154)$$

hence,

$$\langle \hat{v}_x \hat{v}_z \rangle = \langle \hat{\theta} \hat{v}_z \rangle = 1 \quad (155)$$

After normalization, equation (151) becomes

$$\langle |\nabla \times \hat{v}|^2 \rangle = \frac{Ra}{RePr} \frac{\langle \theta v_z \rangle}{\langle v_x v_z \rangle} + Re - Re^2 \langle (1 - \overline{\hat{v}_x \hat{v}_z})^2 \rangle \langle v_x v_z \rangle \quad (156)$$

or

$$\frac{\Phi}{Re} = \frac{Ra}{Re^2 Pr} \frac{\langle \theta v_z \rangle}{\langle v_x v_z \rangle} + 1 - Re \langle v_x v_z \rangle \Lambda \quad (157)$$

where

$$\Phi = \langle |\nabla \times \hat{v}|^2 \rangle \quad (158)$$

$$\Lambda = \langle (1 - \overline{\hat{v}_x \hat{v}_z})^2 \rangle \quad (159)$$

When equations (147) and (148) are substituted into (157),

$$\frac{\Phi}{Re} = \left( 1 + \frac{Ra}{Re^2 Pr^2} \frac{Nu-1}{M_t-1} \right) - (M_t-1) \Lambda \quad (160)$$

or

$$\frac{\Phi}{Re} = T - (M_t-1) \Lambda \quad (161)$$

$$\text{where } T = \left( 1 + \frac{Ra}{Re^2 Pr^2} \frac{Nu-1}{M_t-1} \right) \quad (162)$$

then

$$M_t - 1 = \frac{1}{\Lambda} \left[ T - \frac{\Phi}{\text{Re}} \right] \leq \frac{T}{\Lambda} \quad (163)$$

Similarly, the normalized form of equation (152) is

$$\frac{\langle \theta v_z \rangle^2}{\langle v_x v_z \rangle} \Psi = \text{RePr} \langle \theta v_z \rangle - \text{Re}^2 \text{Pr}^2 \langle \theta v_z \rangle^2 \Omega \quad (164)$$

where

$$\Psi = \langle |\nabla \hat{\theta}|^2 \rangle \quad (165)$$

$$\Omega = \langle (1 - \hat{\theta} \hat{v}_z)^2 \rangle \quad (166)$$

Substituting equations (147) and (148) into equation (164) gives

$$\text{Nu} - 1 = \left( \Omega + \frac{\Psi}{\text{RePr}^2 (M_t - 1)} \right)^{-1} \leq \frac{1}{\Omega} \quad (167)$$

Equations (163) and (167) show that a lower bound must be obtained on the integral quantities  $\Lambda$  and  $\Omega$  in order to seek the upper bounds on  $(M_t - 1)$  and  $(\text{Nu} - 1)$ .

### 3.2 Governing Inequalities

Some inequalities are important to determine upper bounds on heat and momentum flux. First, from Schwarz's inequality,

$$\begin{aligned}
 (\hat{v}_x)^2 &= \left( \int_{-1/2}^z \frac{d\hat{v}_x}{dz} dz \right)^2 \leq \int_{-1/2}^z \left( \frac{d\hat{v}_x}{dz} \right)^2 dz \int_{-1/2}^z dz \\
 &= \hat{z} \int_0^{\hat{z}} \left( \frac{d\hat{v}_x}{d\hat{z}} \right)^2 d\hat{z} = \hat{z} \int_0^1 (\hat{v}_x')^2 d\hat{z} \\
 &\leq \hat{z} \int_{\hat{z}}^1 (\hat{v}_x')^2 d\hat{z}
 \end{aligned} \tag{168}$$

where the prime denotes a derivative with respect to the vertical coordinate; and

$$\hat{z} = z + \frac{1}{2} \tag{169}$$

By taking the horizontal average on equation (168),

$$\overline{(\hat{v}_x)^2} \leq \hat{z} \int_0^1 \overline{(\hat{v}_x')^2} d\hat{z} = \hat{z} \langle (\hat{v}_x')^2 \rangle$$

or

$$\overline{(\hat{v}_x)^2} \leq \hat{z} \langle (\hat{v}_x')^2 \rangle \tag{170}$$

Similarly,

$$\overline{(\hat{\theta})^2} \leq \hat{z} \langle (\hat{\theta}')^2 \rangle \tag{171}$$

and

$$\overline{(\hat{v}_z)^2} \leq \hat{z} \int_0^{\hat{z}} \overline{(\hat{v}_z')^2} d\hat{z} \tag{172}$$

Equation (17a) shows that  $\overline{(\hat{v}'_z)^2}$  is zero on the rigid boundaries but, by definition, it has a nonzero vertical average. Hence,  $\lambda$  is defined as a distance from the lower boundary where  $\hat{v}'_z$  is less than its average value  $\langle \hat{v}'_z \rangle$ . Therefore,  $\hat{z} \leq \lambda$  gives

$$\overline{\hat{v}'_z} \leq \langle (\hat{v}'_z)^2 \rangle \quad (173)$$

and

$$\int_0^{\hat{z}} \overline{(\hat{v}'_z)^2} d\hat{z} \leq \int_0^{\hat{z}} \langle (\hat{v}'_z)^2 \rangle d\hat{z}$$

$$= \hat{z} \langle (\hat{v}'_z)^2 \rangle$$

or

$$\int_0^{\hat{z}} \overline{(\hat{v}'_z)^2} dz \leq \hat{z} \langle (\hat{v}'_z)^2 \rangle \quad (174)$$

Equation (172) and (174) give

$$\overline{(\hat{v}'_z)^2} \leq \hat{z}^2 \langle (\hat{v}'_z)^2 \rangle \quad (175)$$

Again from Schwarz's inequality, it can be found that

$$\overline{(\hat{v}'_x \hat{v}'_z)} \leq \overline{(\hat{v}'_x)^2}^{1/2} \overline{(\hat{v}'_z)^2}^{1/2} \quad (176)$$

by substituting equations (168) and (175);

$$\overline{(\hat{v}'_x \hat{v}'_z)} \leq \hat{z}^{3/2} \langle (\hat{v}'_x)^2 \rangle^{1/2} \langle (\hat{v}'_z)^2 \rangle^{1/2}$$

$$= \left( \frac{\hat{z}}{z_v} \right)^{3/2} \quad (177)$$

where

$$\begin{aligned} z_v &= \langle (\hat{v}'_x)^2 \rangle^{-1/3} \langle (\hat{v}'_z)^2 \rangle^{-1/3} \\ &= (M_t - 1)^{2/3} Re^{-2/3} \langle (v'_x)^2 \rangle^{-1/3} \langle (v'_z)^2 \rangle^{-1/3} \end{aligned} \quad (178)$$

Similarly

$$\overline{(\hat{\theta}'_z)} \leq \left(\frac{\hat{z}}{z_\theta}\right)^{3/2} \quad (179)$$

and

$$\begin{aligned} z_\theta &= \langle (\hat{\theta}') \rangle^{-1/3} \langle (\hat{v}'_z)^2 \rangle^{-1/3} \\ &= Re^{-2/3} Pr^{-2/3} (Nu-1)^{2/3} \langle (\theta')^2 \rangle^{-1/3} \langle (v'_z)^2 \rangle^{-1/3} \end{aligned} \quad (180)$$

At this point, the lower bounds on  $\Lambda$  and  $\Omega$  must be found. By definition,

$$\begin{aligned} \Lambda &= \int_0^1 (1 - \overline{\hat{v}'_x \hat{v}'_z})^2 d\hat{z} \geq 2 \int_0^\lambda (1 - (\frac{\hat{z}}{z_v})^{3/2})^2 d\hat{z} \\ &= 2\lambda \left[ 1 + \frac{1}{4} \left(\frac{\lambda}{z_v}\right)^3 - \frac{4}{5} \left(\frac{\lambda}{z_v}\right)^{3/2} \right] \end{aligned} \quad (181)$$

The function inside [ ] of equation (181) attains its minimum at

$$\frac{\lambda}{z_v} = \left(\frac{8}{5}\right)^{2/3}, \text{ and}$$

$$\Lambda \geq 2\lambda \left[ 1 + \frac{1}{4} \left(\frac{64}{25}\right) - \frac{4}{5} \left(\frac{8}{5}\right) \right] = \frac{10}{25} \lambda \quad (182)$$

However, if  $\lambda/z_v$  is restricted to be less than unit, then

$$\Lambda \geq 2\lambda \left[ 1 + \frac{1}{4} - \frac{4}{5} \right] = \frac{9}{10} \lambda \quad \text{for } \frac{\lambda}{z_v} \leq 1 \quad (183)$$

Similarly, we have

$$\Omega \geq \frac{10}{25} \lambda \quad \text{for} \quad \frac{\lambda}{z_\theta} > 1 \quad (184)$$

and

$$\Omega \geq \frac{9}{10} \lambda \quad \text{for} \quad \frac{\lambda}{z_\theta} \leq 1 \quad (185)$$

From Eqs. (145) through (148), one can find

$$\overline{\hat{v}_x \hat{v}_z} = \frac{\overline{v_x v_z}}{\langle v_x v_z \rangle} = \frac{M_t^{-\beta}}{M_t^{-1}} \quad (186)$$

and

$$\overline{\hat{\theta} \hat{v}_z} = \frac{\overline{\theta v_z}}{\langle \theta v_z \rangle} = \frac{Nu - \Gamma}{Nu - 1} \quad (187)$$

Then equations (177) and (186) give

$$\left(\frac{\hat{z}}{z_v}\right)^{3/2} \geq \frac{M_t^{-\beta}}{M_t^{-1}} \quad (188)$$

Also equations (179) and (187) give

$$\left(\frac{\hat{z}}{z_\theta}\right)^{3/2} \geq \frac{Nu - \Gamma}{Nu - 1} \quad (189)$$

From equation (145),

$$\langle \beta M_t \rangle = \langle \beta^2 \rangle + \text{Re} \langle \beta \overline{v_x v_z} \rangle \quad (190)$$

or

$$M_t = \langle \beta^2 \rangle + \text{Re} \langle \beta \overline{v_x v_z} \rangle \quad (191)$$

By substituting equations (148) and (191) into (141),

$$\begin{aligned} \frac{Ra(Nu-1)}{Re^2 Pr^2} + M_t - \langle \beta^2 \rangle &= \langle |\nabla \times \tilde{v}|^2 \rangle \\ &\geq \langle (v'_z)^2 + (v'_x)^2 \rangle \end{aligned} \quad (192)$$

then

$$\begin{aligned} \langle (v'_z)^2 \rangle &< \langle (v'_x)^2 \rangle \leq \langle (v'_x)^2 \rangle \left[ M_t + \frac{Ra(Nu-1)}{Re^2 Pr^2} \right. \\ &\quad \left. - \langle \beta^2 \rangle - \langle (v'_x)^2 \rangle \right] \end{aligned} \quad (193)$$

Therefore, it can be determined that the function on the right hand side of Eq. (193) attains its maximum at

$$\langle (v'_x)^2 \rangle = \frac{M_t - \langle \beta^2 \rangle + \frac{Ra}{Re^2 Pr^2} (Nu-1)}{2} \quad (194)$$

or

$$\begin{aligned} \langle (v'_x)^2 \rangle^{1/2} \langle (v'_z)^2 \rangle^{1/2} &\leq \frac{M_t - \langle \beta^2 \rangle + \frac{Ra}{Re^2 Pr^2} (Nu-1)}{2} \\ &\leq \frac{M_t}{2} \left( T - \frac{\langle \beta^2 \rangle}{M_t} \right) \end{aligned} \quad (195)$$

As for heat flux, it can be determined from equation (146) that

$$\langle \Gamma Nu \rangle = \langle \Gamma^2 \rangle + RePr \langle \Gamma \overline{\theta v'_z} \rangle \quad (196)$$

or

$$\text{Nu} = \langle \Gamma^2 \rangle + \text{RePr} \langle \Gamma \overline{\theta v_z} \rangle \quad (197)$$

By substituting equation (196) into (143),

$$\text{Nu} - \langle \Gamma^2 \rangle = \langle |\nabla \theta|^2 \rangle \geq \langle (\theta')^2 \rangle \quad (198)$$

or

$$\langle (\theta')^2 \rangle \leq \text{Nu} - \langle \Gamma^2 \rangle \quad (199)$$

Then (192) and (196) give

$$\begin{aligned} \langle (\theta')^2 \rangle \langle (v'_z)^2 \rangle &\leq (\text{Nu} - \langle \Gamma^2 \rangle) (M_t \\ &+ \frac{\text{Ra}(\text{Nu}-1)}{\text{Re}^2 \text{Pr}^2} - \langle \beta^2 \rangle - \langle (v'_x)^2 \rangle) \\ &\leq (\text{Nu} - \langle \Gamma^2 \rangle) (M_t + \frac{\text{Ra}(\text{Nu}-1)}{\text{Re}^2 \text{Pr}^2}) \end{aligned} \quad (200)$$

### 3.3 Bounding Procedure

#### 3.3.1 Upper bound on momentum flux

Before starting derivation, the definition of critical boundary layer depth,  $\lambda$ , discussed in 3.2 should be reviewed. Since a-prior knowledge of whether  $\lambda$  is greater than or less than  $z_v$  is not known, the two cases will be considered separately. First the case,  $\lambda < z_v$  will be investigated. Equation (188) shows the following:

$$\int_0^\lambda \left(\frac{\hat{z}}{z_v}\right)^{3/2} d\hat{z} \geq \int_0^\lambda \left(\frac{M_t - \beta}{M_t - 1}\right) d\hat{z} \quad (201)$$

or

$$\lambda^{5/2} \geq z_v^{3/2} \frac{5}{2} \frac{M_t^\lambda - \int_0^\lambda \beta d\hat{z}}{M_t - 1} \quad (202)$$

Then from equations (178) and (195), equation (202) becomes

$$\lambda^{3/2} \geq \frac{5(M_t - \frac{1}{\lambda} \int_0^\lambda \beta d\hat{z})}{\text{Re}M_t \left( T - \frac{\langle \beta^2 \rangle}{M_t} \right)} \quad (203)$$

Since

$$\begin{aligned} \int_0^\lambda \beta d\hat{z} &\leq \left( \int_0^\lambda \beta^2 d\hat{z} \right)^{1/2} \left( \int_0^\lambda d\hat{z} \right)^{1/2} \\ &\leq \lambda^{1/2} \left( \int_0^\lambda \beta^2 d\hat{z} \right)^{1/2} \end{aligned} \quad (204)$$

Substitute (204) into (203)

$$\lambda^{3/2} \geq \frac{5(1 - \frac{1}{\sqrt{\lambda M_t}} (\int_0^\lambda \beta^2 dz)^{1/2})}{\text{Re}[T - \frac{\langle \beta^2 \rangle}{M_t}]}$$

$$\geq \frac{5(1 - \frac{1}{\sqrt{2\lambda M_t}} \langle \beta^2 \rangle^{1/2})}{\text{Re}[T - \frac{\langle \beta^2 \rangle}{M_t}]} \quad (205)$$

In order to complete the investigation of the case  $\lambda < z_v$ , two special cases must be considered: IA and IB, corresponding to  $\lambda M_t \geq 1$  and  $\lambda M_t < 1$ . For the first, the right hand side of equation (205) can be written as

$$F(a,b) = \frac{5}{\text{Re}} \frac{(1-ab)}{(T-a^2)} \quad (206)$$

where  $a^2 = \frac{\langle \beta^2 \rangle}{M_t}$  (207)

$$b^2 = \frac{1}{2M_t \lambda} \quad (208)$$

Equation (200) attains its minimum at

$$b = \frac{T + a^2}{2a}$$

and

$$F_{\min} = \frac{5}{\text{Re}} \frac{1}{T+a^2} \quad (209)$$

It can be shown from equation (192) that

$$a^2 \leq T$$

or

$$F_{\min} = \frac{5}{\text{Re}} \frac{1}{T+a} \geq \frac{5}{2\text{Re}} \frac{1}{T} \quad (210)$$

Equations (204) and (210) give

$$\lambda^{3/2} \geq \frac{5}{2T\text{Re}} \quad (211)$$

or

$$\lambda \geq \left(\frac{5}{2}\right)^{2/3} T^{-2/3} \text{Re}^{-2/3} \quad (212)$$

Substitute (212) into 183, then

$$\Lambda \geq \frac{9}{10} \frac{5^{2/3}}{2^{2/3}} T^{-2/3} \text{Re}^{-2/3} \quad (213)$$

Equations (163) and (213) give

$$\begin{aligned} M_t - 1 &\leq \frac{10}{9} \frac{2^{2/3}}{5^{2/3}} T^{5/3} \text{Re}^{2/3} \\ &= \frac{5^{1/3}}{9} 2^{5/3} \left(1 + \frac{\text{Ra}}{\text{Re}^2 \text{Pr}^2} \frac{\text{Nu}-1}{M_t-1}\right)^{5/3} \text{Re}^{2/3} \end{aligned} \quad (214)$$

In the second case with  $\lambda M_t < 1$  and  $\lambda < z_v$ , equation (205) can be rewritten as follows:

$$1 \leq \frac{\text{Re}\lambda^{3/2}}{5} \left( T - \frac{\langle \beta^2 \rangle}{M_t} \right) + \frac{1}{\lambda M_t} \int_0^\lambda \beta d\hat{z}$$

$$\leq \frac{\text{Re}}{5} \lambda^{3/2} T + \frac{1}{\sqrt{\lambda M_t}} \left( \int_0^\lambda \beta^2 d\hat{z} \right)^{1/2} \quad (215)$$

$$M_t \leq \frac{E}{5} (\lambda M_t)^{3/2} + G$$

$$\leq \frac{E}{5} + G \quad (216)$$

where

$$E = \frac{\text{Re}}{M_t^{1/2}} T \quad (217)$$

$$G = \left( \frac{1}{\lambda} \int_0^\lambda \beta^2 d\hat{z} \right)^{1/2} \quad (218)$$

Now if  $G \leq E$ , (216) gives

$$M_t \leq \frac{6}{5} E \quad (219)$$

or

$$M_t \leq \frac{6}{5} T M_t^{-1/2} \text{Re} \quad (220)$$

and

$$M_t - 1 \leq M_t \leq \left( \frac{6}{5} \right)^{2/3} T^{2/3} \text{Re}^{2/3} \quad (221)$$

If on the other hand,  $E < G$ , the following inequality results:

$$\lambda^{1/2} < \frac{M_t^{1/2}}{\text{Re}T} \left( \int_0^\lambda \beta^2 d\hat{z} \right)^{1/2} \quad (222)$$

However, from (145), the following can be determined

$$\int_0^\lambda \beta^2 d\hat{z} \leq \int_0^\lambda M_t^2 d\hat{z} = \lambda M_t^2 \quad (223)$$

or

$$\left( \int_0^\lambda \beta^2 d\hat{z} \right)^{1/2} \leq \lambda^{1/2} M_t \quad (224)$$

(222) and (224) give

$$\lambda^{1/2} < \frac{M_t^{3/2}}{\text{Re}T} \lambda^{1/2} \quad (225)$$

or

$$M_t > \text{Re}^{2/3} T^{2/3} \quad (226)$$

It can be shown, that equation (226) constrains the assumption that  $\lambda < z_v$ . Hence, the case for  $M_t \lambda < 1$  and  $E < G$  need not be considered.

Now the case  $\lambda \geq z_v$  must be determined. From equations (145), (147), and (159), the following can be derived:

$$\begin{aligned} \Lambda &= \int_0^1 \left( 1 - \overline{\hat{v}_x \hat{v}_z} \right)^2 d\hat{z} = \left\langle \left( 1 - \frac{\overline{v_x v_z}}{\langle v_x v_z \rangle} \right)^2 \right\rangle \\ &= \left\langle \left( 1 - \frac{M_t - \beta}{M_t - 1} \right)^2 \right\rangle = \frac{\langle \beta^2 \rangle - 1}{(M_t - 1)^2} \end{aligned} \quad (227)$$

Then by substituting equations (178) and (227) into (182),

$$\frac{\langle \beta^2 \rangle - 1}{(M_t - 1)^2} \geq \frac{18}{25} \frac{(M_t - 1)^{2/3}}{\text{Re}^{2/3} \langle (v'_x)^2 \rangle^{1/3} \langle (v'_z)^2 \rangle^{1/3}} \quad (228)$$

Equations (195) and (228) give

$$\frac{\langle \beta^2 \rangle - 1}{(M_t - 1)^{8/3}} \geq \frac{18}{25} \frac{2^{2/3}}{\text{Re}^{2/3}} (M_t - \langle \beta^2 \rangle) + \frac{\text{Ra}}{\text{Re}^2 \text{Pr}^2} (\text{Nu} - 1)^{2/3} \quad (229)$$

or

$$(M_t - 1)^{8/3} \leq \frac{25}{18 \cdot 2^{2/3}} \text{Re}^{2/3} (\langle \beta^2 \rangle - 1) \\ (M_t - \langle \beta^2 \rangle) + \frac{\text{Ra}}{\text{Re}^2 \text{Pr}^2} (\text{Nu} - 1)^{2/3} \quad (230)$$

It is easy to determine that the right hand side of equation (230) attains its maximum at

$$\langle \beta^2 \rangle = \frac{3M_t + \frac{3\text{Ra}}{\text{Re}^2 \text{Pr}^2} (\text{Nu} - 1) + 2}{5} \quad (231)$$

and equation (230) becomes

$$(M_t - 1)^{8/3} \leq \frac{5^{1/3}}{6} (M_t - 1 + \frac{\text{Ra}}{\text{Re}^2 \text{Pr}^2} (\text{Nu} - 1))^{5/3} \text{Re}^{2/3} \\ = \frac{5^{1/3}}{6} (M_t - 1)^{5/3} T^{5/3} \text{Re}^{2/3} \quad (232)$$

or

$$M_t - 1 \leq \frac{5^{1/3}}{6} T^{5/3} \text{Re}^{2/3} \quad (233)$$

## 3.3.2 Upper bound on heat flux

The procedures for determining the upper bounds on heat flux are similar to those in 3.3.1. Again the case for  $\lambda < z_\theta$  must be found. From equation (189), the following is obtained.

$$\int_0^\lambda \left(\frac{\hat{z}}{z_\theta}\right)^{3/2} d\hat{z} \geq \int_0^\lambda \frac{\text{Nu} - \Gamma}{\text{Nu} - 1} d\hat{z} \quad (234)$$

or

$$\lambda^{3/2} \geq \frac{5}{2} z_\theta^{3/2} \frac{\text{Nu} - \frac{1}{\lambda} \int_0^\lambda \Gamma d\hat{z}}{\text{Nu} - 1} \quad (235)$$

(180) and (235) give

$$\lambda^{3/2} \geq \frac{5}{2} \frac{\text{Nu} - \frac{1}{\lambda} \int_0^\lambda \Gamma d\hat{z}}{\text{RePr} \langle \theta' \rangle^{2\frac{1}{2}} \langle (v'_z)^2 \rangle^{\frac{1}{2}}} \quad (236)$$

Substitute (200) into (236) gives

$$\lambda^{3/2} \geq \frac{5}{2} \frac{\text{Nu}^{\frac{1}{2}} - \frac{1}{\lambda \text{Nu}^{\frac{1}{2}}} \int_0^\lambda \Gamma d\hat{z}}{(M_t \text{Re}^2 \text{Pr}^2 + \text{Ra}(\text{Nu} - 1))^{\frac{1}{2}} \left(1 - \frac{\langle \Gamma^2 \rangle}{\text{Nu}}\right)^{\frac{1}{2}}} \quad (237)$$

Since

$$\begin{aligned} \int_0^\lambda \Gamma d\hat{z} &\leq \left(\int_0^\lambda \Gamma^2 d\hat{z}\right)^{\frac{1}{2}} \left(\int_0^\lambda d\hat{z}\right)^{\frac{1}{2}} \\ &\leq \lambda^{\frac{1}{2}} \left(\int_0^\lambda \Gamma^2 d\hat{z}\right)^{\frac{1}{2}} \end{aligned} \quad (238)$$

The substitution of (238) into (237), produces the following results:

$$\lambda^{3/2} \geq \frac{5}{2} \frac{\text{Nu}^{1/2} - \frac{1}{\sqrt{\lambda \text{Nu}}} \left( \int_0^\lambda \Gamma^2 dz \right)^{1/2}}{(M_t \text{Re}^2 \text{Pr}^2 + \text{Ra}(\text{Nu}-1))^{1/2} \left(1 - \frac{\langle \Gamma^2 \rangle}{\text{Nu}}\right)^{1/2}} \quad (239)$$

First the case with  $\lambda \text{Nu} \geq 1$  is investigated. Accordingly (239) can be rewritten as

$$\lambda^{3/2} \geq \frac{5}{2} \frac{\text{Nu}^{-1/2} - \frac{1}{\sqrt{2}} \langle \Gamma^2 \rangle^{1/2}}{(M_t \text{Re}^2 \text{Pr}^2 + \text{Ra}(\text{Nu}-1))^{1/2} \left(1 - \frac{\langle \Gamma^2 \rangle}{\text{Nu}}\right)^{1/2}} \quad (240)$$

It is easy to determine that the function on the right hand side of equation (240) attains its minimum at  $\langle \Gamma^2 \rangle = \frac{\text{Nu}}{2}$  (241)

and equation (240) becomes

$$\lambda^{3/2} \geq \frac{5\text{Nu}^{1/2}}{2\sqrt{2}} (M_t \text{Re}^2 \text{Pr}^2 + \text{Ra}(\text{Nu}-1))^{1/2} \quad (242)$$

or

$$\lambda \geq \frac{5^{2/3}}{2} \text{Nu}^{1/3} (M_t \text{Re}^2 \text{Pr}^2 + \text{Ra}(\text{Nu}-1))^{-1/3} \quad (243)$$

(185) and (243) give

$$\begin{aligned} \Omega &\geq \frac{9}{10} \frac{5^{2/3}}{2} \text{Nu}^{1/3} (M_t \text{Re}^2 \text{Pr}^2 + \text{Ra}(\text{Nu}-1))^{-1/3} \\ &\geq \frac{9}{10} \frac{5^{2/3}}{2} (\text{Nu}-1)^{1/3} (M_t \text{Re}^2 \text{Pr}^2 + \text{Ra}(\text{Nu}-1))^{-1/3} \end{aligned} \quad (244)$$

Substitute (244) into (167); then

$$Nu - 1 \leq \frac{20}{9 \times 5^{2/3}} \left( \frac{M_t Re^2 Pr^2}{Nu-1} + Ra \right)^{1/3} \quad (245)$$

For the case,  $\lambda Nu \leq 1$ , equation (239) may be written as the following:

$$\begin{aligned} Nu &\leq \frac{2\lambda^{3/2}}{5} (M_t Re^2 Pr^2 + Ra (Nu-1))^{1/2} (Nu - \langle \Gamma^2 \rangle)^{1/2} \\ &\quad + \frac{1}{\sqrt{\lambda}} \left( \int_0^\lambda \Gamma^2 d\hat{z} \right)^{1/2} \\ &\leq \frac{2}{5} (\lambda Nu)^{3/2} E + G \leq \frac{2E}{5} + G \end{aligned} \quad (246)$$

where

$$E = [Ra (Nu-1) + M_t Re^2 Pr^2]^{1/2} \frac{1}{Nu} \quad (247)$$

$$G = \frac{1}{\sqrt{\lambda}} \left( \int_0^\lambda \Gamma^2 d\hat{z} \right)^{1/2} \quad (248)$$

In the case where  $G \leq E$ , equation (246) becomes

$$Nu \leq \frac{7}{5} E \leq \frac{7}{5} [M_t Re^2 Pr^2 + Ra (Nu-1)]^{1/2} \frac{1}{Nu} \quad (249)$$

or

$$(Nu-1)^2 \leq Nu^2 \leq \frac{7}{5} \left[ \frac{M_t}{Nu-1} Re^2 Pr^2 + Ra \right]^{1/2} (Nu-1)^{1/2} \quad (250)$$

Then the final form is

$$(Nu-1) \leq \left( \frac{7}{5} \right)^{2/3} \left[ \frac{M_t}{Nu-1} Re^2 Pr^2 + Ra \right]^{1/3} \quad (251)$$

In the case where  $G > E$ , by definition

$$\frac{1}{\sqrt{\lambda}} \left( \int_0^\lambda \Gamma^2 d\hat{z} \right)^{\frac{1}{2}} > [Ra(Nu-1) + M_t Re^2 Pr^2]^{\frac{1}{2}} \frac{1}{Nu} \quad (252)$$

or

$$\lambda^{\frac{1}{2}} < \frac{Nu(Nu-1)^{-\frac{1}{2}}}{\left( Ra + \frac{M_t}{Nu-1} Re^2 Pr^2 \right)^{\frac{1}{2}}} \left( \int_0^\lambda \Gamma^2 d\hat{z} \right)^{\frac{1}{2}} \quad (253)$$

The equation (146) gives

$$\left( \int_0^\lambda Nu^2 d\hat{z} \right)^{\frac{1}{2}} \geq \left( \int_0^\lambda \Gamma^2 d\hat{z} \right)^{\frac{1}{2}} \quad (254)$$

or

$$\lambda^{\frac{1}{2}} Nu \geq \left( \int_0^\lambda \Gamma^2 d\hat{z} \right)^{\frac{1}{2}} \quad (255)$$

Equations (253) and (255) give

$$\frac{Nu^2}{(Nu-1)^2} > \left( Ra + \frac{M_t}{Nu-1} Re^2 Pr^2 \right)^{\frac{1}{2}} \quad (256)$$

Equation (256) constrains the assumption that  $\lambda < z_\theta$  in the same way as equation (226). Hence the case for  $Nu\lambda < 1$  and  $E < G$  need not be considered.

The final stage of this investigation is to determine the upper bound for the case  $\lambda \geq z_\theta$ . From equations (146), (148) and (166),

$$\begin{aligned}
 \Omega &= \int_0^1 (1 - \overline{\theta \hat{v}_z})^2 dz \\
 &= \langle (1 - \frac{\overline{\theta v_z}}{\langle \theta \rangle})^2 \rangle \\
 &= \langle (1 - \frac{Nu - \Gamma}{Nu - 1})^2 \rangle \\
 &= \frac{\langle \Gamma^2 \rangle - 1}{(Nu - 1)^2}
 \end{aligned} \tag{257}$$

Then by substituting (180) and (257) into (184)

$$\begin{aligned}
 \frac{\langle \Gamma^2 \rangle - 1}{(Nu - 1)^2} &\geq \frac{18}{25} \lambda \geq \frac{18}{25} z_\theta \\
 &\geq \frac{18}{25} \frac{(Nu - 1)^{2/3}}{Re^{2/3} Pr^{2/3} \langle (\theta')^2 \rangle^{1/3} \langle (v'_z)^2 \rangle^{1/3}}
 \end{aligned} \tag{258}$$

(200) and (258) give

$$\begin{aligned}
 (Nu - 1)^{8/3} &\leq \frac{25}{18} (\langle \Gamma^2 \rangle - 1) (M_t Re^2 Pr^2 + Ra (Nu - 1))^{1/3} \\
 &\quad \cdot (Nu - \langle \Gamma^2 \rangle)^{1/3}
 \end{aligned} \tag{259}$$

It can easily be determined that the right-hand side of equation (259)

$$\text{attains its maximum at } \langle \Gamma^2 \rangle = \frac{3Nu + 1}{4} \tag{260}$$

and equation (259) becomes

$$(Nu - 1)^{8/3} \leq \frac{25}{18} \frac{3}{2^{8/3}} (Nu - 1)^{4/3} (M_t Re^2 Pr^2 + Ra (Nu - 1))^{1/3} \tag{261}$$

or

$$(\text{Nu}-1) \leq \frac{25}{6 \cdot 2^{8/3}} \left( \frac{M_t \text{Re}^2 \text{Pr}^2}{\text{Nu}-1} + \text{Ra} \right)^{1/3} \quad (262)$$

### 3.3.3 Absolute upper bounds

The upper bounds on heat and momentum flux for different cases have been shown in equations (214), (221), (233), (244), (251), and (262). Therefore it is easy to determine that (214) and (251) are the governing inequalities for finding absolute upper bounds on heat and momentum flux in the case where the Reynolds number is relatively small (say,  $Re \leq 100$ ). On the other hand, (221) and (251) are the chosen inequalities for the larger Reynolds number. These implicit equations (221) and (251) can be solved numerically as shown in Figures (11A) through (11D).

Nickerson (1970) derived a set of inequalities to express the upper bounds on heat and momentum flux for the same problem. However, during the derivation, an additional "single horizontal wave number" assumption was made as Howard (1963) suggested. This assumption is a valid first approximation for a range of Rayleigh numbers; see Busse (1968). Howard assumed that the extreme was satisfied by a single separable eigenvalue or wave number; i.e.,

$$v_z = W(z) \exp [i(k_x x + k_y y)] \quad (263)$$

$$\theta = \Theta(z) \exp [i(k_x x + k_y y)] \quad (264)$$

Based on equations (263) and (264), Nickerson found:

$$M_t - 1 \leq \frac{1}{36} \Phi^{3/4} (3 + 8 \Phi / Re) \quad (265)$$

$$Nu - 1 \leq \frac{5}{16} [\Phi^{-3/8} \Psi^{-3/8} + \frac{45\Psi}{Pr^2 \Phi^{3/4} (12Re + 32\Phi)}]^{-1} \quad (266)$$

where

$$\phi = \left[ \frac{30}{Pr^2 (3Re + 8\phi)} \right]^{8/3} \left[ \frac{135}{121(7\phi - 3Re)} \right]^{11/3} \quad (267)$$

$$\psi = \frac{135Ra}{121(7\phi - 3Re)} \quad (268)$$

The solution of equations (265) and (266) are shown in Figures (12A) ~ (12C). The patterns resulting from these two methods are quite similar; however, the quantity of previous results were smaller (about one half) than the recent one. Since the experimental data are considerably limited now, whether the equations (265) and (266) are also good for the larger Rayleigh number cannot be determined until more data becomes available. At the present time both methods satisfy the numerical experimental data shown in Tables (6) and (7).

Three special cases can be derived from equations (214), (221) and (251). If the Reynolds number is set at zero, then the upper bound on heat flux for turbulent convection within two parallel plates can be found (from equation (251)) as follows:

$$Nu - 1 \leq 1.251 Ra^{1/3} \quad (269)$$

Since a great quantity of laboratory experimental data are available, the details of equation (269) will be discussed in 3.4.

The upper bound on momentum flux for plane Couette flow (no convection) can be determined by setting  $Ra = 0$  in equation (221).

$$M_t - 1 \leq 1.129 Re^{2/3} \quad (270)$$

According to Nickerson (1973), the coefficient 1.129 can be cut down to 0.63 (see Equation (140)) if the symmetrical property of disturbance in the vertical direction are used during analysis. Nickerson (1973) claimed that the appearance of a two-thirds power law for turbulent plane Couette flow should not be surprised since previous analogies show that the Rayleigh number in the convection problem corresponds to the square of the Reynolds number in the plane Couette flow problem. Hence, a Nusselt number proportional to the one-third power of the Rayleigh number might be expected to correspond to a momentum number proportional to the two-thirds power of the Reynolds number.

The third case relates to the larger Reynolds and Rayleigh numbers ( $Re \geq 10Ra \geq 10^4$ ) which might be applied to the atmosphere in the real world. From Figures (11A) through (11D), it can be determined that both the  $(Nu-1)$  and  $(M_t-1)$  are independent of the Rayleigh number and proportional to the two-thirds power of the Reynolds number for larger  $Re$  and  $Ra \leq 0.1 Re$ . This gives

$$M_t - 1 \leq 1.02 Re^{2/3} \quad (271)$$

$$Nu - 1 \leq 1.13 Re^{2/3} \quad (272)$$

### 3.4 The Upper Bound on Heat Flux in Turbulence Convection

The study of turbulent thermal convection has been concerned with the transport of heat through fluid. In these studies the heat transfer can usually be expressed in the form of the following power law:

$$Nu = c Ra^p Pr^q = e Ra^p \quad (273)$$

The experimental values of the constants  $c$ ,  $p$ , and  $q$  in equation (273), as reported by various investigators, were summarized by Lindberg (1970); the details are shown in Table 8. Which indicates that the effect of the Prandtl number is small, and also the value of  $p$  is close to  $1/3$  for all investigations. These significant conclusions can also be found in our upper bound equation (Equation 269). The "one-third-power law" in equation (269) plays an important roll in the upper-bound analysis since it follows the experimental results. If an upper-bound equation does not follow the "one-third-power-law," it can easily be ascertained that the following two cases will occur. Where  $p$  is smaller than  $1/3$ , the predicted upper bound will not cover the actual heat flux if the Rayleigh number is very high. On the other hand, the predicted value is too high to be the effective upper bound for the high Rayleigh number if  $q$  is larger than  $1/3$ . For example, results derived by Busse (1969) and Howard (1963) show

$$Nu - 1 \leq \frac{1}{\sqrt{1035}} Ra^{1/2} \quad (139)$$

$$Nu - 1 \leq \frac{1}{(248)^{3/8}} Ra^{3/8} \quad (137)$$

Thus it can easily be determined that the predicted values from equation (136) and (138) are much larger than the value from equation (269) for

$Ra > 10^{11}$ ; even though the coefficients in (136) and (138) are much smaller than in (269). Note, the heat flux for the larger Rayleigh number ( $Ra > 10^{10}$ ) is the preferable case to be predicted since it actually occurs in the atmosphere, but it is almost impossible to do the experimentation in the laboratory.

Therefore, equation (269) is favorable because a) no additional assumption is necessary; and b) it follows the "one-third-power law."

## Chapter IV

## CONCLUSIONS

In this paper an effort has been made to understand the mechanism of plane Couette flow with a negative temperature gradient. Velocity profile, temperature profile, momentum flux, and heat flux were investigated. For the stable flow, both velocity and temperature profiles keep linear distribution; and the momentum and the heat flux of the flow are unity. The instability of fluid under various conditions was first examined to distinguish the state of the flow by utilizing the linear and nonlinear numerical models. The results confirm that constant shear has a stabilizing effect on the disturbances. However, the critical Rayleigh number for longitudinal roll always remains constant (1707.762) no matter how large a shear is present. Also it was shown that the neutral Rayleigh numbers, found from linear and nonlinear models, are almost identical for non-longitudinal rolls, but quite different for longitudinal rolls.

Then a nonlinear numerical model was generated to predict and investigate the flux and the profiles for turbulent flow within a certain range of Reynolds numbers ( $Re \leq 500$ ) and Rayleigh numbers ( $Ra \leq 500,000$ ). The variation on vertical profiles of mean velocity and temperature was discussed. Also the heat and momentum flux under various conditions were calculated.

Since all numerical studies for turbulent flow are for relatively small Reynolds numbers and large Rayleigh numbers, the convection characteristic dominates the flow motion. Thus the following

results are found: a) Heat flux and momentum flux are linearly correlated; b) Both heat and momentum flux increase with the Rayleigh number, but decrease with an increasing wave angle; c) Heat flux increases as the Reynolds number decreases; d) Heat flux approximately follows the "one-thirds power law" to the Rayleigh number and e) Heat flux attains its maximum at  $\alpha = 0$  (longitudinal roll). The results also show the momentum flux cannot balance for non-longitudinal roll if the Rayleigh number is large; hence, the perturbation with a larger wave angle ( $\alpha \neq 0$ ) can exist only at small Rayleigh numbers for a certain Reynolds number. The above conclusion confirms Chandra's (1938) laboratory results and Kuo's (1963) cloud-form assumptions that the preferred mode of perturbation is a roll-type convection ( $\alpha = 0$ ).

The prediction of heat and momentum flux for larger Reynolds numbers and Rayleigh numbers is still difficult with numerical technique; it is reasonable to determine the upper bound on flux to describe the fluid field. Hence, a theoretical approach based on Malkus' upper bound hypothesis was adopted to derive upper bounds. The upper bounds on heat and momentum flux for heated plane Couette flow are derived. Three special cases can be identified from present upper bounds. It was found that the upper bound on heat flux is proportional to one-thirds power of the Rayleigh number for pure turbulent convection; the upper bound on momentum flux was proportional to the two-thirds power of the Reynolds number for plane Couette flow (no heat). In addition these results show that both upper bound are independent of the Rayleigh number, but proportional to the two-thirds power of

the Reynolds number, if the Reynolds number is ten times the Rayleigh number and both are larger than 10,000.

BIBLIOGRAPHY

## BIBLIOGRAPHY

- Abramowitz, M., and Stegun, I.A., 1965, Handbook of Mathematical Functions, Dover Publications.
- Arakawa, A., 1966, "Computational Design for Long-Term Numerical Integration of Equation of Motion," J. Computational Physics, 1, pp. 119-143.
- Asai, T., 1964, "Cumulus Convection in the Atmosphere with Vertical Wind Shear: Numerical Experiment," J. Meteorological Society of Japan, 42, pp. 245-259.
- Asai, T., 1969, "Three-Dimensional Features of Thermal Convection in a Plane Couette Flow," J. Meteorological Society of Japan, 48, pp. 18-29.
- Brunt, D., 1951, "Experimental Cloud Formation," Compendium of Meteorology, Boston. Amer. Meteor. Soc., pp. 1255-1262.
- Businger, J.A., Wungaard, J.C., Izumi, Y. and Bradley, E.F., 1971, "Flux-Profile Relationships in the Atmospheric Surface Layer," J. Atmospheric Sciences, 28, pp. 181-189.
- Busse, F.H., 1969a, "On Howard's Upper Bound for Heat Transport by Turbulent Convection," J. Fluid Mechanics, 37, pp. 457-477.
- Busse, F.H., 1969b, "Bounds on the Transport of Mass and Momentum by Turbulent Flow Between Parallel Plates," ZAMP, 20, pp. 1-14.
- Busse, F.H., 1970, "Bounds for Turbulent Shear Flow," J. Fluid Mechanics, 41, pp. 219-240.
- Buzbee, B.L., Golub, G.H., Hielsion, C.W., 1970, "On Direct Methods for Solving Poisson's Equation," SIAM J. on Numerical Analysis, 7, pp. 627-656.
- Byatt-Smith, J.G.B., 1971, "An Integral Equation for Unsteady Surface Waves and a Comment on the Boussinesq Equation," J. Fluid Mechanics, 49, pp. 625-633.
- Chandra, K., 1938, "Instability of Fluids Heated From Below," Proc. Roy. Soc., A, 164, pp. 231-242.
- Chandrasekhar, S., 1961, "Hydrodynamic and Hydromagnetic Stability," Oxford: Clarendon Press.
- Chan, R.K., 1970, "Numerical Model for Water Waves," Ph.D. Dissertation, Stanford University.
- Chue, S.H., and McDonald, A.T., 1970, "Application of New Effective Viscosity Model to Turbulent Plane Couette Flow," AIAA, 8, pp. 2076-2078.

- Crowder, H.J. and Dalton, C., 1971, "On the Stability of Poiseuille Flow in Pipe," J. Computational Physics, 7, pp. 12-31.
- Crowley, W.P., 1968, "Numerical Advection Experiments," Monthly Weather Review, 96, pp. 1-11.
- Crowley, W.P., 1970, "A Numerical Model for Viscous, Free-Surface, Barotropic Wind Driven Ocean Circulations," J. Computational Physics, 5, pp. 139-168.
- Dassanayake, D.T.E., 1937, "Study of Some Special Cases of Instability of Fluid Layers, Particularly of Such Cases as Have Applications in Atmosphere," Unpublished Ph.D. Thesis, University of London.
- Davis, S.H., 1968, "Convection in a Box: On the Dependence of Preferred Wave-Number Upon the Rayleigh Number at Finite Amplitude," J. Fluid Mech., 32, pp. 619-624.
- Davis-Jones, R.P., 1970, "Thermal Convection in an Infinite Channel with No-slip Sidewalls," J. Fluid Mech., 44, pp. 695-704.
- Davis-Jones, R.P., 1971, "Thermal Convection in a Horizontal Plane Couette Flow," J. Fluid Mech., 49, pp. 193-205.
- Deardorff, J.W., 1964, "A Numerical Study of Two-Dimensional Parallel-Plate Convection," J. Atmos. Sci., 21, pp. 419-438.
- Deardorff, J.W., 1965, "Gravitational Instability Between Horizontal Plates with Shear," Phys. Fluids, 8, pp. 1027-1030.
- Deardorff, J.W., and Willis, G.E., 1967, "Investigation of Turbulent Thermal Convection Between Horizontal Plates," J. Fluid Mechanics, 28, pp. 675-704.
- Derickson, R.G., 1972, "A Numerical Simulation of a Cold Orographic Cloud System," M.S. Thesis, Colorado State University.
- Donnelly, R.J., Herman, R., Prigogine, I., 1965, Non-equilibrium Thermodynamics Variational Techniques and Stability, The University of Chicago Press.
- Ellingsen, T., Gjevik, B. and Palm, E., 1970, "On the Nonlinear Stability of Plane Couette Flow," J. Fluid Mechanics, 40, pp. 97-112.
- Forsyth, M.J., 1968, Variational Calculus in Science and Engineering, McGraw-Hill Book Company.
- Fox, D.G., and Lilly, D.K., 1972, "Numerical Simulation of Turbulent Flow," Review of Geophysics and Space Physics, 10, pp. 51-72.
- Gallagher, A.P. and Mercer, A. McD., 1962, "On the Behaviour of Small Disturbances in Plane Couette Flow," J. Fluid Mech. 13, pp. 91-100.

- Gallagher, A.P. and Mercer, A. McD., 1964, "On the Behaviour of Small Disturbances in Plane Couette Flow with a Temperature Gradient," Proc. Roy. Soc. London, A, 286, pp. 117-128.
- Gotch, K., and Satoh, M., 1966, "The Stability of a Natural Convection Between Two Parallel Vertical Planes," J. Physical Soc. of Japan, 21, pp. 542-548.
- Graham, A., 1933, "Shear Patterns in An Unstable Layer of Air," Phil. Trans. Roy. Soc., 232, A 714, pp. 285-296.
- Gunness Jr., R.C., and Gebhart, B., 1969, "Stability of Transient Natural Convection," The Physics of Fluid, 12, pp. 1968-1981.
- Hains, F.D., 1971, "Stability of Plane Couette-Poiseuille Flow with Uniform Crossflow," The Physics of Fluid, 14, pp. 1620-1623.
- Halpern, B., 1964, "Upper Bound on Heat Transport by Turbulent Convection," Notes on the 1964 Summer Study Program in Geophysical Fluid Dynamics, 2, pp. 57-68, Woods Hole Oceanographic Institute, Ref. NO. 64-46.
- Hardy, G.H., Littlewood, J.E., and Polya, G., 1969, Inequalities, Cambridge Press.
- Herring, J.R., 1963, "Investigation of Problems in Thermal Convection," J. Atmos. Sci., 20, pp. 325-338.
- Herring, J.R., 1964, "Investigation of Problems in Thermal Convection: Rigid Boundaries," J. Atmos. Sci. 21, pp. 277-290.
- Hess, S.L, 1959, Introduction to Theoretical Meteorology, Holt, Rinehart and Winston.
- Hieber, C.A., and Gebhart, B., 1971, "Stability of Vertical Natural Convection Boundary Layer---Some Numerical Solution," J. Fluid Mechanics, 48, pp. 625-646.
- Hinze, J.O., 1959, Turbulence, McGraw-Hill Book Company.
- Howard, L.N., 1963, "Heat Transport by Turbulent Convection," J. Fluid Mechanics, 17, pp. 405-532.
- Howard, L.N., 1964, "Convection at High Rayleigh Number," Proc. 11th International Congress, Applied Mechanics, pp. 1109-1115.
- IBM, 1970, IBM Scientific Subroutine Package, IBM.
- Ingersoll, A., 1966a, "Convective Instabilities in Plane Couette Flow," Phys. Fluids, pp. 682-689.

- Ingersoll, A., 1966b, "Thermal Convection with Shear at High Rayleigh Number," J. Fluid Mech., 25, pp. 209-228.
- Jeffreys, H., 1926, "The Stability of a Layer of Fluid Heated Below," Phil. Mag., 2, pp. 832-844.
- Kraichnan, R.H., 1962, "Turbulent Thermal Convection at Arbitrary Prandtl Number," The Physics of Fluid, 5, pp. 1374-1389.
- Kuo, H.L., 1963, "Perturbations of Plane Couette Flow in Stratified Fluid and Origin of Cloud Streets," Phys. Fluids, 6, pp. 195-211.
- Kuwabara, S., 1967, "Nonlinear Instability of Plane Couette Flow," The Physics of Fluid, Supplement, pp. 5115-5116.
- Lilly, D.K., 1961, "A Proposed Staggered Grid System For Numerical Integration of Dynamic Equations," Mon. Wea. Rev., 89, pp. 59-63.
- Lilly, D.K., 1964, "Numerical Solutions For the Shape-Preserving Two-Dimensional Thermal Convective Element," J. Atmos. Sci., 21, pp. 83-98.
- Lilly, D.K., 1965, "On the Computational Stability of Numerical Solutions of Time-Dependent Non-Linear Geophysical Fluid Dynamics Problems," Mon. Wea. Rev. 93, p. 11-26.
- Lilly, D.K., 1967, "Nonlinear Instability," Thermal Convection A Colloquium, pp. 229-241.
- Lin, C.C., 1955, The Theory of Hydrodynamic Stability. Cambridge University Press.
- Lin, J.T., and Apelt, C.J., "Stratified Flow Over an Obstacle--A Numerical Experiment," Themis Technical Report No. 7, Fluid Mechanics Program, Colorado State University.
- Lindberg, W.R., 1970, "Theoretical Aspects of Thermohaline Convection," Ph.D. dissertation, Colorado State University.
- Lindberg, W.R., 1971, "An Upper Bound on Transport Processes in Turbulent Thermohaline Convection," J. Physical Oceanography, 1, pp. 187-195.
- Lipps, F.G., 1971, "Two-Dimensional Experiments in Thermal Convection with Vertical Shear," J. Atmospheric Sciences, 28, pp. 3-19.
- Lumley, J.L. and Panofsky, H.A., 1964, The Structure of Atmospheric Turbulence, John Wiley and Sons, New York.

- Malkus, W.V.R., 1954a, "Discrete Transitions in Turbulent Convection," Proc. Royal Soc. A, 225, pp. 185-195.
- Malkus, W.V.R., 1954b, "The Heat Transport and Spectrum of Thermal Turbulence," Proc. Royal Soc. A, 225, pp.196-212.
- Malkus, W.V.R., 1956, "Outline of a Theory of Turbulent Shear Flow," J. Fluid Mechanics, 5, pp. 521-239.
- Malkus, W.V.R., 1964, "Boussinesq Equations," Notes on the 1964 Summer Study Program in Geophysical Fluid Dynamics, 1, pp. 1-12, Woods Hole Oceanographic Institute, Ref. No. 64-46.
- Malkus, W.V.R., 1968, "Absolute Stability and Upper Bounds on Turbulent Transport," Paper presented at the SIAM meeting, Toronto, Canada, 12 June 1968.
- Meksyn, D., and Stuart, J.T., 1951, "Stability of Viscous Motion Between Parallel Planes for Finite Disturbances," Proc. Royal Soc. A, 208, pp. 517-526.
- Mihaljan, J.M., 1962, "A Rigorous Exposition of the Boussinesq Approximations Applicable to a Thin Layer of Fluid," Astrophys. J., 136, pp. 1126-1133.
- Moore, M.J., and R.R. Long, 1971, "An Experimental Investigation of Turbulent Stratified Shear Flow," J. Fluid Mechanics, 49, pp. 635-655.
- Mori, Y., and Y. Uchida, 1966, "Forced Convective Heat Transfer Between Horizontal Flat Plates," Int. J. Heat Mass Transfer, 9, pp. 803-817.
- Nakayama, W., Hwang, G.J., and Cheng, K.C., 1970, "Thermal Instability in Plane Poiseuille Flow," J. Heat Transfer, 92, pp. 61-68.
- Nickerson, E.C., 1965, "A Numerical Experiment in Buoyant Convection Involving the Use of a Heat Source," J. The Atmosphere Science, 22, pp. 412-418.
- Nickerson, E.C., 1969, "Upper Bounds on the Torque in Cylindrical Couette Flow," J. Fluid Mechanics, 38, pp. 807-815.
- Nickerson, E.C., 1970, "The Turbulent Transport of Heat and Momentum," Technical Report, Fluid Mechanics Program, Colorado State University.
- Nickerson, E.C., 1973, "An Upper Bound on the Stress in Plane Couette Flow," to be published in ASME.
- Ogura, Y., and Yagihashi, 1969, "A Numerical Study of Convection Rolls in a Flow Between Horizontal Parallel Plates," J. Meteorological Soc. of Japan, 47, pp. 205-217.
- Pai, S.I., 1953, "On Turbulent Flow Between Parallel Plates," J. Applied Mechanics, 20, pp. 109-114.

- Phillips, A.C., and Walker, G.T., 1932, "The Forms of Stratified Clouds," Quart. J.R. Meteor. Soc., 58, pp. 23030.
- Potter, M.C., 1971, "Linear Stability of Turbulent Flow Profile," The Physics of Fluid, 14, pp. 1323-1325.
- Rao, K.N., Narasimha, R., and Narayanan, M.A.B., 1971, "The Bursting Phenomenon in a Turbulent Boundary Layer," J. Fluid Mechanics, 48, pp. 339-352.
- Reichardt, H., 1959, "Gesetzmässigkeiten Der Geradlinigen Turbulenten Couettestromung," Rep. 22, Max-Plank-Inst., Gottengen.
- Reynolds, W.C., and Tiedesman, W.G., 1967, "Stability of Turbulent Channel Flow with Application to Malkus' Theory," J. Fluid, Mechanics, 27, pp. 253-272.
- Robertson, J.M., 1959, "On Turbulent Plane Couette Flow," 6th Midwestern Conference of Fluid Mechanics, pp. 169-182.
- Schlichting, H., 1968, Boundary-Layer Theory, McGraw-Hill Book Co.
- Squire, W., 1960, "A Unified Theory of Turbulent Flow--II. Plane Couette Flow," Appl. Sci. Res. 49, pp. 393-410.
- Stewartson, K. and Stuart, J.T., 1971, "A Nonlinear Instability Theory for a Wave System in Plane Poiseuille Flow," J. Fluid Mechanics, 48, pp. 529-545.
- Stuart, J.T., 1971, "Nonlinear Stability Theory," Annual Review of Fluid Mechanics, pp. 347-370.
- Terada, T., 1928, "Some Experiments on Periodic Columnar Formation of Vortices Caused by Convection," Report Aeron. Res. Inst. Tokyo, 3, pp. 1-46.
- Vest, C.M., and Arpaci, V.S., 1969, "Stability of Natural Convection in a Vertical Slot," J. Fluid Mechanics, 36, pp. 1-15.
- Yamada, T., 1971, "Numerical and Wind Tunnel Simulation of Response of Stratified Shear Layers to Nonhomogeneous Surface Features," Ph.D. dissertation, Fluid Mechanics Program, Colorado State University.
- Yih, C.S., 1965, Dynamics of Nonhomogeneous Fluids, Macmillan Company.

APPENDIXES

## Appendix I

## GALERKIN METHOD

The Galerkin method proposed by B.G. Galerkin in 1915, is used to find the approximate solution for the ordinary differential equation, partial differential equation, or integral equation. This method is especially convenient for boundary-value problems. If  $u$  is the solution of the linear equation  $L(u) = f$  with corresponding boundary condition, then theoretically  $u$  can be expanded as the series form of

$$u(x,y,z) = \sum_{i=1}^{\infty} a_i Q_i(x,y,z) \quad (A1)$$

Here  $Q_1$  is chosen to satisfy the boundary conditions and also is linearly independent. The partial sum of Eq. A1 can be written as

$$u_n = \sum_{i=1}^N a_i Q_i \quad (A2)$$

In order that  $u_n$  be the exact solution of the given equation, it is necessary that  $R(u_n) = L(u_n) - f$  be identically equal to zero. This requirement, if  $R(u_n)$  is considered continuous, is equivalent to the requirement of the orthogonality of the expression  $R(u_n)$  to all the functions of the system  $Q_k$ ,  $k = 1, N$ ; or

$$\int_V R(u_n) \cdot Q_k^* dV = \int_V (L(u_n) - f) \cdot Q_k^* dV = 0 \quad k = 1, N \quad (A3)$$

Thus, if Eq. A3 holds, then

$$\lim_{N \rightarrow \infty} R(u_n) = 0 \quad (A4)$$

which can be proven as follows. Now let  $\eta(x,y,z)$  be an arbitrary function satisfying the continuity and homogeneous boundary conditions.

then  $\eta$  can be expressed as

$$\eta(x,y,z) = \sum_{k=1}^{\infty} c_k Q_k^* \quad (A5)$$

and 
$$\int_V \lim_{N \rightarrow \infty} R(u_n) \eta(x,y,z) dV = \int_V \lim_{N \rightarrow \infty} R(u_n) \sum_{k=1}^{\infty} c_k Q_k^* dV$$

$$= \lim_{N \rightarrow \infty} \sum_{k=1}^{\infty} c_k \int_V R(u_n) Q_k^* dV = \sum_{k=1}^{\infty} c_k \int_V R(u_n) Q_k^* dV = 0 \quad (A6)$$

or

$$\lim_{N \rightarrow \infty} \int_V R(u_n) \eta(x,y,z) dV = 0 \quad (A6)$$

for arbitrary  $\eta$ , so that it implies

$$\lim_{N \rightarrow \infty} R(u_n) = 0$$

This is the basic ideal for Galerkin method. Here  $Q_k^*$  is the complex conjugate of  $Q_k$ . From Eqs. A2 and A3,

$$\begin{aligned} \int_V (L(\sum_{i=1}^N a_i Q_i) - f) Q_k^* dV &= \int_V L(\sum_{i=1}^N a_i Q_i) Q_k^* dV - \int_V f Q_k^* dV \\ &= 0 \quad k = 1, N \end{aligned} \quad (A7)$$

Since  $Q_i$  is the known function, a system of simultaneous linear equations for  $a_i$  can be obtained. If  $\langle u, v \rangle$  is the inner product of  $u$  and  $v$ , then Eq. 7 can be rewritten as:

$$\langle L(Q_1), Q_1 \rangle a_1 + \langle L(Q_2), Q_1 \rangle a_2 + \dots + \langle L(Q_N), Q_1 \rangle a_N = \langle f, Q_1 \rangle$$

$$\langle L(Q_1), Q_2 \rangle a_1 + \langle L(Q_2), Q_2 \rangle a_2 + \dots + \langle L(Q_N), Q_2 \rangle a_N = \langle f, Q_2 \rangle$$

. . . . .



$$y_n' = \sum a_i (ix^{i-1} - (i+1)x^i)$$

$$y_n'' = \sum a_i ((i^2-i)x^{i-2} - (i^2+i)x^{i-1})$$

$$L(y) - f = y'' + y - x = \sum a_i ((i^2-i)x^{i-1} - (i^2+i)x^{i-1} + x^i - x^{i+1}) - x = 0$$

then from Eq. A3

$$\int_0^1 (\sum a_i ((i^2-i)x^{i-2} - (i^2+i)x^{i-1} + x^i - x^{i+1}) - x) \cdot$$

$$(x^k - x^{k+1}) dx = 0$$

$$k = 1, N$$

Take  $N = 2$  for instance,

$$\int_0^1 (a_1(-2+x-x^2) + a_2(2-6x+x^2-x^3)-x)(x-x^2) dx = 0$$

$$\int_0^1 (a_1(-2+x-x^2) + a_2(2-6x-x^2-x^3)-x)(x^2-x^3) dx = 0$$

or  $a_1 = 71/369$  and  $a_2 = 7/41$

Hence  $y_2 = x(1-x)(71/369+7x/41)$ ;

with the same procedure

$$y_1 = x(1-x)5/18$$

The results are as follows:

s	$y_1$	$y_2$	$y_{\text{exact}}$
0.25	0.0521	0.0440	0.0440
0.50	0.0693	0.0694	0.0698
0.75	0.0520	0.0600	0.0600

In order to solve Eqs. 50-52 numerically by the Galerkin method, the two variables  $W(z)$  and  $\theta(z)$  are expanded in series form as in Eqs. 67 and 68 which satisfy the boundary conditions (Eq. 52). Then from the principle of the Galerkin method, Eqs. 77 and 78 are established. Substituting Eqs. 67, 68, 50 and 51 into Eqs. 77 and 78 and set  $\sigma = 0$ , results in

$$\int_{-1/2}^{1/2} \sum_{n=1}^N \{ (G_n'' - 2k^2 G_n'' + k^4 G_n) A_n + \text{Re} k_x ((H_n'' - k^2 H_n) \bar{U} - H_n \bar{U}'') B_n - \text{Ra} k_x^2 L_n D_n \} G_m dz = 0 \quad m = 1, N \quad (\text{A9})$$

$$\int_{-1/2}^{1/2} \sum_{n=1}^N \{ -\text{Re} k_x ((G_n'' - k^2 G_n) \bar{U} - G_n) A_n + (H_n - 2k^2 H_n'' + k^4 H_n) B_n - \text{Ra} k_x^2 M_n E_n \} H_m dz = 0 \quad m = 1, N \quad (\text{A10})$$

$$\int_{-1/2}^{1/2} \sum_{n=1}^N \{ (L_n'' - k^2 L_n) D_n + \text{Re} \text{Pr} k_x \bar{U} M_n E_n - \bar{T}' G_n A_n \} L_m dz = 0 \quad m = 1, N \quad (\text{A11})$$

$$\int_{-1/2}^{1/2} \sum_{n=1}^N \{ -\bar{T}' H_n B_n - \text{Re} \text{Pr} k_x \bar{U} L_n D_n + (M_n'' - k^2 M_n) E_n \} M_m dz = 0 \quad m = 1, N \quad (\text{A12})$$

If we define

$$C_{1mn} = \int_{-1/2}^{1/2} (G_n'' - 2k^2 G_n'' + k^4 G_n) G_m dz$$

$$C_{2mn} = \int_{-1/2}^{1/2} ((k^2 U + \bar{U}'') H_n - H_n \bar{U}'') G_m dz$$

$$C_{3mn} = \int_{-1/2}^{1/2} L_n G_m dz$$

$$C_{4mn} = \int_{-1/2}^{1/2} ((\bar{U}'' + k^2 \bar{U}) G_n - \bar{U} G_n'') H_m dz$$

$$C_{5mn} = \int_{-1/2}^{1/2} (H_n - 2k^2 H_n'' + k^4 H_n) H_m dz$$

$$C_{6mn} = \int_{-1/2}^{1/2} M_n H_m dz$$

$$C_{7mn} = \int_{-1/2}^{1/2} \bar{T}' G_n L_m dz$$

$$C_{8mn} = \int_{-1/2}^{1/2} (L_n'' - k^2 L_n) L_m dz$$

$$C_{9mn} = \int_{-1/2}^{1/2} \bar{U} M_n L_m dz$$

$$C_{10mn} = \int_{-1/2}^{1/2} \bar{T}' H_n M_m dz$$

$$C_{11mn} = \int_{-1/2}^{1/2} \bar{U} L_n M_m dz$$

$$C_{12mn} = \int_{-1/2}^{1/2} (M_n'' - k^2 M_n) M_m dz$$

Hence Eqs. A9-A12 will be

$$\sum_{n=1}^N (C_{1mn} A_n - \text{Re} k_x C_{2mn} B_n - \text{Ra} k^2 C_{3mn} D_n) = 0 \quad m = 1, N \quad (\text{A13})$$

$$\sum_{n=1}^N (C_{4mn} \text{Re} k_x A_n + C_{5mn} B_n - \text{Ra} k^2 C_{6mn} E_n) = 0 \quad m = 1, N \quad (\text{A14})$$

$$\sum_{n=1}^N (-C_{7mn} A_n + C_{9mn} D_n + \text{Re} \text{Pr} k_x C_{9mn} E_n) = 0 \quad m = 1, N \quad (\text{A15})$$

$$\sum_{n=1}^N (-C_{10mn} B_n - \text{Re} \text{Pr} k_x C_{11mn} D_n + C_{12mn} E_n) = 0 \quad m = 1, N \quad (\text{A16})$$

The matrix form of Eqs. A13-A16 are the same as Eq. 79 in 2.1. As previously stated, the determinant is equal to zero indicating the state

of neutral stability, i.e.,

$$F(\alpha, k, Ra, Re, Pr) = \begin{vmatrix} X_{11} & X_{12} & & & & & X_{1N} \\ X_{21} & X_{22} & & & & & X_{2N} \\ \cdot & \cdot & \cdot & \cdot & \cdot & \cdot & \cdot \\ \cdot & \cdot & \cdot & \cdot & \cdot & \cdot & \cdot \\ X_{N1} & X_{N2} & & & & & X_{NN} \end{vmatrix} = 0 \quad (81a)$$

The elemental matrix  $X_{mn}$  is defined as:

$$X_{mn} = \begin{bmatrix} C_{1mn} & -Re\sin(\alpha)C_{2mn} & Rak^2 C_{3mn} & 0 \\ Re\sin(\alpha)C_{4mn} & C_{5mn} & 0 & -Rak^2 C_{6mn} \\ -C_{7mn} & 0 & C_{8mn} & RePr\sin(\alpha)C_{9mn} \\ 0 & -C_{10mn} & -RePr\sin(\alpha)C_{11mn} & C_{12mn} \end{bmatrix}$$

A trial and error method is used to solve Eq. 81a by setting certain value of  $\alpha$ ,  $k$ ,  $Ra$ ,  $Re$  and  $Pr$  in order to adjust the determinant to be zero.

## Appendix II

(Excerpted from Vest &amp; Arpaci (1969))

It will now be proven that the real part of the wave speed,  $\sigma_r$ , must be zero if the solutions,  $W$  and  $\theta$  are of the form (67) or (68).

The equations and boundary conditions governing a small disturbance with the complex wave speed  $\sigma$  are:

$$W'''' - 2k^2 W'' + k^4 W - RaK^2 \theta - ik_x \text{Re}[(\bar{U} - \frac{\sigma}{k_x})(W'' - k^2 W) - \bar{U}'' W] = 0 \quad (B1)$$

$$\theta'' - k^2 \theta - W \bar{T}' - ik_x \text{RePr}(\bar{U} - \frac{\sigma}{k_x}) \theta = 0 \quad (B2)$$

$$\theta(\pm \frac{1}{2}) = W(\pm \frac{1}{2}) = W'(\pm \frac{1}{2}) = 0 \quad (B3)$$

where

$$\bar{U}(z) = -z, \quad \bar{T}(z) = \frac{T_o}{\Delta T} - z - \frac{1}{2} \quad (B4)$$

Equations (B1) and (B2) are multiplied respectively by  $W^*$  and  $\theta^*$ , the conjugates of  $W$  and  $\theta$ , and integrated over  $(-\frac{1}{2}, +\frac{1}{2})$ . Suitable integrations by parts and utilization of conditions (B3) and (B4) yield:

$$\int_{-1/2}^{1/2} (|W''|^2 + 2k^2 |W'|^2 + k^4 |W|^2) dz + i k_x \text{Re} \left\{ \int_{-1/2}^{1/2} ((\bar{U}' + k^2 \bar{U}) |W|^2 - \bar{U} W'' W^*) dz - \frac{\sigma}{k_x} \int_{-1/2}^{1/2} (|W'|^2 + k^2 |W|^2) dz \right\} - Ra \int_{-1/2}^{1/2} k^2 \theta W^* dz = 0 \quad (B5)$$

and

$$-\int_{-1/2}^{1/2} (|\theta'|^2 + k^2|\theta|^2) dz + i k_x \text{RePr} \left\{ \frac{\sigma}{k_x} \int_{-1/2}^{1/2} |\theta|^2 dz \right. \\ \left. - \bar{U} |\theta|^2 \right\} - \int_{-1/2}^{1/2} \bar{W} \bar{T}' \theta^* dz = 0 \quad (\text{B6})$$

$$\int_{-1/2}^{1/2} ((\bar{U}'' + k^2 \bar{U}) |W|^2 - \bar{U} W'' W^*) dz \\ = i \int_{-1/2}^{1/2} \bar{U} (\phi_o'' \phi_e - \phi_e'' \phi_o) dz \quad (\text{B7})$$

$$\int_{-1/2}^{1/2} \theta W^* dz = \int_{-1/2}^{1/2} (\tau_o \phi_e + \tau_o \phi_o) dz \quad (\text{B8})$$

$$\int_{-1/2}^{1/2} \bar{T}' W \theta^* dz = \int_{-1/2}^{1/2} \bar{T}' (\phi_e \tau_e + \phi_o \tau_o) dz \quad (\text{B9})$$

and

$$\int_{-1/2}^{1/2} \bar{U} |\theta|^2 dz = 0 \quad (\text{B10})$$

Eqs. (B7)-(B10) exist since by definition  $\phi_e$ ,  $\tau_e$ ,  $\bar{T}'$  are even with respect to  $z$ ; and  $\phi_o$ ,  $\tau_o$ ,  $\bar{U}$  are odd functions. Using the results above, equations (B5) and (B6) can be rewritten in terms of their explicit real and imaginary parts. The imaginary parts of (B5) and (B6) are respectively:

$$-\text{Re} \sigma \tau \int_{-1/2}^{1/2} (|W'|^2 + k^2 |W|^2) dz = 0 \quad (\text{B11})$$

and

$$\text{RePr} \sigma \tau \int_{-1/2}^{1/2} |\theta|^2 dz = 0 \quad (\text{B12})$$

Since both of these integrals are definite, it is necessary that

$$\sigma_r = 0$$

(B13)

## Appendix III

## Derivation of Equations

Before deriving the equations which were used in the previous chapters, the following important theorems and identities are listed:

## A. Leibniz's theorem

$$\begin{aligned} \frac{d}{dc} \int_{a(c)}^{b(c)} f(x,c) dx &= \int_{a(c)}^{b(c)} \frac{\partial}{\partial c} f(x,c) dx \\ &+ f(b,c) \frac{db}{dc} - f(a,c) \frac{da}{dc} \end{aligned} \quad (C1)$$

if  $a$  and  $b$  are constants;

$$\frac{d}{dc} \int_a^b f(x,c) dx = \int_a^b \frac{\partial}{\partial c} f(x,c) dx \quad (C2)$$

## B. Vector identities

$$\nabla^2 \vec{A} = \nabla(\nabla \cdot \vec{A}) - \nabla \times (\nabla \times \vec{A}) \quad (C3)$$

$$\vec{A} \cdot (\nabla \times \vec{B}) = \vec{B} \cdot (\nabla \times \vec{A}) - \nabla \cdot (\vec{A} \times \vec{B}) \quad (C4)$$

$$\nabla \cdot (\phi \vec{A}) = (\nabla \phi) \cdot \vec{A} + \phi (\nabla \cdot \vec{A}) \quad (C5)$$

$$\vec{A} \cdot (\vec{B} \cdot \nabla) \vec{A} = \frac{1}{2} \vec{B} \cdot \nabla (\vec{A} \cdot \vec{A}) \quad (C6)$$

## C1. Prove

$$\begin{aligned} \iiint \frac{\partial}{\partial q} ( \quad ) dx dy dz \\ = \frac{\partial}{\partial q} \iiint ( \quad ) dx dy dz = 0 \quad q = x, y, \text{ or } z \end{aligned} \quad (C7)$$

From Eq. C2,

$$\begin{aligned} \iiint \frac{\partial}{\partial q} ( \quad ) dx dy dz &= \iiint \frac{\partial}{\partial q} f ( \quad ) dx dy dz \\ &= \int \frac{\partial}{\partial q} \iint ( \quad ) dx dy dz = \frac{\partial}{\partial q} \iiint ( \quad ) dx dy dz \end{aligned}$$

Since  $\iiint ( ) dx dy dz$  is no variation along  $x$ ,  $y$ , and  $z$ . Where  $q$  one of the  $x$ ,  $y$ , or  $z$ . Hence

$$\frac{\partial}{\partial q} \iiint ( ) dx dy dz = 0 \quad q = x, y, \text{ or } z$$

By the shorthand notation (Eq. 30)

$$\left\langle \frac{\partial}{\partial q} ( ) \right\rangle = \frac{\partial}{\partial q} \langle ( ) \rangle = 0 \quad q = x, y, \text{ or } z \quad (C7)$$

Similarly

$$\overline{\frac{\partial}{\partial q} ( )} = \frac{\partial}{\partial a} \overline{( )} = 0 \quad a = x, \text{ or } y \quad (C8)$$

## C2. Derivation of equation (21)

The steady state equation of Eq. 3

$$\vec{V} \cdot \nabla T = \kappa \nabla^2 T \quad (C9)$$

The horizontal average of Eq. C9 is

$$\overline{\vec{V} \cdot \nabla T} = \overline{\kappa \nabla^2 T} \quad (C10)$$

Since

$$\begin{aligned} \overline{\vec{V} \cdot \nabla T} &= \overline{\nabla \cdot \vec{V} T} - \overline{T(\nabla \cdot \vec{V})} \\ &= \frac{\partial}{\partial x} \overline{(V_x T)} + \frac{\partial}{\partial y} \overline{(V_y T)} + \frac{\partial}{\partial z} \overline{(V_z T)} \\ &= \frac{\partial}{\partial z} \overline{(V_z T)} = \frac{\partial}{\partial z} \overline{(V_z \theta + V_z \bar{T})} \\ &= \frac{\partial}{\partial z} \overline{V_z \theta} + \frac{\partial}{\partial z} \overline{(V_z \bar{T})} = \frac{\partial}{\partial z} \overline{V_z \theta} \\ \overline{V^2 T} &= \overline{\nabla^2 (\bar{T} + \theta)} = \overline{\nabla^2 \bar{T}} + \overline{\nabla^2 \theta} \\ &= \overline{\nabla^2 T} = \frac{d^2}{dz^2} \bar{T} \end{aligned}$$

then from Eq. C10

$$\frac{d}{dz} (\overline{V_z \theta}) = \frac{d^2}{dz^2} \overline{T} \quad (C11)$$

or

$$S = \overline{V_z \theta} - \kappa \frac{d\overline{T}}{dz}$$

By definition of Nusselt number

$$\begin{aligned} \text{Nu} &= \frac{\text{actual vertical heat flux}}{\text{pure conductive vertical heat flux}} \\ &= \frac{S}{\kappa \Delta T / D} \end{aligned}$$

The dimensionless form of Eq. C12 is

$$S = \Delta U \Delta T \overline{V_z \theta} - \frac{\Delta T}{D} \kappa \frac{d\overline{T}}{dz}$$

or

$$\text{Nu} = \text{RePr} \overline{V_z \theta} - \frac{d\overline{T}}{dz} \quad (21)$$

C3. Derivation of equation (22)

From steady-state form of Eq. 6

$$\vec{\nabla} \cdot \vec{\nabla} \overline{V} + \nabla \overline{\pi} - \frac{\text{Ra}}{\text{Re}^2 \text{Pr}} \overline{\theta} \vec{k} = \frac{1}{\text{Re}} \nabla^2 \overline{V} \quad (C16)$$

$$\overline{\theta} = 0 \quad (C17)$$

$$\nabla \overline{\pi} = \frac{\partial}{\partial z} \overline{\pi} \vec{k} \quad (C18)$$

$$\begin{aligned}
 \overline{\nabla^2 \vec{V}} &= \frac{\partial^2}{\partial z^2} \vec{V} = \frac{\partial^2}{\partial z^2} (\overline{U} \vec{i} + \hat{v}) \\
 &= \frac{d^2}{dz^2} \overline{U} \vec{i} = \frac{d^2}{dz^2} (\overline{U} \sin \alpha \vec{i}_*) \\
 &\quad + \frac{d^2}{dz^2} (\overline{U} \cos \alpha \vec{j}_*)
 \end{aligned} \tag{C19}$$

$$\begin{aligned}
 \overline{\vec{v} \cdot \nabla \vec{V}} &= \overline{\vec{v} \cdot \nabla v_x} \vec{i} + \overline{\vec{v} \cdot \nabla v_y} \vec{j} + \overline{\vec{v} \cdot \nabla v_z} \vec{k} \\
 &= \overline{\nabla \cdot (v_x \vec{V})} \vec{i} - \cancel{\overline{v_x \nabla \cdot \vec{V}} \vec{i}} + \overline{\nabla \cdot (v_y \vec{V})} \vec{j} \\
 &\quad - \overline{v_y \nabla \cdot \vec{V}} \vec{j} + \overline{\nabla \cdot (v_z \vec{V})} \vec{k} - \cancel{\overline{v_z \nabla \cdot \vec{V}} \vec{k}} \\
 &= \overline{\nabla \cdot (v_x \vec{V})} \vec{i} + \overline{\nabla \cdot (v_y \vec{V})} \vec{j} + \overline{\nabla \cdot (v_z \vec{V})} \vec{k} \\
 &= \frac{d}{dz} (\overline{v_x v_z} \vec{i} + \overline{v_y v_z} \vec{j} + \overline{v_z^2} \vec{k}) \\
 &= \frac{d}{dz} ((\overline{U} + v_x) v_z \vec{i} + \overline{v_y v_z} \vec{j} + \overline{v_z^2} \vec{k}) \\
 &= \frac{d}{dz} (\overline{v_x v_z} \vec{i} + \overline{v_y v_z} \vec{j} + \overline{v_z^2} \vec{k})
 \end{aligned} \tag{C20}$$

Substitution of Eqs. C17-C20 gives

$$\overline{v_y v_z} = \text{constant}$$

$$\frac{dv_z^2}{dz} + \frac{d}{dz} \overline{\pi} = \text{constant}$$

$$\frac{d^2 \overline{U}}{dz^2} = \frac{d\overline{U}}{dz} \text{Re } v_x v_z$$

or

$$M_o = \frac{d\bar{U}}{dz} - \operatorname{Re} \overline{v_x v_z} \quad (\text{Along } x\text{-axis}) \quad (22)$$

Similarly, for (m,n,z) system, it gives

$$M_{om} = \frac{d\bar{U}}{dz} \sin\alpha - \operatorname{Re} \overline{v_m v_z} \quad (23)$$

$$M_{on} = \frac{d\bar{U}}{dz} \cos\alpha - \operatorname{Re} \overline{v_n v_z} \quad (24)$$

## C4. Derivation of equation (26)

Taking dot on Eq. 6 with perturbation velocity and then taking volume average on that gives:

$$\begin{aligned} \langle \tilde{v} \cdot \frac{\partial \tilde{V}}{\partial t} \rangle + \langle \tilde{v} \cdot (\tilde{V} \cdot (\tilde{V} \cdot \nabla) \tilde{V}) \rangle + \langle \tilde{v} \cdot \nabla \pi \rangle \\ = \langle \tilde{v} \cdot \frac{Ra}{Re^2 Pr} \theta \vec{k} \rangle + \frac{1}{Re} \langle \tilde{v} \cdot \nabla \tilde{V} \rangle \end{aligned} \quad (C21)$$

Since

$$\begin{aligned} \langle \tilde{v} \cdot \nabla \pi \rangle &= \langle \nabla \cdot (\pi \tilde{v}) \rangle - \langle \cancel{\pi \tilde{v} \cdot \nabla} \rangle \\ &= \nabla \cdot \langle \tilde{v} \pi \rangle = 0 \end{aligned} \quad (C22)$$

$$\langle \tilde{v} \cdot \theta \vec{k} \rangle = \langle v_z \theta \rangle = \langle \overline{v_z \theta} \rangle \quad (C23)$$

$$\begin{aligned} \langle \tilde{v} \cdot \frac{\partial \tilde{V}}{\partial t} \rangle &= \langle \tilde{v} \cdot \frac{\partial \tilde{v}}{\partial t} \rangle + \langle \tilde{v} \cdot \frac{\partial \bar{U}}{\partial t} \vec{i} \rangle \\ &= \frac{1}{2} \frac{\partial}{\partial t} \langle \tilde{v} \cdot \tilde{v} \rangle + \langle v_x \frac{\partial \bar{U}}{\partial t} \rangle \\ &= \frac{1}{2} \frac{\partial}{\partial t} \langle |\tilde{v}|^2 \rangle = \frac{\partial}{\partial t} K' \end{aligned} \quad (C24)$$

$$\begin{aligned} \langle \tilde{v} \cdot \nabla^2 \tilde{v} \rangle &= \langle \tilde{v} \cdot \nabla^2 \tilde{v} \rangle + \langle \tilde{v} \cdot \nabla^2 \bar{U} \vec{i} \rangle \\ &= \langle \tilde{v} \cdot [\nabla(\nabla \cdot \tilde{v}) - \nabla_x(\nabla_x \tilde{v})] \rangle + \langle v_x \nabla^2 \bar{U} \rangle \\ &= \langle \nabla_x(\nabla_x \tilde{v}) \rangle \\ &= - \langle (\nabla_x \tilde{v}) \cdot (\nabla_x \tilde{v}) - \nabla \cdot [\tilde{v} (\nabla_x \tilde{v})] \rangle \\ &= - \langle (\nabla_x \tilde{v}) \cdot (\nabla_x \tilde{v}) \rangle \end{aligned} \quad (C25)$$

$$\langle \tilde{v} \cdot (\tilde{V} \cdot \nabla) \tilde{V} \rangle = \langle \tilde{v} \cdot (\tilde{V} \cdot \nabla) (\bar{U} \vec{i} + \tilde{v}) \rangle$$

$$\begin{aligned}
&= \langle \tilde{v} \cdot (\tilde{V} \cdot \nabla) \tilde{v} \rangle + \langle v_x (\tilde{V} \cdot \nabla) \bar{U} \rangle \\
&= \frac{1}{2} \langle (\tilde{V} \cdot \nabla) |\tilde{v}|^2 \rangle + \langle v_x v_z \frac{d\bar{U}}{dz} \rangle \\
&= \langle \overline{v_x v_z} \frac{d\bar{U}}{dz} \rangle \tag{C26}
\end{aligned}$$

Substitution of Eqs. C22-C26 into C21 gives

$$\begin{aligned}
\frac{\partial}{\partial t} (K') &= - \langle v_x v_z \frac{d\bar{U}}{dz} \rangle + \frac{Ra}{PrRe^2} \langle \overline{v_z \theta} \rangle \\
&\quad - \frac{1}{Re} \langle |\nabla \times \tilde{v}|^2 \rangle \tag{26}
\end{aligned}$$

C5. Derivation of equation (27)

Taking dot product on Eq. 6 with velocity and then volume average to that equation gives

$$\begin{aligned}
\langle \tilde{v} \cdot \frac{\partial \tilde{V}}{\partial t} \rangle &+ \langle \tilde{v} \cdot (\tilde{V} \cdot \nabla) \tilde{V} \rangle + \langle \tilde{v} \cdot \nabla \pi \rangle \\
&= \frac{Ra}{Re^2 Pr} \langle \tilde{v} \cdot \theta \vec{k} \rangle + \frac{1}{Re} \langle \tilde{v} \cdot \nabla^2 \tilde{V} \rangle \tag{C27}
\end{aligned}$$

since

$$\begin{aligned}
\langle \tilde{v} \cdot \nabla \pi \rangle &= \langle \nabla \cdot (\pi \tilde{V}) \rangle - \langle \pi \nabla \cdot \tilde{V} \rangle \\
&= \nabla \cdot \langle \pi \tilde{V} \rangle = 0 \tag{C28}
\end{aligned}$$

$$\langle \tilde{v} \cdot \theta \vec{k} \rangle = \langle v_z \theta \rangle = \langle \overline{v_z \theta} \rangle \tag{C30}$$

$$\begin{aligned}
\langle \tilde{v} \cdot \frac{\partial \tilde{V}}{\partial t} \rangle &= \frac{1}{2} \frac{\partial}{\partial t} \langle \tilde{V} \cdot \tilde{V} \rangle = \frac{1}{2} \frac{\partial}{\partial t} \langle \bar{U}^2 \rangle + \frac{\partial}{\partial t} \langle \bar{U} v_x \rangle \\
&\quad + \frac{1}{2} \frac{\partial}{\partial t} \langle \tilde{v} \cdot \tilde{v} \rangle = \frac{\partial}{\partial t} (\bar{K}) + \frac{\partial}{\partial t} (K') \tag{C31}
\end{aligned}$$

$$\begin{aligned}
\langle \vec{v} \cdot \nabla^2 \vec{v} \rangle &= \langle \bar{u} \vec{i} \cdot \nabla^2 \vec{v} \rangle + \langle \tilde{v} \cdot \nabla^2 \vec{v} \rangle \\
&= \langle \bar{u} \nabla^2 (\bar{u} + v_x) \rangle - \langle |\nabla \times \tilde{v}|^2 \rangle \\
&= \langle \bar{u} \frac{d^2 \bar{u}}{dz^2} \rangle + \langle \bar{u} \nabla^2 v_x \rangle - \langle |\nabla \times \tilde{v}|^2 \rangle \\
&= \langle \bar{u} \frac{d^2 \bar{u}}{dz^2} \rangle - \langle |\nabla \times \tilde{v}|^2 \rangle \tag{C32}
\end{aligned}$$

$$\begin{aligned}
\langle \vec{v} \cdot (\vec{v} \cdot \nabla) \vec{v} \rangle &= \langle \frac{1}{2} \vec{v} \cdot \nabla |\vec{v}|^2 \rangle \\
&= \frac{1}{2} [ \langle \nabla \cdot (\vec{v} |\vec{v}|^2) \rangle - \langle |\vec{v}|^2 \nabla \cdot \vec{v} \rangle ] \\
&= 0 \tag{C33}
\end{aligned}$$

Substitution of Equations C28-C33, and 26 into Eq. C27 gives

$$\frac{\partial \bar{K}}{\partial t} = \langle \frac{v_x v_z}{v} \frac{d\bar{u}}{dz} \rangle + \frac{1}{\text{Re}} \langle \bar{u} \frac{d^2 \bar{u}}{dz^2} \rangle \tag{C34}$$

From the theorem of integration by parts

$$\int \bar{u} \frac{d^2 \bar{u}}{dz^2} dz = \bar{u} \frac{d\bar{u}}{dz} \Big|_{-1/2}^{1/2} - \int \left( \frac{d\bar{u}}{dz} \right)^2 dz \tag{C35}$$

Substitution of Eq. C34 into Eq. C35 gives

$$\frac{\partial \bar{K}}{\partial t} = \langle \frac{v_x v_z}{v} \frac{d\bar{u}}{dz} \rangle + \frac{1}{2\text{Re}} \frac{d(\bar{u}^2)}{dz} \Big|_{-1/2}^{1/2} - \frac{1}{\text{Re}} \int \left( \frac{d\bar{u}}{dz} \right)^2 dz \tag{27}$$

## C6 Derivation of equation (33)

From Equation 7

$$\frac{\partial T}{\partial t} + \vec{V} \cdot \nabla T = \frac{1}{\text{RePr}} \nabla^2 T \quad (7)$$

$$\langle \theta \frac{\partial T}{\partial t} \rangle + \langle \theta \vec{V} \cdot \nabla T \rangle = \langle \frac{\theta}{\text{RePr}} \nabla^2 T \rangle \quad (32)$$

$$\begin{aligned} \langle \theta \frac{\partial T}{\partial t} \rangle &= \langle \cancel{\theta \frac{\partial T}{\partial t}}^0 \rangle + \langle \theta \frac{\partial \theta}{\partial t} \rangle \\ &= \frac{1}{2} \langle \frac{\partial \theta^2}{\partial t} \rangle = \frac{\partial}{\partial t} \langle \frac{1}{2} \theta^2 \rangle \\ &= \frac{\partial I'}{\partial t} \end{aligned} \quad (C36)$$

$$\begin{aligned} \langle \theta \vec{V} \cdot \nabla T \rangle &= \langle \theta (\vec{V} \cdot \nabla \theta) + \theta (\vec{V} \cdot \nabla \bar{T}) \rangle \\ &= \langle \frac{1}{2} \vec{V} \cdot \nabla \theta^2 \rangle + \langle \theta v_z \frac{d\bar{T}}{dz} \rangle = \langle \theta v_z \frac{d\bar{T}}{dz} \rangle \\ &+ \frac{1}{2} \langle \cancel{\nabla \cdot \vec{V} \theta^2}^0 - \cancel{\theta^2 \nabla \cdot \vec{V}}^0 \rangle = \langle \theta v_z \frac{d\bar{T}}{dz} \rangle \end{aligned} \quad (C37)$$

$$\begin{aligned} \langle \theta \nabla^2 T \rangle &= \langle \cancel{\theta \nabla^2 T}^0 \rangle + \langle \theta \nabla^2 \theta \rangle \\ &= \langle \theta \nabla \cdot \nabla \theta \rangle = \langle \cancel{\nabla \cdot \theta \nabla \theta}^0 \rangle - \langle \nabla \theta \cdot \nabla \theta \rangle \\ &= - \langle |\nabla \theta|^2 \rangle \end{aligned} \quad (C38)$$

Substitution of Equation (C36) through (C38) into (32) gives

$$\frac{\partial I'}{\partial t} + \langle \theta v_z \frac{d\bar{T}}{dz} \rangle = \frac{-1}{\text{RePr}} \langle |\nabla\theta|^2 \rangle \quad (33)$$

## Appendix IV

## Time-splitting Method

In this section, the finite difference form for transport equations are derived by the time-splitting scheme. According to this scheme, the integration of governing equations are separated by two parts. First the equation is integrated along the m-axis which is independent of z ; then it is integrated along the z-axis. Equation 109 becomes

$$\frac{\partial P}{\partial t} = -V_m \frac{\partial P}{\partial m} + C_1 \frac{\partial^2 P}{\partial m^2} + C_2 \frac{\partial Q}{\partial m} \quad (D1)$$

and

$$\frac{\partial^2 P}{\partial t^2} = -V_m \frac{\partial}{\partial m} \left( \frac{\partial P}{\partial t} \right) - \frac{\partial V_m}{\partial t} \frac{\partial P}{\partial m} + C_1 \frac{\partial^2}{\partial m^2} \left( \frac{\partial P}{\partial t} \right) + C_2 \frac{\partial^2 \theta}{\partial m \partial t} \quad (D2)$$

Substitution of Eq. D1 into Eq. D2 gives

$$\begin{aligned} \frac{\partial^2 P}{\partial t^2} &= V_m^2 \frac{\partial^2 P}{\partial m^2} = V_m \frac{\partial}{\partial m} \left( C_1 \frac{\partial^2 P}{\partial m^2} + C_2 \frac{\partial \theta}{\partial m} \right) \\ &\quad - \frac{\partial V_m}{\partial t} \frac{\partial P}{\partial m} + C_1 \frac{\partial^2}{\partial m^2} \left( \frac{\partial P}{\partial t} \right) + C_2 \frac{\partial^2 \theta}{\partial m \partial t} \end{aligned} \quad (D3)$$

According to Taylor's expansion theory, P can be expanded with respect to t .

$$P_{j,k}^{\ell+\frac{1}{2}} = P_{j,k}^{\ell} + \frac{\partial P}{\partial t} \Big|_{j,k}^{\ell} \Delta t + \frac{\partial^2 P}{\partial t^2} \Big|_{j,k}^{\ell} \frac{\Delta t^2}{2} + O(\Delta t^3) \quad (D4)$$

Equations D1 , D2 , and D4 give

$$\begin{aligned}
 P_{j,k}^{\ell+1/2} &= P_{j,k}^{\ell} - V_m \left. \frac{\partial P}{\partial m} \right|_{j,k}^{\ell} \Delta t + C_1 \left. \frac{\partial^2 P}{\partial m^2} \right|_{j,k}^{\ell} \Delta t \\
 &+ C_2 \left. \frac{\partial Q}{\partial m} \right|_{j,k}^{\ell} \Delta t + V_m^2 \left. \frac{\partial^2 P}{\partial m^2} \right|_{j,k}^{\ell} \frac{\Delta t}{2}
 \end{aligned} \tag{D3}$$

$$+ \text{(High order terms)} \tag{D5}$$

or

$$\begin{aligned}
 P_{j,k}^{\ell+1/2} &\approx P_{j,k}^{\ell} - \frac{\Delta t}{2\Delta m} (V_m)_{j,k}^{\ell} (P_{j+1,k}^{\ell} - P_{j-1,k}^{\ell}) \\
 &+ \left[ \frac{1}{2} \left( \frac{\Delta t}{\Delta m} (V_m)_{j,k}^{\ell} \right)^2 + C_1 \frac{\Delta t}{(\Delta m)^2} \right] (P_{j+1,k}^{\ell} \\
 &- 2 P_{j,k}^{\ell} + P_{j-1,k}^{\ell}) + \frac{\Delta t}{2\Delta m} C_2 (Q_{j+1,k}^{\ell} - Q_{j-1,k}^{\ell})
 \end{aligned} \tag{125}$$

Similarly, it can be integrated along z=axis direction only.

Equation (109) becomes

$$\frac{\partial P}{\partial t} = -V_z \frac{\partial P}{\partial z} + C_1 \frac{\partial^2 P}{\partial z^2} \tag{D6}$$

and

$$\begin{aligned}
 \frac{\partial^2 P}{\partial t^2} &= -V_z \frac{\partial}{\partial z} \left( \frac{\partial P}{\partial t} \right) - \frac{\partial V_z}{\partial t} \frac{\partial P}{\partial z} + C_1 \frac{\partial^2 P}{\partial z^2 \partial t} \\
 &= V_z^2 \frac{\partial^2 P}{\partial z^2} + \frac{\partial}{\partial z} \left( C_1 \frac{\partial^2 P}{\partial z^2} \right) - \frac{\partial V_z}{\partial t} \frac{\partial P}{\partial z} + C_1 \frac{\partial^3 P}{\partial z^2 \partial t}
 \end{aligned} \tag{D7}$$

as in equation D4, it gives

$$P_{j,k}^{\ell+1} = P_{j,k}^{\ell+\frac{1}{2}} + \left. \frac{\partial P}{\partial t} \right|_{j,k}^{\ell+\frac{1}{2}} \Delta t + \left. \frac{\partial^2 P}{\partial t^2} \right|_{j,k}^{\ell+\frac{1}{2}} \frac{\Delta t^2}{2} + O(\Delta t^3) \quad (D8)$$

Substitute D6 and D7 into D8

$$\begin{aligned} P_{j,k}^{\ell+1} = & P_{j,k}^{\ell+\frac{1}{2}} - V_z \left. \frac{\partial P}{\partial z} \right|_{j,k}^{\ell+\frac{1}{2}} \Delta t + C_1 \left. \frac{\partial^2 P}{\partial z^2} \right|_{j,k}^{\ell+\frac{1}{2}} \Delta t \\ & + V_z^2 \left. \frac{\partial^2 P}{\partial z^2} \right|_{j,k}^{\ell+\frac{1}{2}} \frac{\Delta t^2}{2} + (\text{high order terms}) \end{aligned} \quad (D9)$$

or

$$\begin{aligned} P_{j,k}^{\ell+1} \approx & P_{j,k}^{\ell+\frac{1}{2}} - \frac{\Delta t}{2\Delta z} (V_z)_{j,k}^{\ell+\frac{1}{2}} (P_{j,k+1}^{\ell+\frac{1}{2}} - P_{j,k-1}^{\ell+\frac{1}{2}}) \\ & + \left[ \frac{1}{2} \left( \frac{\Delta t}{\Delta z} (V_z)_{j,k}^{\ell+\frac{1}{2}} \right) + \frac{\Delta t}{(\Delta z)^2} C_1 \right] (P_{j,k+1}^{\ell+\frac{1}{2}} - 2P_{j,k}^{\ell+\frac{1}{2}} \\ & + P_{j,k-1}^{\ell+\frac{1}{2}}) \end{aligned} \quad (126)$$

FIGURES

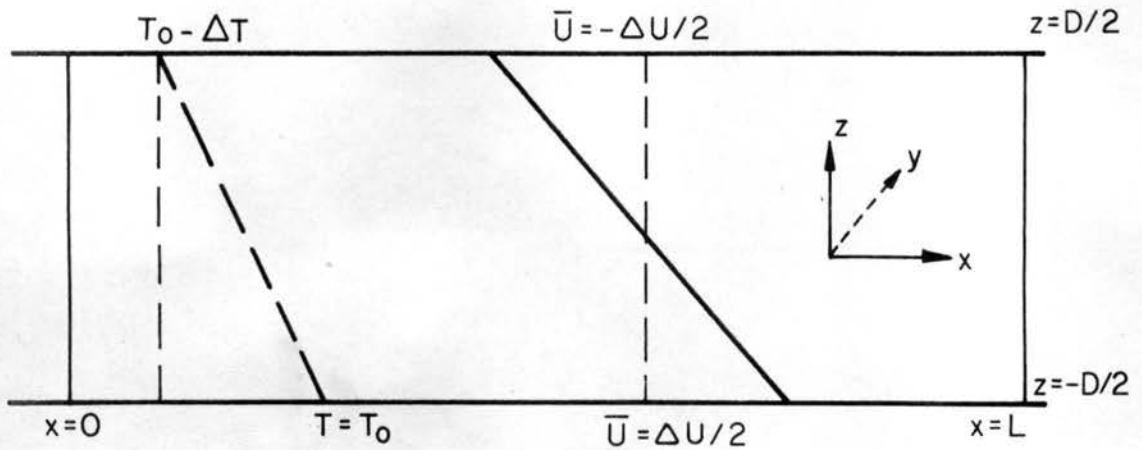


Figure 1 A vertical cross section of the model for thermal convection in the presence of vertical shear.

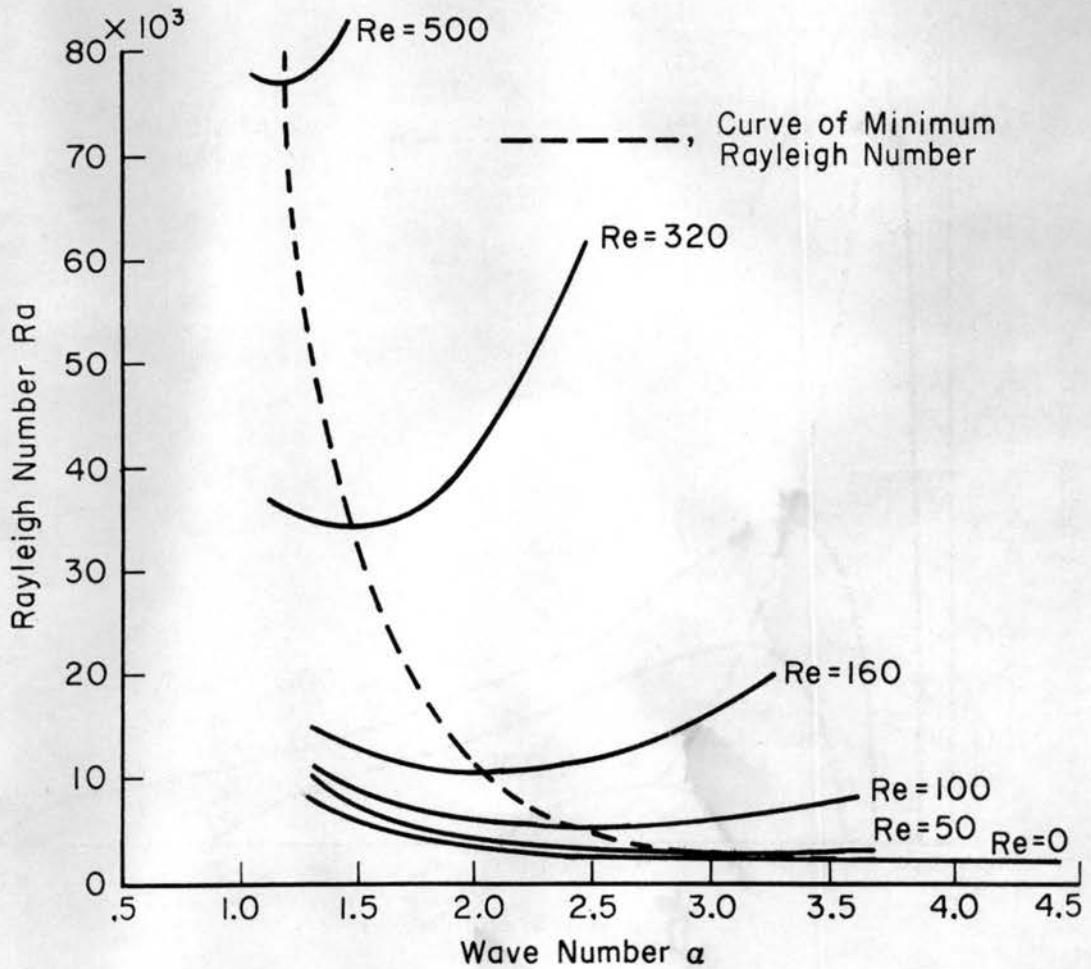


Figure 2 Neutral stability curves for various Reynolds numbers obtained from linear stability theory (Transverse roll).

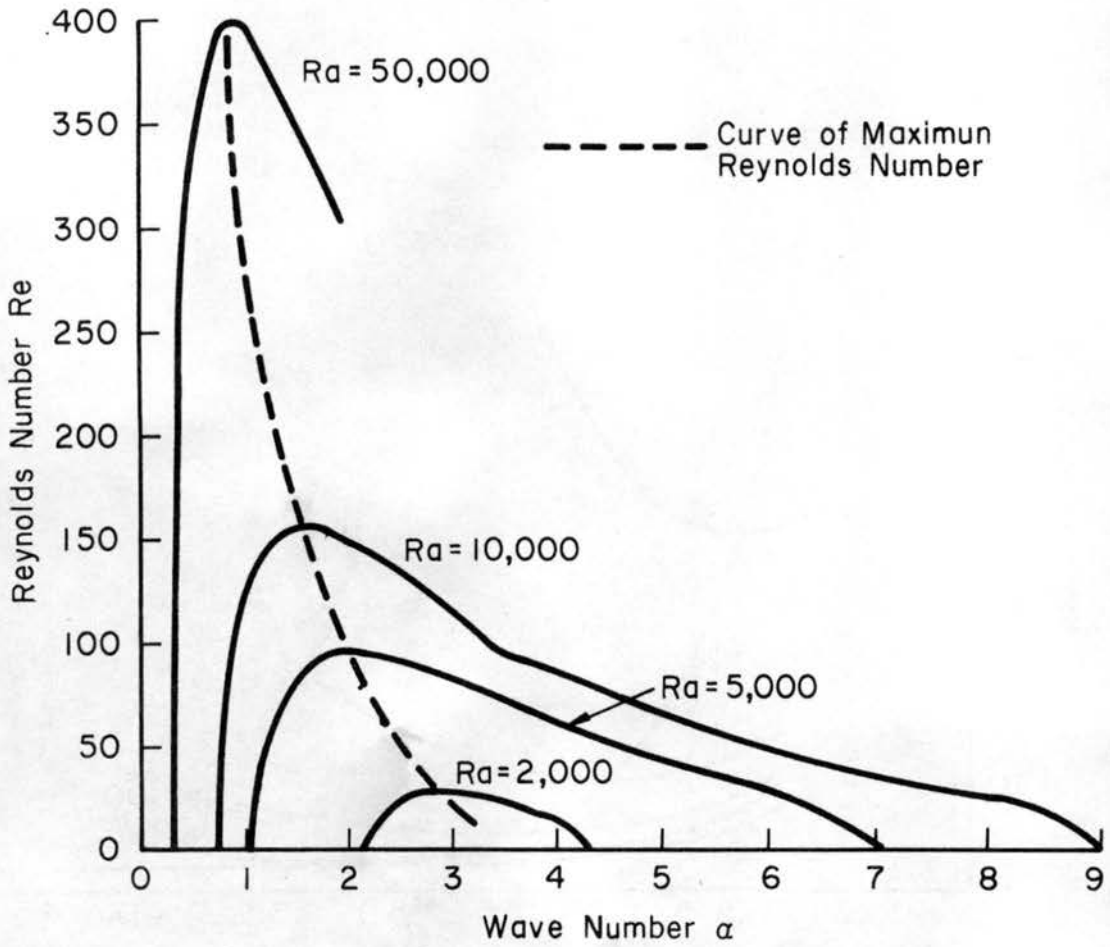


Figure 3 Neutral stability curves for various Rayleigh numbers obtained from linear stability theory (Transverse roll).

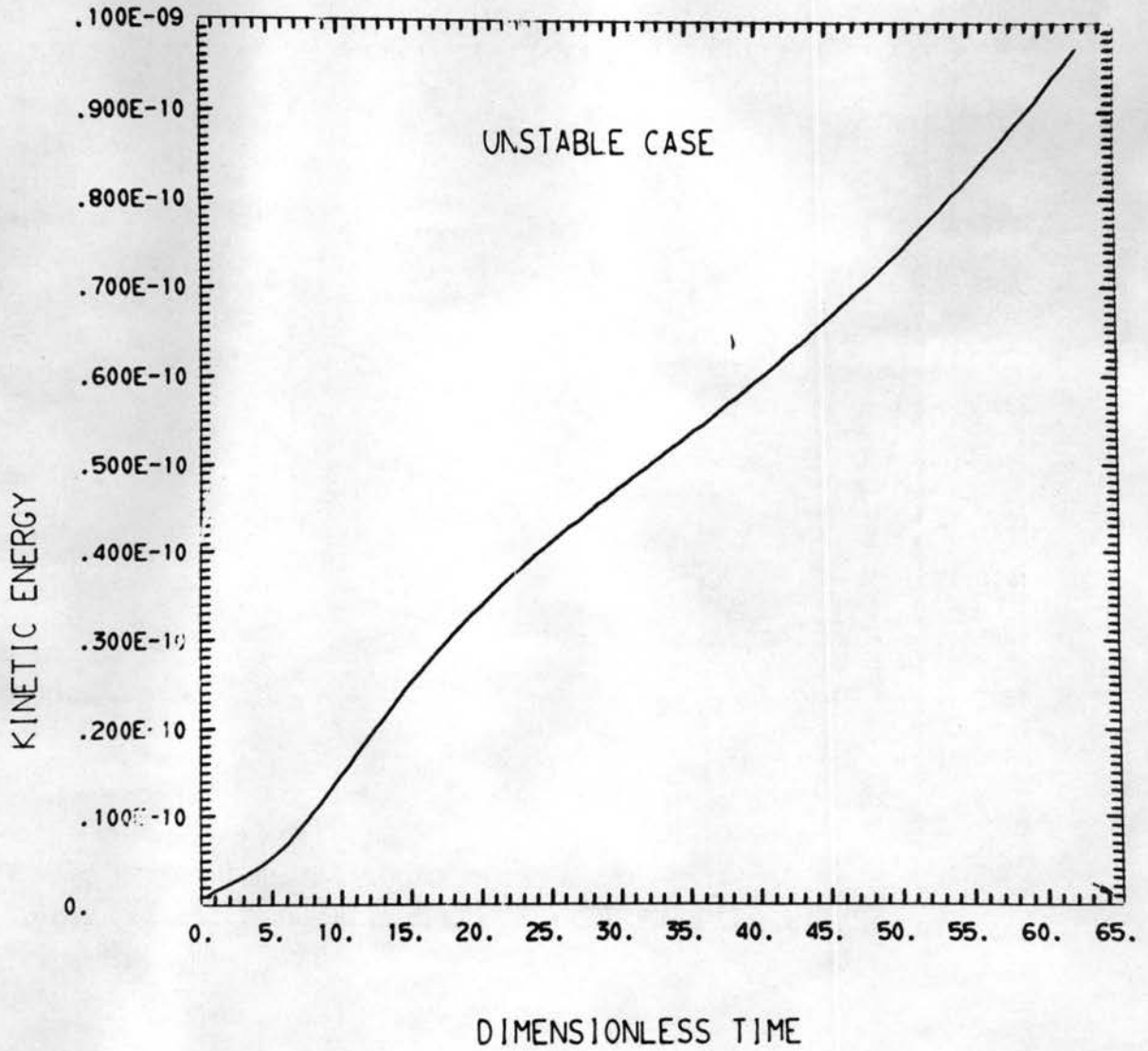


FIGURE 4A. VARIATION OF KINETIC ENERGY OF DISTURBANCE

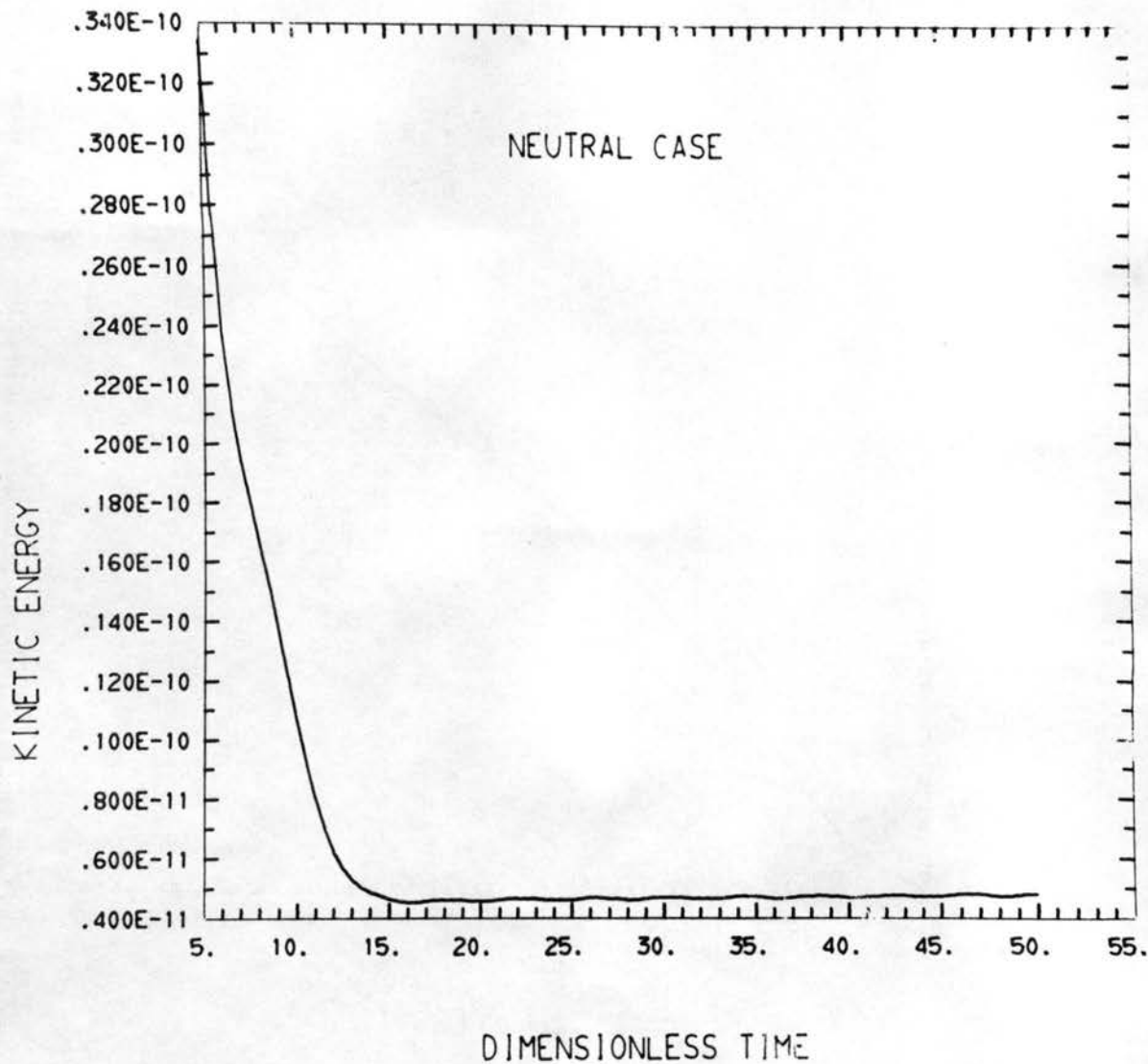


FIGURE 4B. VARIATION OF KINETIC ENERGY OF DISTURBANCE

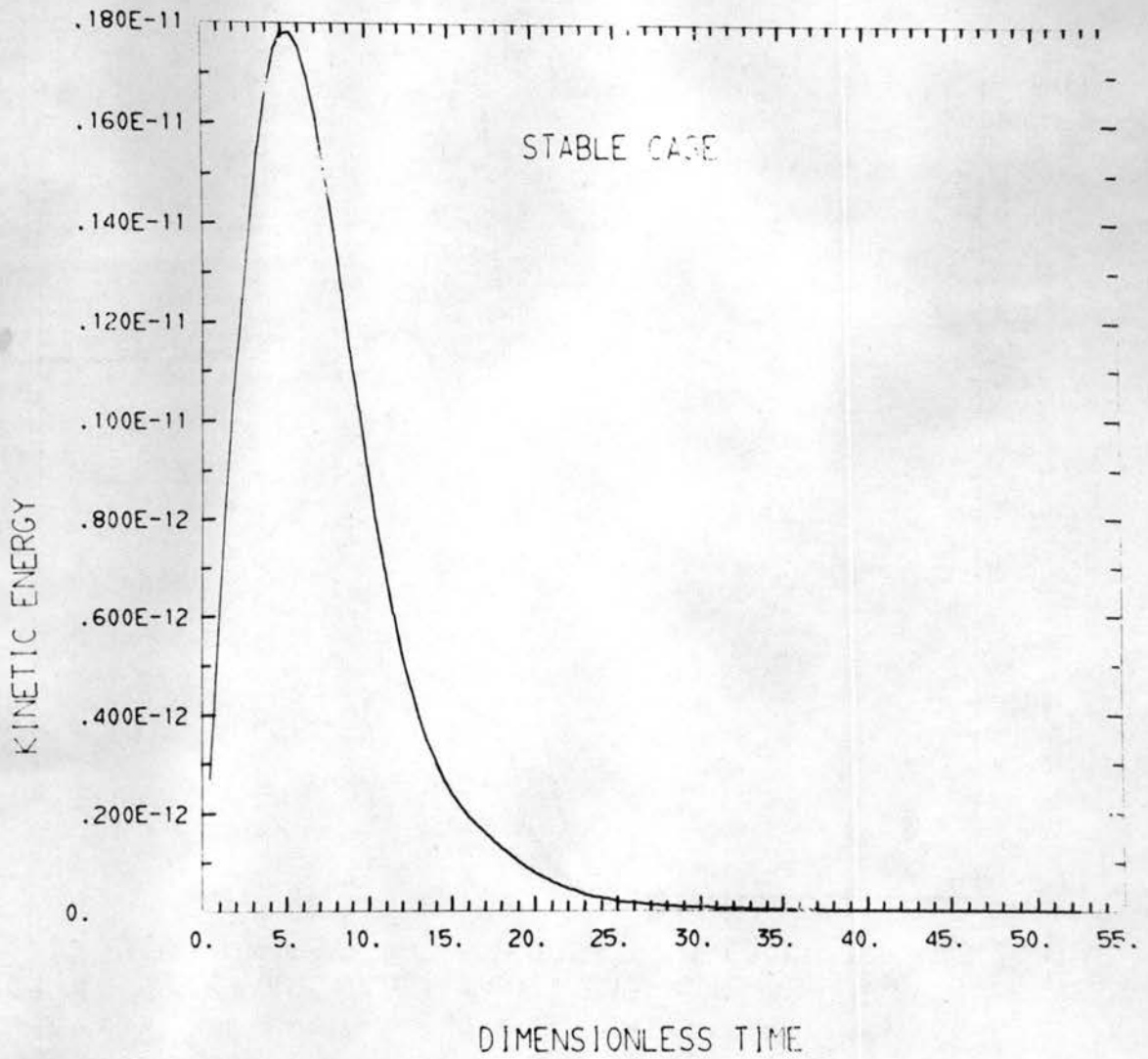


FIGURE 4C. VARIATION OF KINETIC ENERGY OF DISTURBANCE

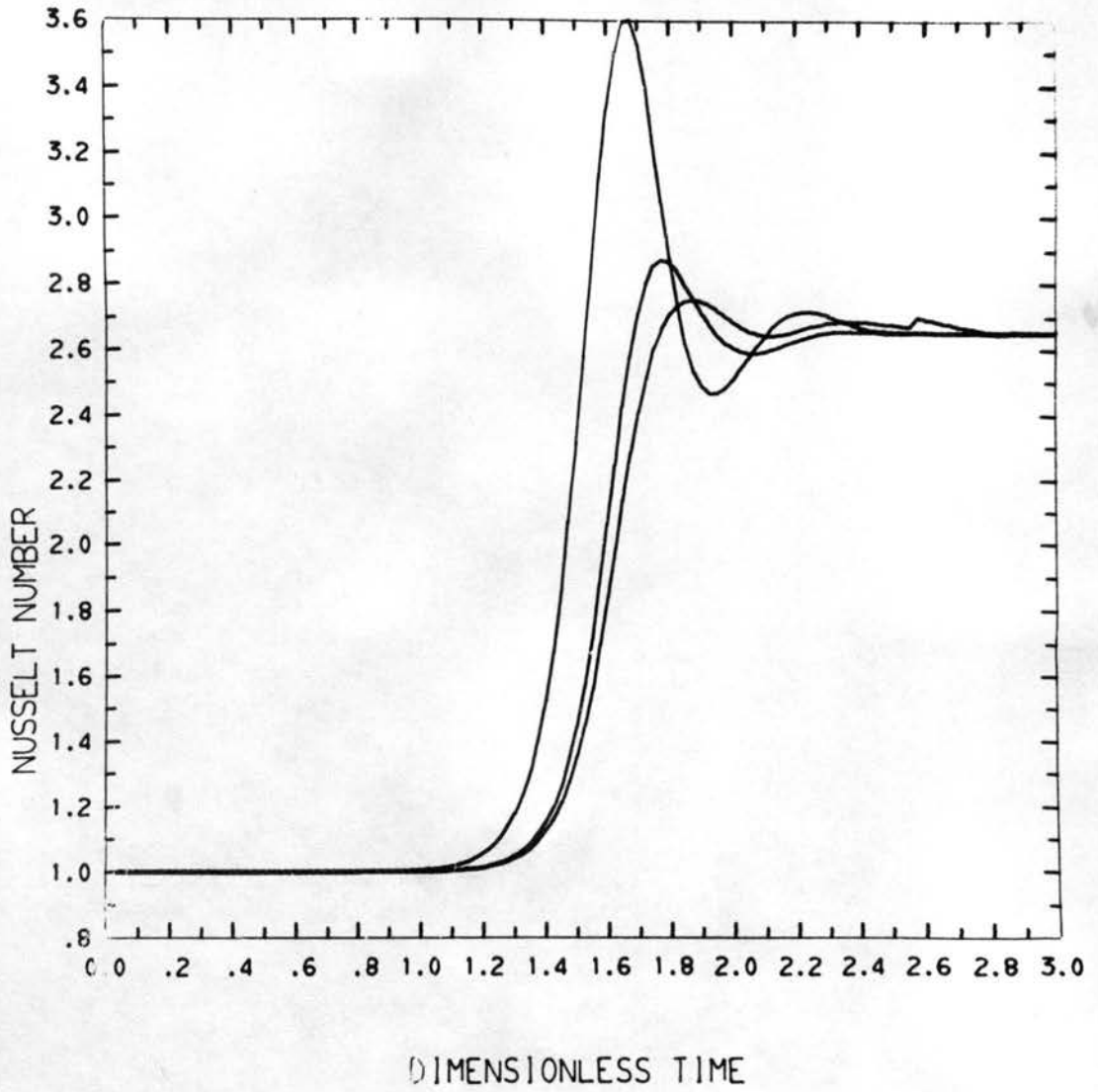


FIGURE. 5 VARIATION OF NU AT THREE VERTICAL POSITIONS

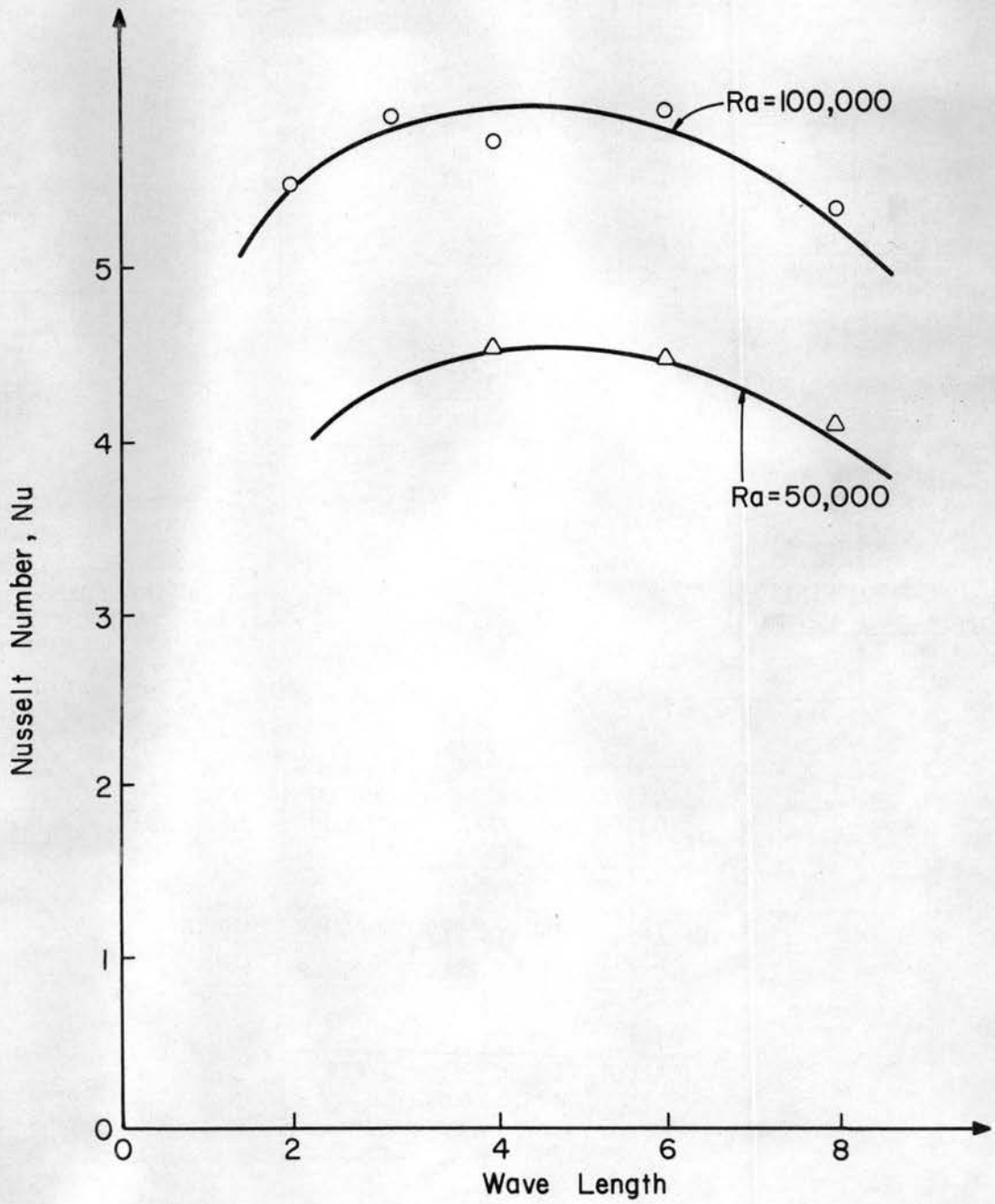


Figure 6. Nusselt number as a function of the dimensionless horizontal wave length for  $Re = 160$  and  $\alpha = 0$ .

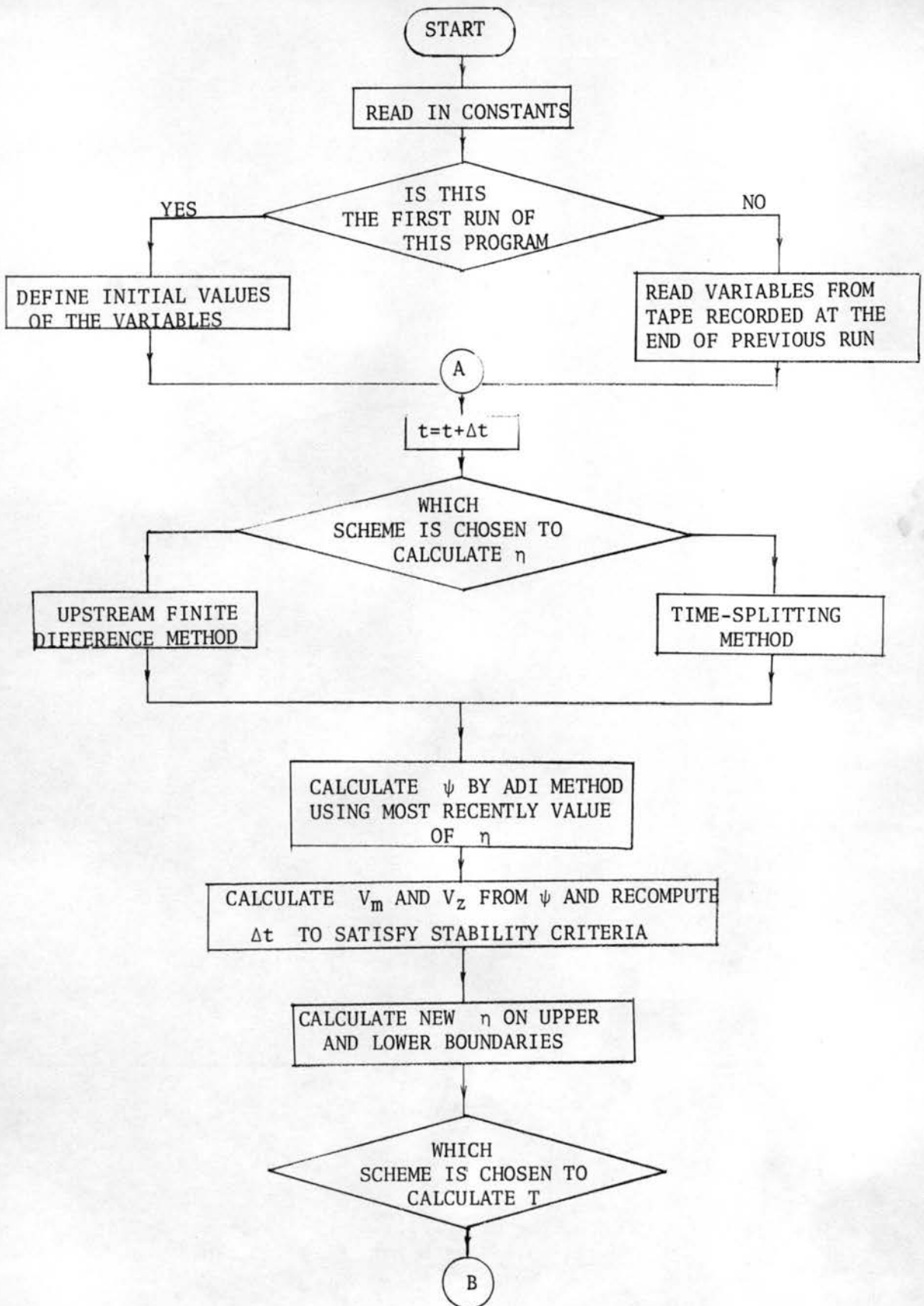


Figure 7 Flow chart of nonlinear program



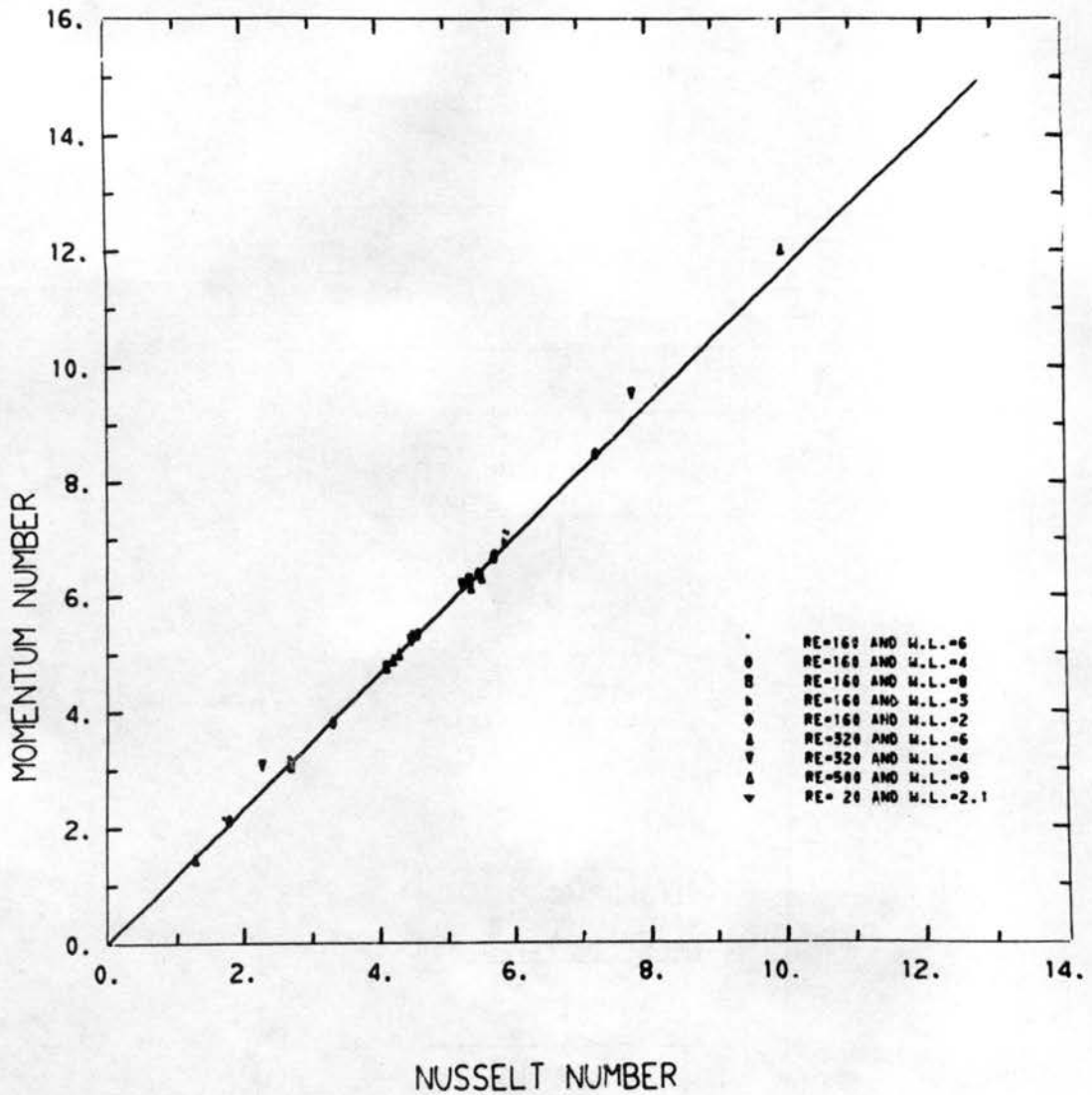
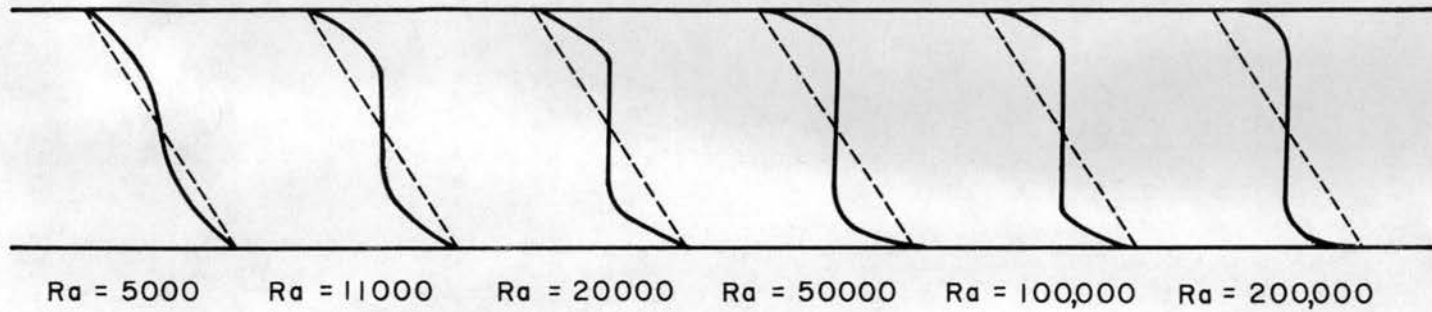


FIGURE 8. RELATION BETWEEN NU AND  $-M_0$  FOR LONGITUDINAL ROLLS

Mean Temperature Profile



Mean Velocity Profile

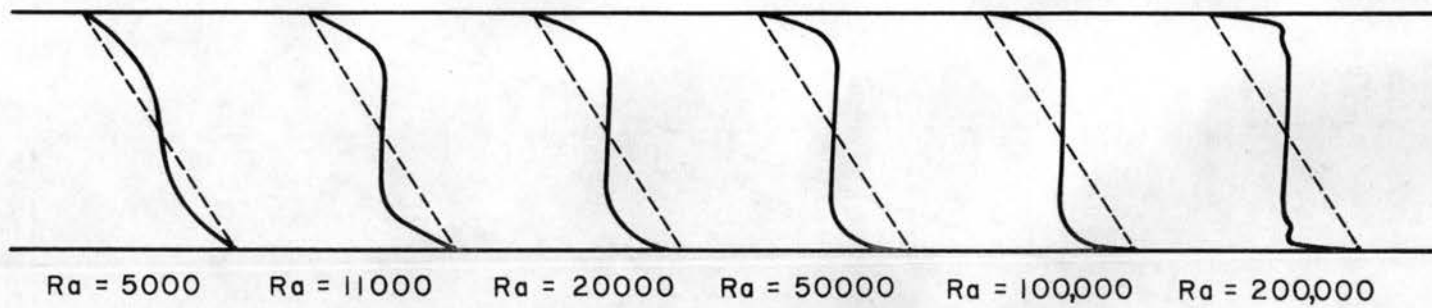


Figure 9 Mean temperature and velocity profiles for  $Re = 160$ ,  $\alpha = 0$ , Wave length = 4 .

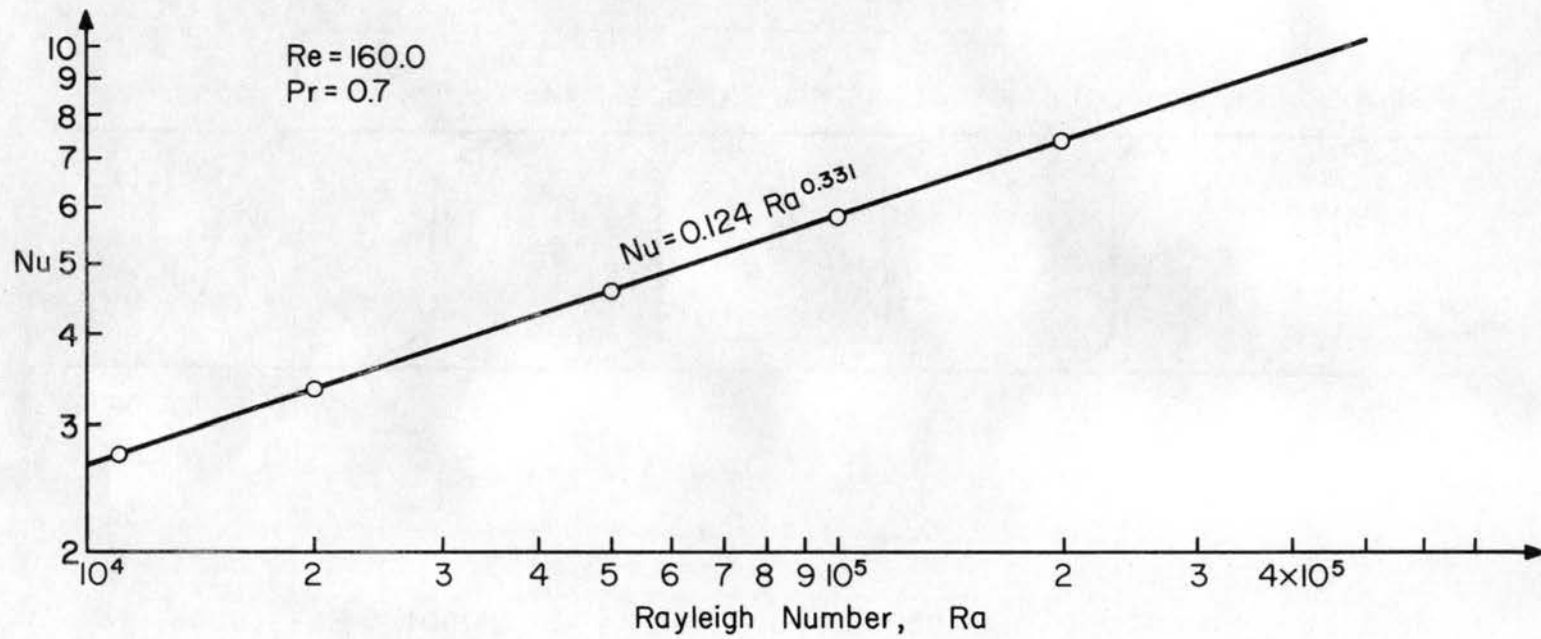


Figure 10. Nusselt number as a function of Rayleigh number in logarithmic scale.

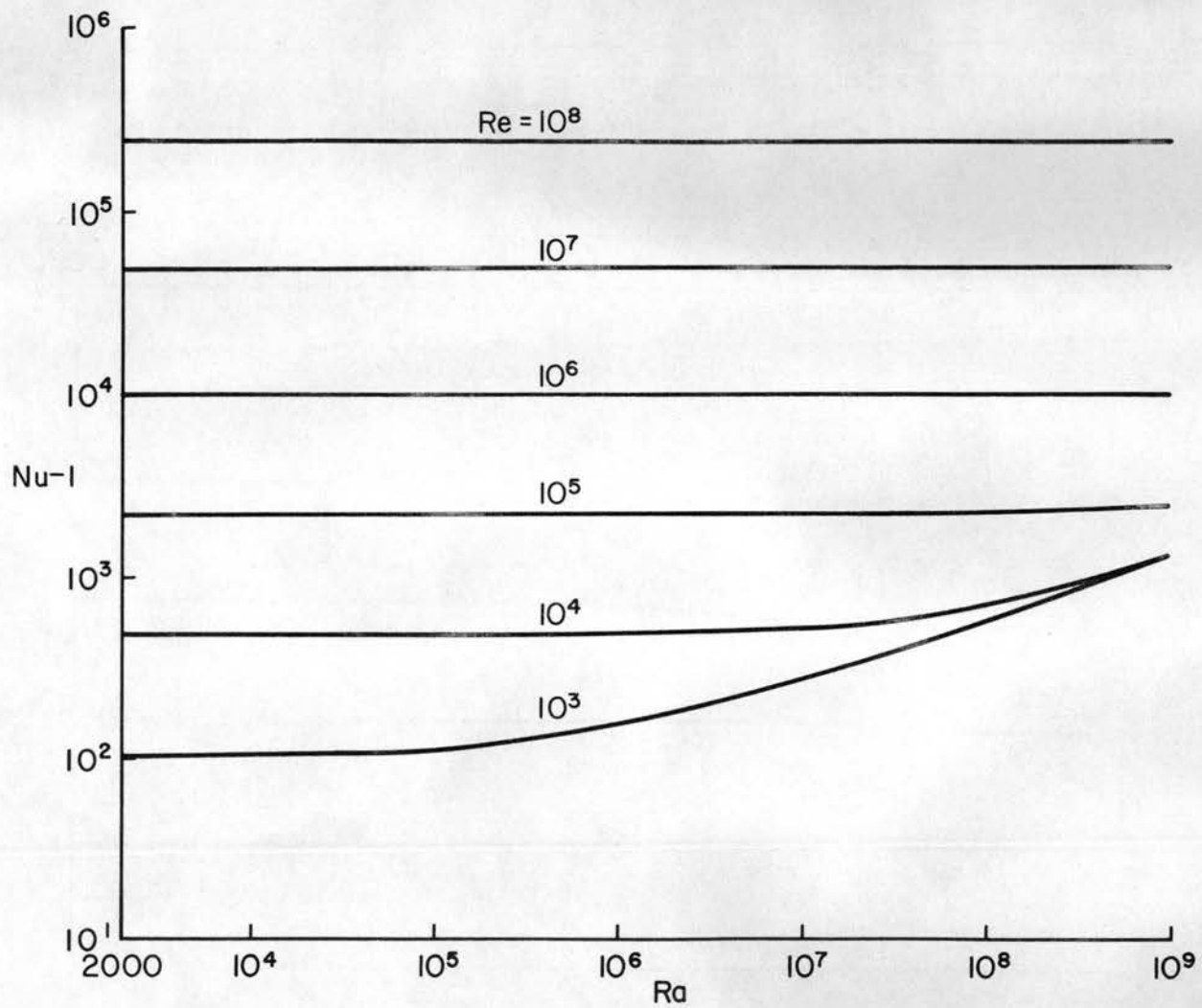


Figure 11A. Upper bound on heat flux in terms of Rayleigh and Reynolds numbers ( $Pr = 0.7$ ).

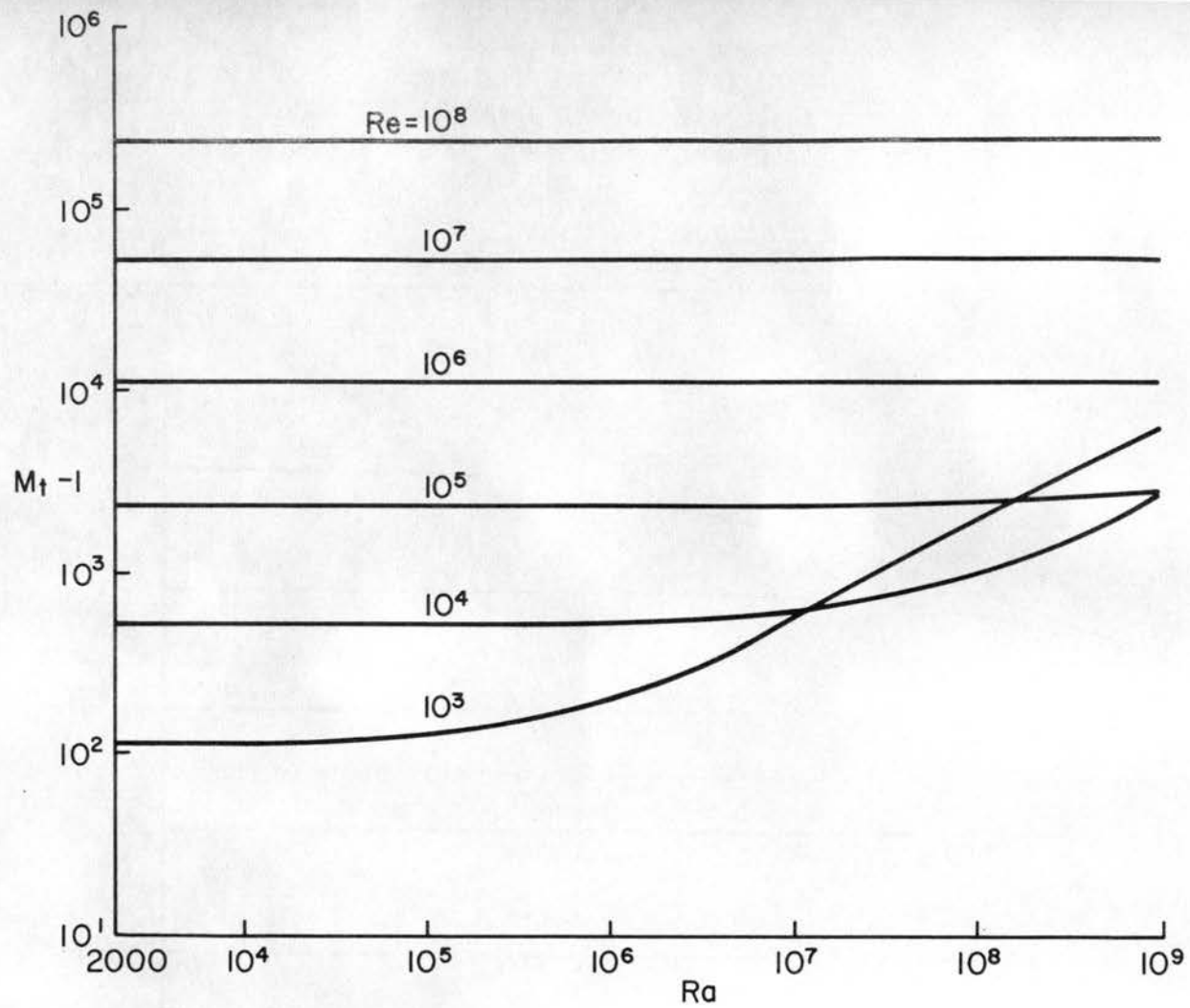


Figure 11B. Upper bound on momentum flux in terms of Rayleigh and Reynolds numbers ( $Pr = 0.7$ ).

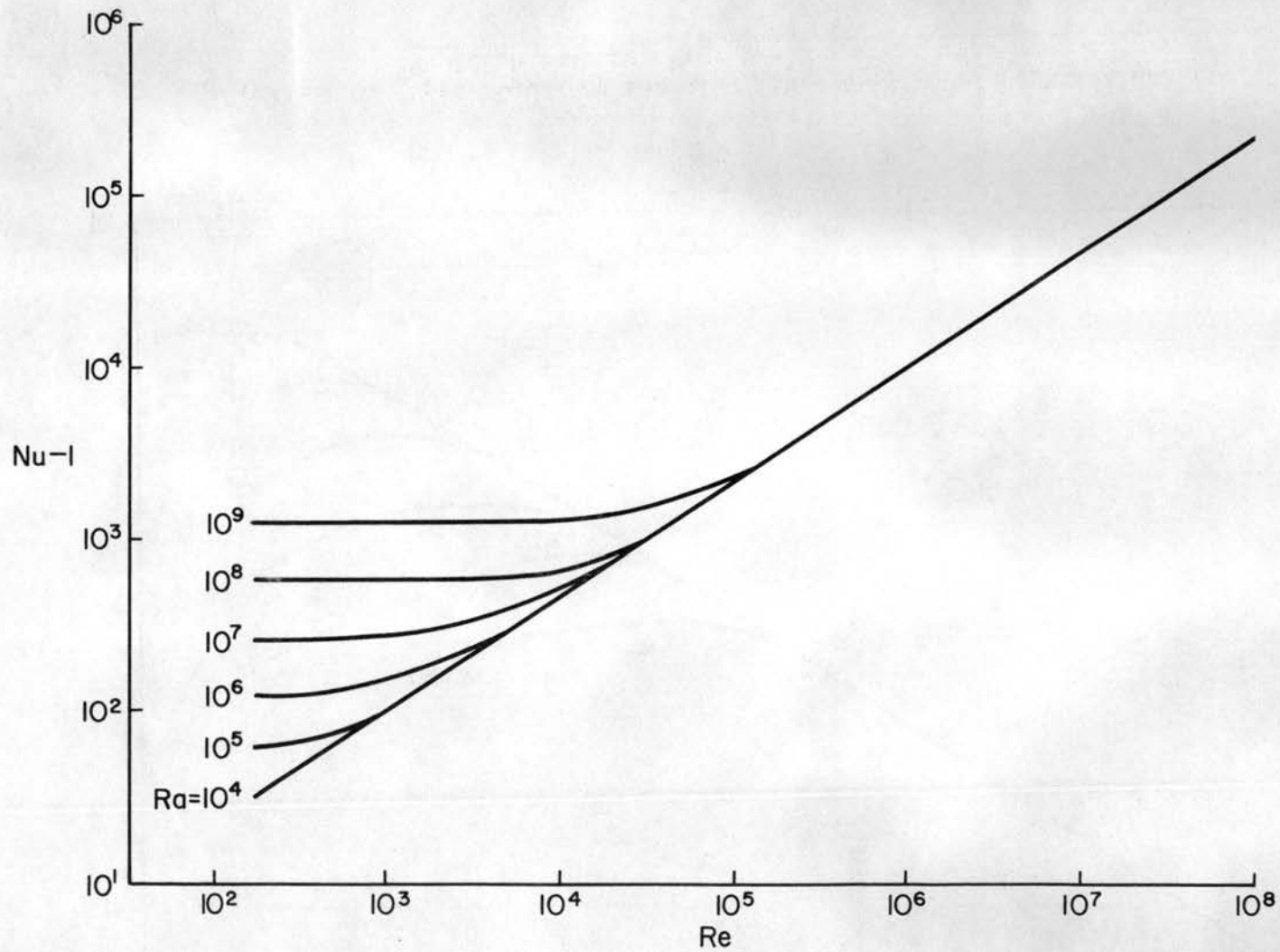


Figure 11C. Upper bound on heat flux in terms of Reynolds and Rayleigh numbers ( $Pr = 0.7$ ).

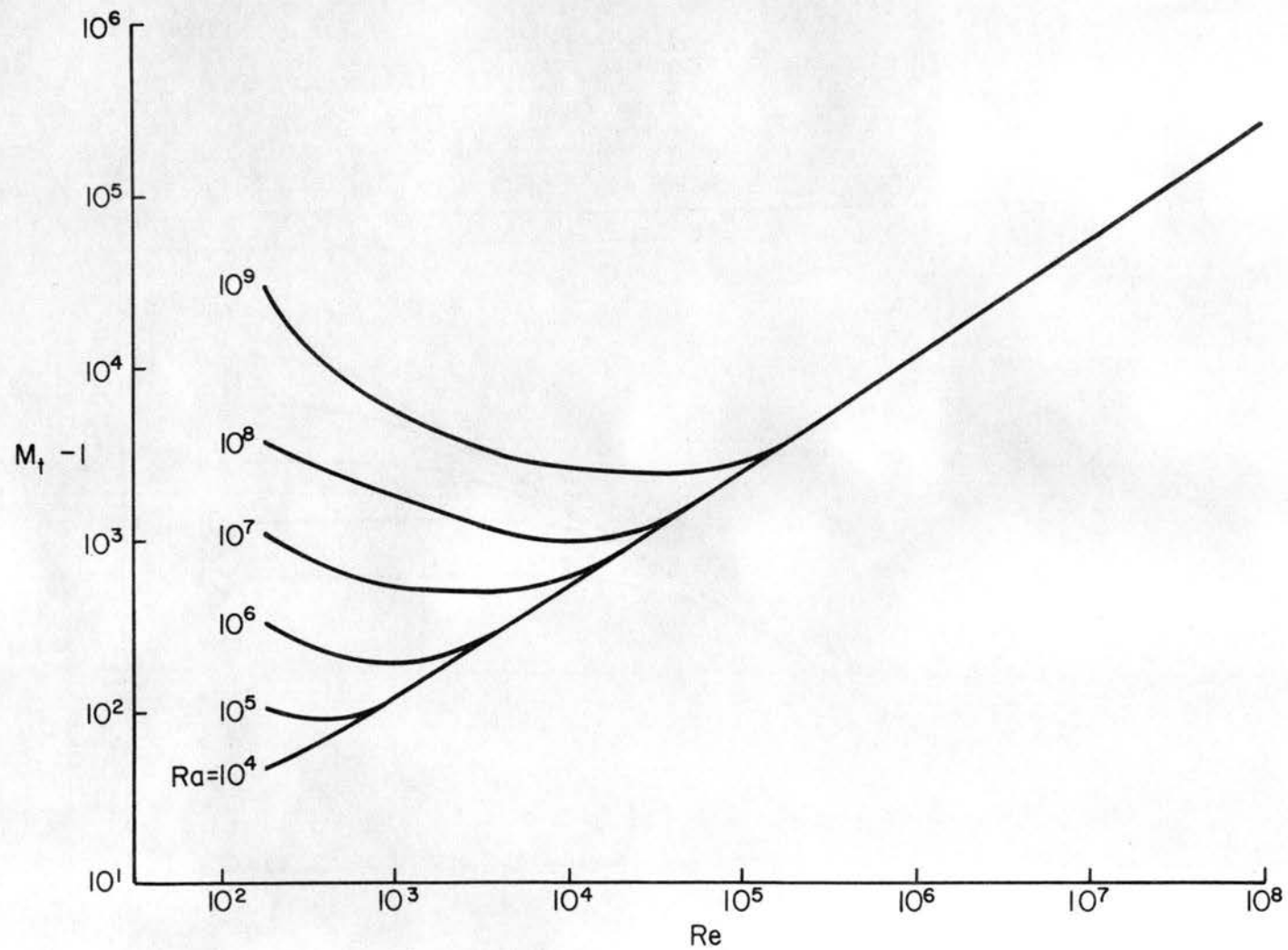


Figure 11D. Upper bound on momentum flux in terms of Reynolds and Rayleigh numbers ( $Pr = 0.7$ ).

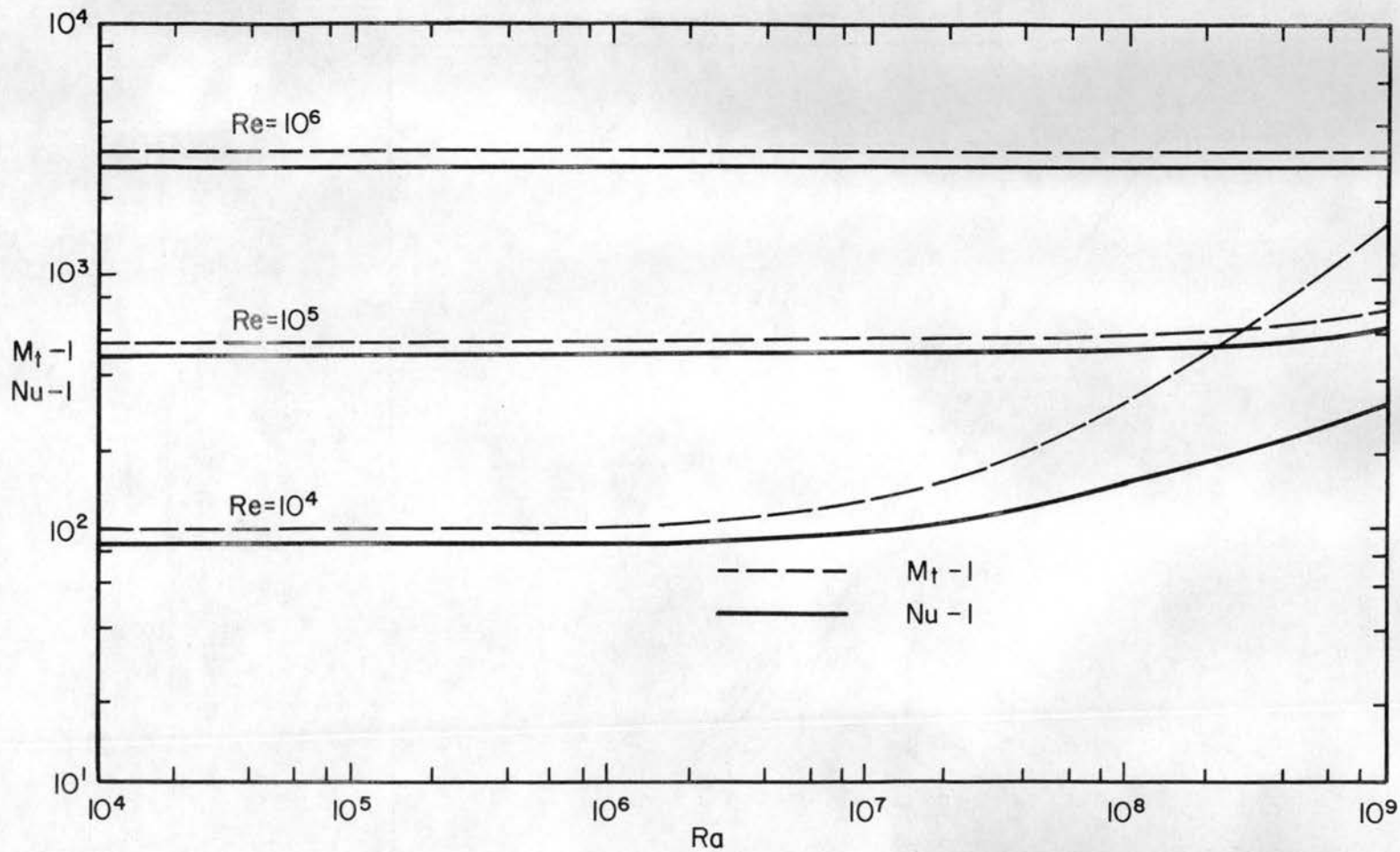


Figure 12A. Upper bounds on heat and momentum flux in terms of Rayleigh and Reynolds numbers for a different single-wave-number assumption ( $Pr = 0.7$ ). (From Nickerson (1970)).

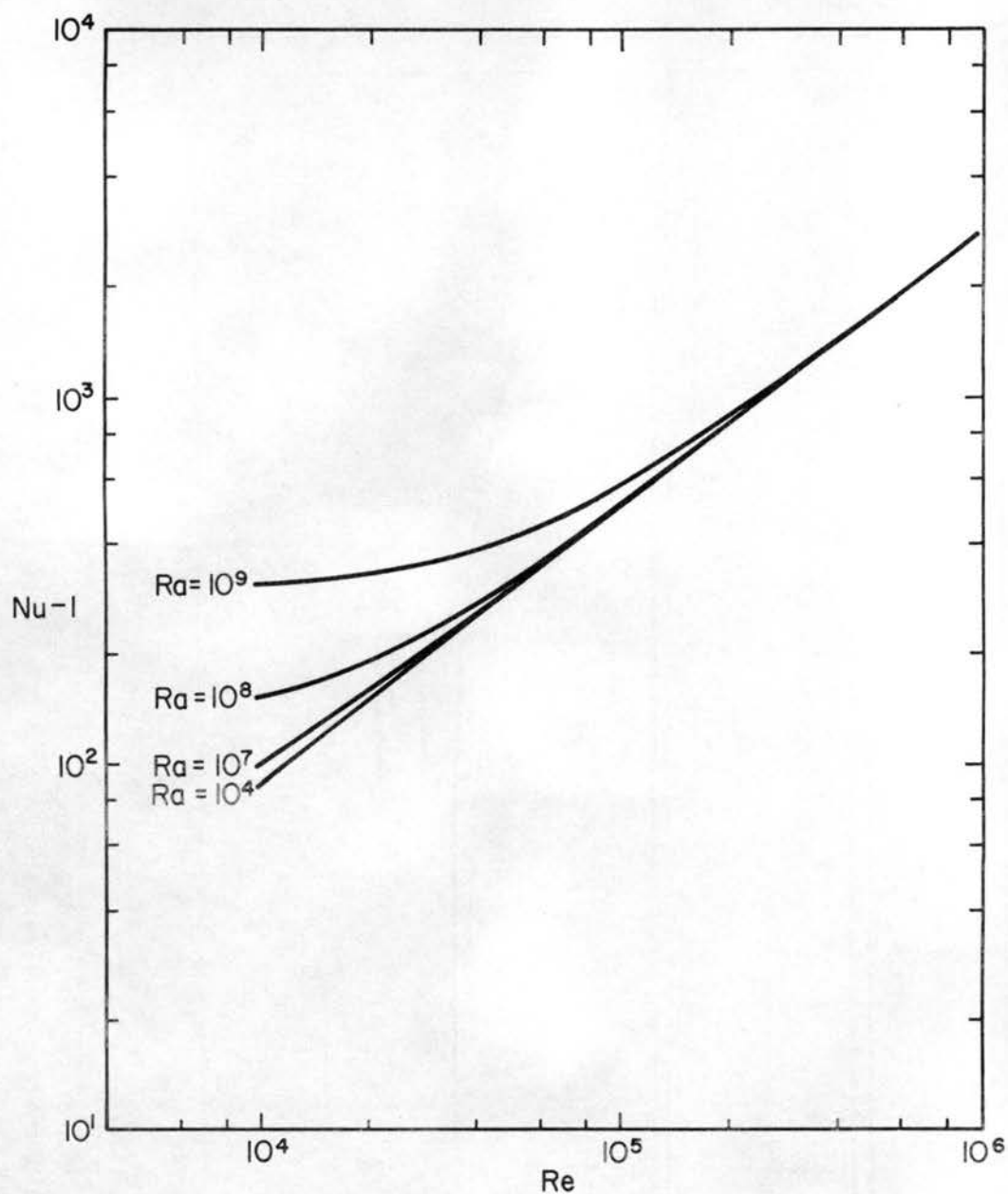


Figure 12B. Upper bound on heat flux in terms of Reynolds and Rayleigh numbers for a different single-wave-number assumption ( $Pr = 0.7$ ). (From Nickerson (1970)).

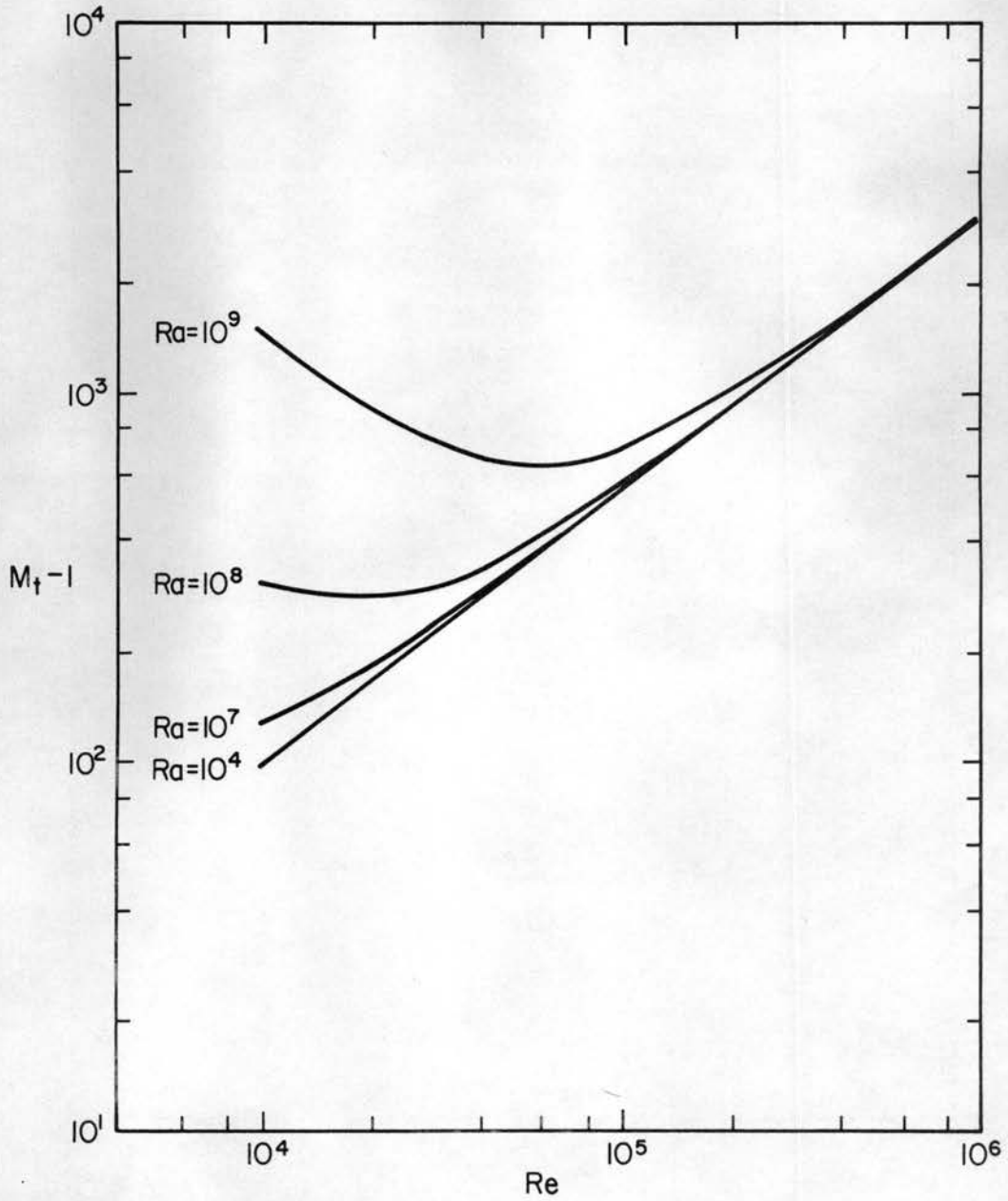
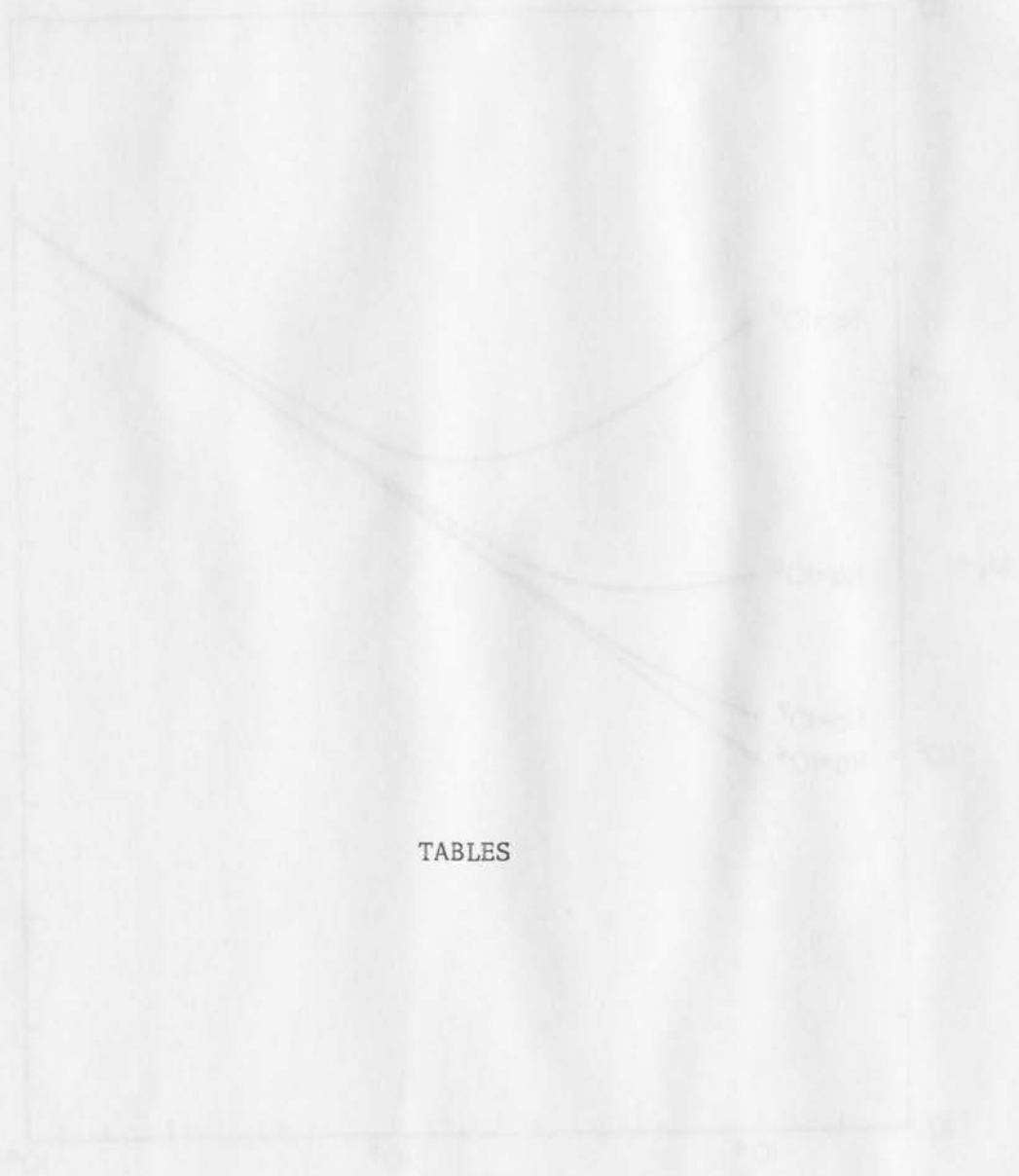


Figure 12C. Upper bound on momentum flux in terms of Reynolds and Rayleigh numbers for a different single-wave-number assumption ( $Pr = 0.7$ ). (From Nickerson (1970)).



TABLES

TABLE I  
 Summary of the results of the experiments on the effect of the concentration of the solution on the rate of the reaction. The rate was measured by the amount of gas evolved in a given time. The temperature was kept constant at 25°C. The concentration of the solution was varied from 0.1 M to 1.0 M. The rate of the reaction increased with increasing concentration of the solution.

Run	Source	$\Delta U$ (cm/sec)	$\Delta T$ ( $^{\circ}C$ )	Depth (cm)	Width (cm)	B=W/D	Re	Ra	Type of Rolls
1	Dassanayake	0.5	40	1.0	30.48	30.48	3.19	4132.45	Trans-Longit
2	Brunt	10.	58	0.8	30.48	38.1	51.02	3067.93	Longitudinal
3	Brunt	9.	90	0.8	30.48	38.1	45.92	4760.58	Transverse
4	Chandra	1.7	90	0.8	30.48	38.1	8.67	4760.58	Trans-Longit
5	Chandra	2.3	103	0.7	30.48	43.54	10.27	3649.88	Polyg-Longit
6	Chandra	10.	29	1.6	30.48	19.05	102.04	12271.72	Longitudinal
7	Chandra	2.3	47	1.6	30.48	19.05	23.47	19888.6	No Longitud.
8.	Chandra	1.3	13	1.6	30.48	19.05	13.27	5501.1	Longitudinal
9	Chandra	6.	100	1.6	30.48	19.05	61.22	42316.29	Longitudinal
10	Chandra	6.	100	0.7	30.48	43.54	26.79	3543.57	Longitudinal
11	Chandra	2.3	91	0.6	30.48	50.8	11.73	2030.69	Longitudinal

Table I Experimental data for Heated Plane Couette Flow

Re	Source	Wave Number $\alpha$									
		0.4	0.8	1.2	1.6	2.0	2.4	2.8	3.2	3.6	4.0
0	Present Data	32393	8688	4324	2830	2177	1869	1735	1709.5	1762	1879
	G & M	32432	8680	4328	2832	2176	1864	1736	1712	1760	1880
20	Present Data	---	8786	4427	2939	2297	2002	1889	1890	1976	2138
50	Present Data	---	---	4965	3519	2940	2738	2756	2939	---	---
100	Present Data	34774	11139	6919	5682	5455	5818	6721	8306	---	---
	Present Data	38492	15001	11139	10639	11772	14544	20072	---	---	---
160	G & M	38712	15200	11336	10840	12000	14816	20432	---	---	---
	Present Data	56865	34783	35156	43698	61892	---	---	---	---	---
320	G & M	57704	35496	35808	44384	62744	---	---	---	---	---
	Present Data	925917	77377	97101	140368	---	---	---	---	---	---

Table 2 Values of Rayleigh number for neutral stability obtained from linear stability theory [G & M refers to the values of Rayleigh number obtained from the data of Gallagher and Mercer (1965)].

Reynolds Number	0	20	50	100	160	320	500
Critical Ra	1707.784	1877.14	2723.02	5446.81	10589.993	33775.69	76461.9
Corresponding Wave Number	3.11	2.99	2.56	1.93	1.502	0.973	0.704

Table 3 Critical Rayleigh Number with its corresponding Reynolds Number for transverse roll (see also in Figure 2).

Rayleigh Number	2,000	5,000	10,000	50,000
Critical Re	26.3604	93.3609	154.125	397.598
Corresponding Wave Number	2.91	2.00	1.53	0.84

Table 4 Critical Reynolds Number with its corresponding Rayleigh Number for transverse roll (see also in Figure 3).

Re	Wave Length	$\alpha$	Linear	Nonlinear	
				Present	Lipp's
160	4.0	0	2901	1725	---
		$\pi/8$	3933	3635	---
		$\pi/4$	6563	6582	---
		$3\pi/8$	9388	9429	---
		$\pi/2$	10614	10660	10400
	3.0	$\pi/2$	12261	12267	---
	6.0	$\pi/2$	11990	12217	---
320	6.0	0	5412	2200	---
		$3\pi/8$	29368	29760	---
		$\pi/2$	33933	34354	33000

Table 5. Comparison of neutral Rayleigh number from linear and nonlinear method [Lipp's refers the data from Lipp's (1971) paper].

## Heat Flux

Ra	Wave Angle				
	0	$\pi/8$	$\pi/4$	$3\pi/8$	$\pi/2$
20,000	3.310	3.203	2.684	2.658	2.768
50,000	4,569	4,605	4.386	3.445	3.507
100,000	5.721	5.336	5.114	4.127	4.910
200,000	7.232	6.669	6.427	6.334	5.018
300,000	---	7.5106	---	7.112	6.987

## Momentum Flux

Ra	Wave Angle				
	0	$\pi/8$	$\pi/4$	$3\pi/8$	$\pi/2$
20,000	-3.882	-3.211	-1.782	-1.023	-0.594
50,000	-5.353	-4.680	-2.868	-0.781	U.B.
100,000	-6.704	-5.207	-2.928	U.B.	U.B.
200,000	-8.462	-6.244	-3.661	U.B.	U.B.
300,000	---	-6.759	---	U.B.	U.B.

(U.B. refers to unbalanced momentum flux)

Table 6. Heat flux and momentum flux at various wave angles for  $Re = 160$  and wavelenth = 4.

$\alpha$		Reynolds Number		
		160	320	500
		Wave Number		
		4.	6.	9.
0	5,000	1.765	1.0	1.0
	11,000	2.679	2.691	1.283
	50,000	4.569	4.290	4.215
	100,000	5.721	5.367	4.486
	200,000	7.232	5.706	5.535
	300,000	---	6.696	---
	500,000	---	9.975	9.406
$\pi/2$	5,000	1.0	1.0	1.0
	10,000	1.0	1.0	1.0
	20,000	2.768	1.0	1.0
	50,000	3.507	1.0	1.0
	100,000	4.910	3.524	1.0
	200,000	5.018	4.062	3.431
	500,000	---	7.015	5.133

Table 7. Nusselt number for various Reynolds number and Rayleigh number at  $\alpha = 0$  and  $\alpha = \pi/2$ .

Investigator	Year	Range of Ra Examined	C	p	q
O'Toole & Silveston	1961	$10^5 - 10^9$	.104	.305	.084
Mull & Reiher	1930	$10^5 - 10^6$	.068	.333	0
Schmidt & Silveston	1959	$10^5 - 10^7$	.10	.310	.05
Globe & Dropkin	1959	$10^5 - 10^8$	.069	.333	.074
Di Federico & Foraboschi	1966	$10^4 - 10^7$	.092	.333	0
Malkus	1954a	$10^5 - 10^9$	.052	.325	0
Somerscles & Gasda	1969	$10^5 - 10^8$	.196	.283	0

Table 8 Experimental values of the constants in equation (273) as reported by various investigators.